

Development, Disease, and Regeneration: Using Zebrafish to Model Neurological Perturbations.

By

Robert J. Thorn

B.A., Columbia University, 2010

Thesis

Submitted in partial fulfillment of the requirements for the degree of Doctor of Philosophy in the
Division of Biology of Medicine at Brown University

PROVIDENCE, RHODE ISLAND

May 2018

© Copyright 2018 by Robert J. Thorn

This dissertation by Robert J. Thorn is accepted in its present form by the Department of Molecular Biology, Cell Biology and Biochemistry as satisfying the dissertation requirement for the degree of Doctor of Philosophy.

Date: _____

Dr. Robbert Creton, Advisor

Recommended to the Graduate Council

Date: _____

Dr. Alison DeLong, Reader

Date: _____

Dr. Anne Hart, Reader

Date: _____

Dr. Kimberly Mowry, Reader

Date: _____

Dr. Gary Wessel, Reader

Date: _____

Dr. Neel Aluru, Reader

Approved by the Graduate Council

Date: _____

Dr. Andrew Campbell,
Dean of the Graduate School

Curriculum Vitae

ROBERT J. THORN

Address: Box G-L106C
185 Meeting Street
Providence, RI 02912

Telephone:(401) 863-6512 [Lab]
(914) 907-7067 [Cell]
Email: Robert_Thorn@Brown.edu

EDUCATION

Doctor of Philosophy

Molecular Biology, Cell Biology and Biochemistry Expected in 2018
Brown University, Providence, RI
Thesis: “Development, Disease, and Regeneration: Using Zebrafish to Model Neurological Perturbations”

Bachelor of Arts

Biochemistry 2010
Neuroscience and Behavior 2010
Columbia University, Columbia College, New York, NY

RESEARCH EXPERIENCE

Graduate Thesis 06/2013 – Present
Brown University, Providence, RI *Advisor: Robbert Creton*

Laboratory Technician 05/2010 – 08/2012
Columbia University Medical Center, New York, NY *Advisor: Frank Costantini*

Molecular Biology Laboratory Undergraduate 06/2009 – 05/2010
Columbia University Medical Center, New York, NY *Advisor: Frank Costantini*

PUBLICATIONS

Clift D., Richendrfer H., **Thorn R.J.**, Colwill R.M., Creton R. High-throughput analysis of behavior in zebrafish larvae: effects of feeding. *Zebrafish*. 2014; 11 (5) : 455-461

Clift D.E., **Thorn R.J.**, Passarelli E.A., Kapoor M., LoPiccolo M.K., Richendrfer H.A., Colwill R.M., Creton R. Effects of embryonic cyclosporine exposures on brain development and behavior. *Behav Brain Res*. 2015; 282 : 117-24

Thorn R.J., Clift DE, Ojo O, Colwill RM, Creton R. The loss and recovery of vertebrate vision examined in microplates. *PLoS One* 2017 Aug 17;12(8):e0183414.

RESEARCH PRESENTATIONS

Thorn R.J., Bestoso D., Richendrfer H., Creton R. The Effects of Cyclosporine A on Zebrafish Brain Development. Brown University MCB Department Retreat Poster, August 2013

Thorn R.J., Bestoso D., Richendrfer H., Creton R. The Effects of Cyclosporine A on Zebrafish Brain Development. Brown University MCB Department Retreat Poster, August 2014

Thorn R.J., Brown University MCB Department Data Club, The Role of Calcineurin in Zebrafish Brain Development, January 2015

Thorn R.J., Fast Track Presentation, Northeast Regional Society for Developmental Biology (NESDB) Meeting Poster, Woods Hole, MA, May 2015

Thorn R.J., Bestoso D., Creton R. The Role of Calcineurin in Zebrafish Brain Development. Northeast Regional Society for Developmental Biology (NESDB) Meeting Poster, Woods Hole, MA, May 2015

Thorn R.J., Bestoso D., Creton R. The Role of Calcineurin in Zebrafish Brain Development. MCB Department Retreat Poster, September 2015

Thorn R.J., Brown University MCB Department Data Club, Regulatory subunits of calcineurin differentially direct early zebrafish brain and development, November 2015

Thorn R.J., Fast Track Presentation, Northeast Regional Society for Developmental Biology (NESDB) Meeting Poster, Woods Hole, MA, May 2016

Thorn R.J., Clift D.E., Creton R. Differing Roles for Calcineurin Regulatory Subunits in Zebrafish Brain Development. Fast-Track Presentation and Poster Presentation. Northeast Regional Society for Developmental Biology (NESDB) 2016

Thorn R.J., Brown University MCB Department Data Club, Regulatory subunits of calcineurin differentially direct early zebrafish brain and development, November 2016

Thorn R.J., Bestoso D., Oladele O., Seto R., Creton R. Analyzing Eye Ablation and Regeneration in Zebrafish. MCB Department Retreat Poster, September 2017

AWARDS AND HONORS

Abstract Selected for Fast Track Presentation	<i>NESDB 2015</i>
2nd Place Graduate Student Poster Award	<i>NESDB 2015</i>
MCB Department Student Service Award	<i>MCB Department Retreat, 2015</i>

COMMITTEES AND SERVICE

Student Member of MCBGP Admissions Committee, Brown University, 2014–2015

Mentor, MCBGP First Year Mentoring Program, Brown University, 2014-2015

Organizer, MCBGP First Year mentoring program, Brown University, 2015-2016

Mentor, MCBGP First Year Mentoring Program, Brown University, 2016-2017

MEMBERSHIP IN SOCIETIES

Society for Developmental Biology (SDB), 2014-2018

Genetics Society of America (GSA), 2016-2017

TEACHING EXPERIENCE

Teaching Certificates:

Certificate IV Course Brown University	Sheridan Teaching Center <i>Fall 2016 – Spring 2018</i>
Certificate I Discussion Leader Brown University	Sheridan Teaching Center <i>Fall 2017</i>
Certificate I Discussion Leader Brown University	Sheridan Teaching Center <i>Fall 2016</i>
Completed Certificate IV Course Brown University	Sheridan Teaching Center <i>Fall 2015 – Spring 2016</i>
Completed Certificate I Course Brown University	Sheridan Teaching Center <i>Fall 2014 – Spring 2015</i>

Course Instruction:

Instructor Brown University - Summer at Brown	CEBI0932 –Molecular Biology and Biochemistry <i>Summer 2017</i>
Teaching Assistant Brown University - Summer at Brown	CEBI0932 –Molecular Biology and Biochemistry <i>Summer 2016</i>
Teaching Assistant Brown University	BIOL 1310 Analysis of Development <i>Fall 2013</i>

Teaching Assistant
Columbia University

Science Honors Program in Organic Chemistry
Fall2009 - Spring2010

Teaching Assistant
Columbia University

CHEM C3543 Organic Chemistry Lab,
Summer 2008-Fall 2009

Facilitation:

STEM Study Group Leader
Brown University

The Leadership Alliance
Summer 2015

Science Education Fellow
Columbia University

TLQP Math/Science Workshop
Summer 2009

Guest Lectures:

Guest Lecture – Branching Morphogenesis
Brown University

BIOL 1310 Analysis of Development
Fall 2014

Guest Lecture – Branching Morphogenesis
Brown University

BIOL 1310 Analysis of Development
Fall 2013

Acknowledgements:

First, to the Creton Lab, especially Dr. Robbert Creton, my thesis advisor, for taking on an overambitious first year as his first PhD student. To Danielle Bestoso, lab manager extraordinaire, for managing me throughout my time in lab and making lab feel like home. To Geoff Williams, cohabitant of the Leduc bioimaging facility with the Creton lab, for training me and making sure I did not break any microscopes.

To Dr. Alison DeLong, Dr. Anne Hart, Dr. Kimberly Mowry and Dr. Gary Wessel, my thesis committee, for all their support and advice throughout the years. They helped rein in my ideas and challenge me as a scientist. A special thank you to Dr. Kimberly Mowry, for allowing me space in her lab to further my training at a time when I needed it most. Without her and the rest of the Mowry Lab I would still be trying to figure out how to do a Western Blot.

To the students of MCB, both past and present. The MCB community has been an extremely strong source of support, friendship, and roommates. To Sam, Melissa and (future) baby Freedlander for being a source of family in New England. To my friends from Tuckahoe High School, for always keeping me grounded and helping me keep things into perspective. To Jenna Kotak, who has been my rock, my bulldog, my partner and my best friend.

To my family, both blood related and not. Thank you for the words of encouragement and love, even when you did not know that fish do in fact have brains. To my sister, Ariana Thorn, for not letting me take myself too seriously. To my parents, Robert and Christine Thorn for cultivating my interest in science throughout my life. For

taking time out of their Saturday mornings in high school to drive me to New York City so I could take even more science classes.

To my late grandparents, Antoinette and Vincent Giuliano. Their love and support throughout my formative years helped shape me into the man I am today. I dedicate this thesis to my Grandmother. In 2013 she was introducing me as her grandson “the doctor” and five years later I am making that a reality.

Table of Contents

Title Page	i
Copyright Page	ii
Signature Page	iii
Curriculum Vitae	iv
Acknowledgements	viii
Table of Contents	x
List of Tables and Figures	xiii

Chapter 1: Introduction	1
Abstract	2
Zebrafish as a model to study brain development and behavior	5
Zebrafish as a disease model of human disease and toxicology	6
Developmental toxicity of immunosuppressant drugs	8
Calcineurin/NFAT signaling	10
Calcineurin in the nervous system	11
Overview of the retina	12
Eye Diseases	12
Zebrafish as a model to test the loss and recovery of vision	13
Overview of Thesis Research	14
References	15
Figures	20

Chapter 2: Effects of embryonic cyclosporine exposures on brain development and behavior	23
Abstract	24
Introduction	25
Materials and Methods	27

Results	31
Discussion	38
References	42
Figures	44
Chapter 3: Examining Calcineurin Inhibition in the Developing Zebrafish Brain	52
Abstract	53
Introduction	53
Materials and Methods	56
Results	63
Discussion	67
References	71
Figures	73
Chapter 4: The loss and recovery of vertebrate vision examined in microplates	79
Abstract	80
Introduction	80
Materials and Methods	82
Results	91
Discussion	99
References	104
Figures	106
Chapter 5: Conclusion	113
Zebrafish, what are they good for?	114
Expanding toolbox, expanded results	115
Cyclosporine and beyond	117

Alternative Medications	119
Zebrafish model of Calcineurin inhibition	120
Calcineurin inhibition in Down syndrome	122
The calcineurin conundrum	122
Tissue specific calcineurin inhibition	124
Assay for the loss and recovery of vision	126
“Eye” can see clearly now	127
Regeneration or recovery?	128
The good, the bad, and the ugly	129
Final thoughts	130
References	131
Appendix A: High-throughput analysis of behavior in zebrafish larvae: effects of feeding.	134
Appendix B: Updates and additions to behavioral assays	155
Appendix C: Test of zebrafish response to visual stimuli of primary and secondary colors	164

List of Tables and Figures

Chapter 1: Introduction

Figure 1. Overview of early zebrafish development	20
Figure 2. Zebrafish brain at 3 days post fertilization	21
Figure 3. Model of the Calcineurin signaling pathway	22

Chapter 2: Effects of embryonic cyclosporine exposures on brain development and behavior

Figure 1. Critical or sensitive periods in human development	44
Figure 2. Cyclosporine exposures affect eye size.	45
Figure 3. Cyclosporine exposures affect brain size	46
Figure 4. Sensitive periods for eye and brain defects.	47
Figure 5. Larval morphology at 5 dpf	48
Figure 6. Automated analysis of behavior in a five-lane plate.	49
Figure 7. Behavioral defects at 5 dpf.	50
Figure 8. Summary of sensitive periods in zebrafish development.	51

Chapter 3: Examining Calcineurin Inhibition in the Developing Zebrafish Brain

Figure 1. Immunolabeling for Calcineurin B in Zebrafish	73
Figure 2. Western Blot for Calcineurin B in Zebrafish	74
Figure 3. Effects of Calcineurin B knockdown in zebrafish	75
Figure 4. Effect of Calcineurin B knockdown on apoptosis	76
Figure 5. Effects of separate knockdown of Calcineurin B subunits on zebrafish	77
Figure 6. Effects of separate knockdown of Calcineurin B subunits on zebrafish behavior	78

Chapter 4: The loss and recovery of vertebrate vision examined in microplates

Figure 1. Imaging system for automated analyses of behavior	106
---	-----

Figure 2. Visual stimuli in 5-lane plates	107
Figure 3. Visual stimuli in 6-well plates	108
Figure 4. Effects of UV illumination examined in 5-lane plates	109
Figure 5. Effects of UV illumination examined in 6-well plates	110
Figure 6. Visual defects after pde6c knockdown	111
S1 Table. Assays for visually-guided behaviors in 5 day old zebrafish larvae	112

Appendix A: High-throughput analysis of behavior in zebrafish larvae: effects of feeding.

Figure 1. Imaging of zebrafish larvae in five-lane plates	152
Figure 2. The behavior of 6- and 7-day-old zebrafish larvae is affected by feeding	153
Figure 3. Fish-to-Fish Distance	154

Appendix B: Updates and additions to behavioral assays

Figure 1. 96-well plate setup	161
Figure 2. Response of zebrafish to audio stimulus	162
Figure 3. Habituation of zebrafish to a visual stimulus.	163

Appendix C: Test of zebrafish response to visual stimuli of primary and secondary colors

Figure 1. Test of zebrafish visual response in lanes with primary and secondary colors.	169
Figure 2. Test of zebrafish visual response to cyan colored stimuli.	170

Chapter 1: Introduction

Abstract

As medical technologies advance, effective vertebrate models of human disease are vital to determine safety and efficacy of treatments. My research has further developed zebrafish as a model to investigate vertebrate neurological development and disease.

Zebrafish are well suited for use as a model of vertebrate disease. A mixed population of male and female fish can produce hundreds of embryos on a daily basis. The embryos are transparent, develop externally, and can be imaged live by light microscopy throughout development. They are accessible to genetic manipulation and have many genes that are homologous to human disease genes. Zebrafish larvae display robust stereotyped behaviors that can be assayed to detect subtle brain defects.

In my thesis work, I used zebrafish to model developmental sensitivities to immunosuppressant drugs that may be prescribed during human fetal development. My research indicated that these drugs have a negative effect on brain and behavioral development. I've shown that zebrafish are also useful in testing neurodevelopmental toxicity of small molecules. Additionally, I have used morpholinos in zebrafish to knock down calcineurin, whose decreased signaling has been implicated in Down syndrome disease phenotypes. My research displayed developmental brain defects and behavioral defects in the calcineurin morphants, potentially due to increased apoptosis early in development. This model can also be utilized to test pharmaceuticals that may treat Down syndrome phenotypes. Finally, I used zebrafish as a high-throughput model for the loss and recovery of vertebrate vision. My work showed that zebrafish behavior can be used as a method to detect loss and recovery of larval zebrafish vision in multi-well plates.

This model will be useful in testing compounds to treat human visual diseases, especially those that may be used in conjunction with promising stem cell therapies.

Overall my research has made strides in using zebrafish as a vertebrate model of neurodevelopmental aberrations and potential therapeutic screening of pharmaceutical compounds.

Introduction

As medical technologies continue to advance, it becomes more important to find effective methods to test new medical interventions. Few drugs make it from conception to market, and such failures add to the rising cost of drug development. This need is especially pressing for diseases affecting the nervous system. The brain is one of the most complex organs, consisting of billions of neurons and trillions of connections [1], which makes it extremely difficult to model *in vitro*. In humans, neural development begins at three weeks post conception and continues for at least 20 years, through childhood and adolescence [2]. Although toxicant screening is challenging, it is critical considering the extended period of brain development, which includes several specific periods of sensitivity. Additionally, genetic aberrations may lead to disruption of neural development that can be difficult to treat due to the complexity of the disruption [3–5]. Similarly, more effective testing is needed for age-related brain diseases. As the human population ages and grows, cognitive decline becomes more prevalent and an even more vital area of research. There are a myriad of aging-related, neurodegenerative diseases, such as Amyotrophic Lateral Sclerosis (ALS), Alzheimer’s Disease, and dementia [6–8]. For these reasons, an effective *in vivo* model system to study the complexities of brain development and aging is essential. The zebrafish (*Danio rerio*) has become a popular model for screening drugs and modeling human disease, as will be discussed in this dissertation.

Zebrafish as a model to study brain development and behavior

With recent advances in genome sequencing and genetic technology, zebrafish have become an outstanding vertebrate model to research human disease. Zebrafish develop quite rapidly, allowing a view of vertebrate development on a shorter time scale than most traditional vertebrate model organisms. At fertilization, the zygote is composed of a single cell sitting atop the yolk and enveloped by the chorion [9]. The first cell division takes 30 to 45 minutes and the following cleavages occur at approximately 15-minute intervals. At approximately 6 hours post fertilization (hpf), gastrulation occurs and the body plan begins to take shape. By 24hpf (Fig 1a), the embryo has a distinct body plan with a beating heart, prominent eyes and a prototype vertebrate brain with different brain regions [10]. At this stage, embryos will twitch within their chorion and sensory response circuits start to become evident [10]. By 3 days post fertilization (dpf) (Fig 1c) the embryos have hatched from the chorion and although no metamorphosis occurs, they are now termed larvae [11]. At 3dpf, the zebrafish larvae can swim freely within water and will show more robust response to light, touch, and sound. By 5dpf (Fig 1e), the swim bladder of the larvae is inflated and while the yolk sac is still present, the larvae will forage for food and display robust behavior in response to visual stimuli and sound [12,13]. Zebrafish reach sexual maturity at 2 to 3 months post fertilization and can be used as breeders to spawn additional embryos.

Zebrafish offer many advantages over traditional vertebrate models of genetics and development. One small tank of fish can produce hundreds of fertilized embryos daily, allowing for fast and easy collection of many fish. Zebrafish embryos develop externally, are transparent and are quick to develop, growing from one cell to a patterned

body with a beating heart in the span of one day. They are perfect for screening of small molecules as they can be treated by immersing the developing embryos into a bath of the compound. Additionally, zebrafish display robust and replicable stereotyped behaviors starting at 5dpf. These factors make zebrafish ideal for high-throughput use to model human disease, developmental sensitivities, and to screen potential treatments.

Many techniques have been developed for studying brain development and behavior *in vivo* during zebrafish development [12,14–18]. Since the larvae are transparent, transgenic lines that express fluorescent proteins in the brain are a favorite tool among researchers. Standard fluorescent lines, such as GFP under the post-mitotic neuron promoter *elavl3*, allow researchers to assess size and shape of the brain *in vivo* during development (Fig 2). Additionally, many high-throughput methods to assess zebrafish brain development involve testing behavioral profiles [19,20]. While this does not exactly illuminate what is structurally wrong in the brain, it provides insight into subtler functional defects. These behavioral profiles can be used to test small molecule compounds, and it is known that compounds affecting the same subtypes of neurons will show similar behavioral profiles [13,19]. More recent technologies have allowed the imaging of zebrafish brain activity in larvae during specific behaviors [21,22].

Zebrafish as a model of human disease and toxicology

Zebrafish have 25 chromosomes and in the most recent whole genome sequence showed that 71.4% of human protein coding genes have at least one zebrafish ortholog [23]. The orthology between human and zebrafish genes was determined through the use of EnsemblCompara Genetrees [24] to compare protein coding sequences of the

genomes. The similarity between human and zebrafish genomes make zebrafish a great model for testing human genetic disorders. Shared receptors and pathways make zebrafish a useful model to test toxicity of pharmaceutical compounds [20,25–27]. These tests can offer advanced and valuable insight into how such molecules might alter human development, including neurodevelopment, since these molecules will target the orthologous receptors in zebrafish.

Small molecules, including pharmaceuticals, are commonly found as contaminants in the environment [19,28]. It is important to have an efficient way to test the potential impact on both human and animal development to know how better to assess and mitigate the risks associated with these compounds. Testing these compounds in zebrafish has emerged as an efficient method of assessing how they may alter development [16,19,29]. Not only are zebrafish good models to test how environmental toxicants may alter the development of the affected aquatic organisms, but they are also useful as a model of human development since there are common developmental pathways between humans and zebrafish [23,26,30]. Humans may be exposed to compounds during development due to contact with toxicants present in the environment or due to the mother taking medications that can cross the placenta. Zebrafish are especially useful as a method to test compounds that are not widely used during fetal development as there may not be enough effected individuals to generate enough interest to fund traditional developmental toxicity studies.

Developmental toxicity of immunosuppressant drugs

Immunosuppressant drugs have revolutionized the field of transplant medicine. The first immunosuppressant drugs were natural products isolated from fungi [31,32]. Prior to the discovery of immunosuppressant drugs patients required an exact match to receive solid organs, which was exceptionally rare. Once immunosuppressant drugs were discovered, slight mismatches were permitted between the patient and the donor, allowing these lifesaving procedures to become more common [33]. Two frequently used immunosuppressant drugs are cyclosporine and tacrolimus (FK506). Cyclosporine and tacrolimus both need to bind to an accessory immunophilin (cyclophilin A for cyclosporine, or FK506 binding protein (FKBP) for FK506) to actively suppress the immune system [34]. These immunosuppressant-immunophilin complexes can then inhibit the serine/threonine phosphatase calcineurin to suppress immune system activation [35].

In normal functioning T-cells, calcineurin would dephosphorylate a transcription factor called the Nuclear Factor of Activated T-cells or NFAT (Fig 3). Dephosphorylation of NFAT leads to a conformational change that unveils a nuclear localization signaling, allowing NFAT to be translocated to the nucleus where it can activate a transcriptional cascade [36,37]. This conformational change also gives NFAT a higher affinity for DNA [38]. NFAT activation is crucial for T-cell function and by inhibiting calcineurin, a patient's immune system is suppressed and will not reject the transplanted organ. While these compounds are used to suppress the immune system, they also block calcineurin phosphatase activity indiscriminately [34], which may lead to drug side effects.

Many studies have focused on the adverse effects of cyclosporine on patients, which have linked cyclosporine to effects such as nephrotoxicity, hepatotoxicity, neurotoxicity, and cardiotoxicity [39]. While cyclosporine has been shown to be potentially harmful to an adult, the research on the potential role of cyclosporine in a developing fetus has been sparse. Its role in development is especially important as cyclosporine can cross the placenta and affect the fetus if the mother is prescribed it while pregnant [40]. Studies that examined the effects of cyclosporine during development have shown that it negatively effects the development of the hepatic, nephritic, cardiovascular, and neuronal systems [41–44].

Transplant patients will need to take immunosuppressants throughout their lives. As a result, if a woman who had an organ transplant became pregnant, her fetus would be exposed to these same drugs. Cyclosporine and tacrolimus are considered Class C Drugs by the FDA, meaning that not much is known about their developmental risks, but that their benefits (i.e. avoiding organ rejections) outweigh the known risks [45,46]. Zebrafish provide an excellent model for testing possible consequences of taking immunosuppressant drugs during pregnancy. It was recently discovered that there are sensitive periods of cyclosporine exposure during development [47], the results of which show the importance of assessing the developmental risks associated with these compounds. While transplant patients cannot stop immunosuppressant treatment, it is essential for family planning purposes that parents are informed of the potential risks of taking immunosuppressants during pregnancy.

Calcineurin/NFAT signaling

Calcineurin is a calcium dependent, serine/threonine phosphatase that is part of the protein phosphatase p family of phosphatases [48]. Calcineurin is composed of a catalytic (or A) subunit and a regulatory (or B) subunit (Fig 3), and remains inactive until it forms a heterotrimer with calmodulin [49]. Substrates dock to calcineurin through two known binding motifs: the PxIxIT motif, which has a docking area on the calcineurin A subunit [50,51]; and the more recently discovered LxVP motif, which docks at the interface between calcineurin A and B subunits [51,52]. Since the active site of calcineurin shows nonspecific phosphatase activity, the docking sites on calcineurin have been implicated in determining substrate specificity.

NFATs are a family of transcription factors that are known enzymatic targets of calcineurin [48,53]. There are five known members of the NFAT family, four of which are regulated by calcineurin: NFATc1, NFATc2, NFATc3, and NFATc4 [53]. There are many mechanisms by which calcineurin/NFAT signaling can be regulated in normally functioning cells. One way is to regulate the amount of calcium in the cytoplasm [34,54]. Additionally, calcineurin enzymatic activity can be inhibited by various proteins in the cell. The regulator of calcineurin (RCAN), a Kinase Anchoring Protein 79 (AKAP79), and Calcineurin Binding Protein 1 (Cabin1) all contain PxIxIT motifs that interact with calcineurin to directly inhibit its activity by outcompeting substrates [55–57]. Finally, this signaling pathway can be regulated via modulation of NFAT phosphorylation. Kinases in the cytoplasm and the nucleus act to keep NFATs in their hyperphosphorylated states. Kinases such as casein kinase 1 (CK1), glycogen-synthase kinase 3 (GSK3), and dual-specificity tyrosine-phosphorylation-regulated kinase 1A (DYRK1A) are responsible for

phosphorylating NFATs in the nucleus to deactivate NFAT activity and mark the NFAT for nuclear export [58–60]. These multiple layers of control over calcineurin/NFAT signaling allow for precise regulation of calcineurin/NFAT signaling during development.

Calcineurin in the nervous system

Although calcineurin has been extensively studied in the immune system, it was first identified in the brain and calcineurin has been reported to compose approximately 1% of all the protein in the brain [61]. Studies in cell culture have shown that calcineurin has a variety of roles throughout neuronal development [62–66]. Mouse neural progenitor cell culture research has indicated that calcineurin/NFAT signaling plays roles in survival, proliferation, and differentiation of these cells [62]. In mouse embryonic stem cells, calcineurin signaling may trigger neural induction via direct silencing by dephosphorylating the Smad1/5 transcription factors, which are required for neural induction [63]. Calcineurin has also been shown to play a role neuronal survival and axonal guidance [64,65]. In addition, calcineurin has a possible role in signaling in Down syndrome [67,68].

Down syndrome is a neurodevelopmental syndrome in humans, is caused by the presence of an extra copy of the 21st chromosome. Two genes on the 21st chromosome, DYRK1A and DSCR1, are regulators of calcineurin signaling. DYRK1A, a kinase located in the nucleus, can phosphorylate NFAT, beginning the process that exports NFAT from the nucleus [67]. DSCR1 (also called RCAN) is a direct inhibitor of calcineurin signaling. DSCR1 inhibits calcineurin by competing for binding to the PxxIT

motif on calcineurin [69], which is different from CsA and FK506 interactions with the LxVP site-binding pocket. Currently it is unknown which, if any, of the phenotypes of Down syndrome are associated with the 1.5 fold over-expression of these genes (effectively inhibiting calcineurin signaling). What has been shown is that that these genes alone are sufficient for delayed neuronal differentiation and certain behavioral phenotypes in mice [67,68]. This evidence has directed research towards the role of calcineurin in brain development.

Overview of the retina

The human eye is a complex organ that can sense light and translate that signal into a picture of the world. The light sensing ability of the eye is due to photoreceptors in the retina. Two types of photoreceptors are present in the retina: rods and cones [70]. Rods function best in low light conditions and lack any color information [71]. Cones are functional in bright light conditions and are responsible for high-acuity color vision [71,70]. Humans have trichromatic vision, meaning that the human eye has three types of cones that each sense a different color of light. These colors are red, green and blue [72].

Eye diseases

Visual impairments affect 285 million people worldwide, 39 million of which are blind and 246 million have low vision [73]. These diseases are especially concerning as the population ages and becomes more susceptible to diseases like glaucoma, cataracts, macular degeneration, and diabetic retinopathy [74]. The National Eye Institute has projected that the number of Americans over the age of 40 who have low vision or

blindness will increase by over 300%, from 4 million to 13 million by the year 2050. In the past decade, substantial progress has been made in ocular surgery and it may eventually be possible to restore vision by regenerating neural connections in the visual system. It was recently reported that a stem cell based therapy was successful in restoring vision in patients affected by age-related macular degeneration [75]. This successful phase 1 clinical trial is an exciting step towards treatment of visual diseases in humans.

Zebrafish as a model to examine the loss and recovery of vision

Zebrafish are ideally suited to study retinal regeneration and disease. For one, zebrafish have the innate ability to regenerate their retina [76,77], allowing researchers to interrogate the factors that are involved in such regeneration. Previously, mice have been used as a model used to examine retinal regeneration as they also have regenerative capacity [78]. However, mice are adapted for low light conditions with rod-dominated retina, in opposition to human vision which is adapted for bright light conditions [79,80]. Their vision is also dichromatic, meaning they only have two color sensing cones (red and green) [80,81]. Zebrafish are adapted for bright light environments with cone-dominated retina and tetrachromatic vision, including three cones homologous to humans and an additional cone sensitive to UV light [82,83]. The presence of red, green, and blue light sensing cones and a cone-dominated retina make zebrafish great models for human vision. Researchers have also taken advantage of their visual behaviors to assess loss and recovery of vision in zebrafish. Previous studies have used the optokinetic response (OKR) [18,84], optomotor response (OMR) [85,86], responses to light [16,87], and response to directed visual stimuli [12] as high-throughput ways to assess zebrafish

vision. This combination of factors allows research on zebrafish to be an effective tool for assessing degenerative eye diseases. With the increased research in stem cell therapies and the first successful phase 1 clinical trial [75] to treat retinal diseases, zebrafish models of retinal regeneration will also offer a high-throughput method for testing potential stem cell treatment co-therapies.

Overview of thesis research

In this dissertation, I will describe how we have used zebrafish as a model to test neurotoxicity, neurodevelopmental diseases, and regeneration. I will discuss how we examined the effects of immunosuppressant drugs on the developing brain (Chapter 2), how we modeled calcineurin inhibition to gain insights into Down syndrome (Chapter 3), and how we updated our behavioral assay to detect the loss and recovery of vision using zebrafish (Chapter 4). These studies together show how zebrafish can be useful in modeling human neurobiology, and how such models can be useful in testing and discovering potential therapies for human disorders.

References:

1. Pakkenberg B, Gundersen HJG. Neocortical Neuron Number in Humans : 1997; **320**:312–320.
2. Stiles J, Jernigan TL. The basics of brain development. *Neuropsychol Rev* 2010; **20**:327–348.
3. Meshalkina DA, N. Kizlyk M, V. Kysil E, *et al.* Zebrafish models of autism spectrum disorder. *Exp Neurol* 2018; **299**:207–216.
4. Bathelt J, Astle D, Barnes J, Raymond FL, Baker K. Structural brain abnormalities in a single gene disorder associated with epilepsy, language impairment and intellectual disability. *NeuroImage Clin* 2016; **12**:655–665.
5. Homberg JR, Kyzar EJ, Stewart AM, *et al.* Improving treatment of neurodevelopmental disorders: recommendations based on preclinical studies. *Expert Opin Drug Discov* 2016; **11**:11–25.
6. C. Reese L, Tagliatalata G. A Role for Calcineurin in Alzheimers Disease. *Curr Neuropharmacol* 2011; **9**:685–692.
7. Tagliatalata G, Rastellini C, Cicalese L. Reduced Incidence of Dementia in Solid Organ Transplant Patients Treated with Calcineurin Inhibitors. *J Alzheimer's Dis* 2015; **47**:329–333.
8. Kipanyula MJ, Kimaro WH, Etet PFS. The Emerging Roles of the Calcineurin-Nuclear Factor of Activated T-Lymphocytes Pathway in Nervous System Functions and Diseases. *J Aging Res* 2016; **2016**.
9. Kimmel CB, Ballard WW, Kimmel SR, Ullmann B, Schilling TF. Stages of embryonic development of the zebrafish. *Dev Dyn* 1995; **203**:253–310.
10. Kimmel CB, Ballard WW, Kimmel SR, Ullmann B, Schilling TF. Stages of embryonic development of the zebrafish. *Dev Dyn* 1995; **203**:253–310.
11. Westerfield M. *The zebrafish book. A guide for the laboratory use of zebrafish (Danio rerio)*. 4th Editio. Eugene: Univ. of Oregon Press; 2007.
12. Thorn RJ, Clift DE, Ojo O, Colwill RM, Creton R. The loss and recovery of vertebrate vision examined in microplates. *PLoS One* 2017; **12**:e0183414.
13. Bruni G, Rennekamp AJ, Velenich A, *et al.* Zebrafish behavioral profiling identifies multitarget antipsychotic-like compounds. *Nat Chem Biol* 2016; **12**:559–566.
14. Colwill RM, Creton R. Imaging escape and avoidance behavior in zebrafish larvae. *Rev Neurosci* 2011; **22**:63–73.
15. Scott CA, Marsden AN, Slusarski DC. Automated, high-throughput, in vivo analysis of visual function using the zebrafish. *Dev Dyn* 2016; **245**:605–613.
16. Rihel J, Prober D a, Arvanites A, *et al.* Zebrafish behavioral profiling links drugs to biological targets and rest/wake regulation. *Science* 2010; **327**:348–51.
17. Orger MB, Smear MC, Anstis SM, Baier H. Perception of Fourier and non-Fourier motion by larval zebrafish. *Nat Neurosci* 2000; **3**:1128–1133.
18. Brockerhoff SE, Hurley JB, Janssen-Bienhold U, Neuhauss SC, Driever W, Dowling JE. A behavioral screen for isolating zebrafish mutants with visual system defects. *Proc Natl Acad Sci U S A* 1995; **92**:10545–9.
19. Richendrfer H, Creton R. Cluster analysis profiling of behaviors in zebrafish larvae treated with antidepressants and pesticides. *Neurotoxicol Teratol* 2017.
20. Bruni G, Rennekamp AJ, Velenich A, *et al.* Zebrafish behavioral profiling identifies

- multitarget antipsychotic-like compounds. *Nat Chem Biol* 2016; **12**:559–566.
21. Kim DH, Kim J, Marques JC, *et al.* Pan-neuronal calcium imaging with cellular resolution in freely swimming zebrafish. *Nat Methods* 2017; **14**:1107–1114.
 22. Ahrens MB, Li JM, Orger MB, *et al.* Brain-wide neuronal dynamics during motor adaptation in zebrafish. *Nature* 2012; **485**:471–7.
 23. Howe K, Clark MD, Torroja CF, *et al.* The zebrafish reference genome sequence and its relationship to the human genome. *Nature* 2013; **496**:498–503.
 24. Vilella AJ, Severin J, Ureta-Vidal A, Heng L, Durbin R, Birney E. EnsemblCompara GeneTrees: Complete, duplication-aware phylogenetic trees in vertebrates. *Genome Res* 2009; **19**:327–335.
 25. Wolman MA, Jain RA, Liss L, Granato M. Chemical modulation of memory formation in larval zebrafish. *Proc Natl Acad Sci* 2011; **108**:15468–15473.
 26. Wolman M, Granato M. Behavioral genetics in larval zebrafish: learning from the young. *Dev Neurobiol* 2012; **72**:366–72.
 27. Baraban SC, Dinday MT, Hortopan GA. Drug screening in Scn1a zebrafish mutant identifies clemizole as a potential Dravet syndrome treatment. *Nat Commun* 2013; **4**:1–10.
 28. Ali S, Champagne DL, Richardson MK. Behavioral profiling of zebrafish embryos exposed to a panel of 60 water-soluble compounds. *Behav Brain Res* 2012; **228**:272–283.
 29. Kokel D, Bryan J, Laggner C, *et al.* Rapid behavior-based identification of neuroactive small molecules in the zebrafish. *Nat Chem Biol* 2010; **6**:231–237.
 30. Rinkwitz S, Mourrain P, Becker TS. Zebrafish: an integrative system for neurogenomics and neurosciences. *Prog Neurobiol* 2011; **93**:231–243.
 31. Kahan BD. Cyclosporine: the agent and its actions. *Transplant Proc* 1985; **17**:5–18.
 32. Ochiai T, Nakajima K, Nagata M, *et al.* Effect of a new immunosuppressive agent, FK 506, on heterotopic cardiac allotransplantation in the rat. *Transplant Proc* 1987; **19**:1284–6.
 33. Azzi JR, Sayegh MH, Mallat SG. Calcineurin inhibitors: 40 years later, can't live without. *J Immunol* 2013; **191**:5785–5791.
 34. Hogan PG, Chen L, Nardone J, Rao A. Transcriptional regulation by calcium, calcineurin, and NFAT. *Genes Dev* 2003; **17**:2205–32.
 35. Barbarino JM, Staats CE, Venkataramanan R, Klein TE, Altman RB. PharmGKB summary: cyclosporine and tacrolimus pathways. *Pharmacogenet Genomics* 2013; **23**:563–85.
 36. Ruff VA, Leach KL. Direct demonstration of NFATp dephosphorylation and nuclear localization in activated HT-2 cells using a specific NFATp polyclonal antibody. *J Biol Chem* 1995; **270**:22602–22607.
 37. Shaw KT, Ho AM, Raghavan A, *et al.* Immunosuppressive drugs prevent a rapid dephosphorylation of transcription factor NFAT1 in stimulated immune cells. *Proc Natl Acad Sci U S A* 1995; **92**:11205–11209.
 38. Loh C, Shaw KT, Carew J, *et al.* Calcineurin binds the transcription factor NFAT1 and reversibly regulates its activity. *J Biol Chem* 1996; **271**:10884–91.
 39. Rezzani R. Cyclosporine A and adverse effects on organs: histochemical studies. *Prog Histochem Cytochem* 2004; **39**:85–128.
 40. Flechner SM, Katz AR, Rogers AJ, Van Buren C, Kahan BD. The presence of cyclosporine in body tissues and fluids during pregnancy. *Am J Kidney Dis* 1985; **5**:60–3.

41. Rezzani R, Rodella L, Bianchi R. Cyclosporine and pregnancy in the rat. *Transplantation* 1997; **63**:164–7.
42. Tendron A, Decramer S, Justrabo E, Gouyon J-B, Semama DS, Gilbert T. Cyclosporin A administration during pregnancy induces a permanent nephron deficit in young rabbits. *J Am Soc Nephrol* 2003; **14**:3188–96.
43. Beis D, Bartman T, Jin S-W, *et al.* Genetic and cellular analyses of zebrafish atrioventricular cushion and valve development. *Development* 2005; **132**:4193–204.
44. Uhing MR, Goldman AS, Goto MP. Cyclosporin A-induced embryopathy in embryo culture is mediated through inhibition of the arachidonic acid pathway. *Proc Soc Exp Biol Med* 1993; **202**:307–14.
45. FDA. U.S. Food and Drug Administration. CFR - Code of Federal Regulations Title 21. <http://www.accessdata.fda.gov/scripts/cdrh/cfdocs/cfcfr/CFRSearch.cfm?fr=20157> 2014; (retrieved).
46. Babalola O, Strober BE. Management of psoriasis in pregnancy. *Dermatol Ther* 2013; **26**:285–292.
47. Clift DE, Thorn RJ, Passarelli EA, *et al.* Effects of embryonic cyclosporine exposures on brain development and behavior. *Behav Brain Res* 2015; **282**:117–24.
48. Hemenway CS, Heitman J. Calcineurin. Structure, function, and inhibition. *Cell Biochem Biophys* 1999; **30**:115–51.
49. Guerini D. Calcineurin: not just a simple protein phosphatase. *Biochem Biophys Res Commun* 1997; **235**:271–5.
50. Aramburu J, Garcia-Cózar F, Raghavan a, Okamura H, Rao a, Hogan PG. Selective inhibition of NFAT activation by a peptide spanning the calcineurin targeting site of NFAT. *Mol Cell* 1998; **1**:627–37.
51. Rodríguez A, Roy J, Martínez-Martínez S, *et al.* A conserved docking surface on calcineurin mediates interaction with substrates and immunosuppressants. *Mol Cell* 2009; **33**:616–26.
52. Liu J, Masuda ES, Tsuruta L, Arai N, Arai K. Two independent calcineurin-binding regions in the N-terminal domain of murine NF-ATx1 recruit calcineurin to murine NF-ATx1. *J Immunol* 1999; **162**:4755–61.
53. Macian F. NFAT proteins: Key regulators of T-cell development and function. *Nat Rev Immunol* 2005; **5**:472–484.
54. Ramachandran K V, Hennessey JA, Barnett AS, *et al.* Calcium influx through L-type CaV1.2 Ca²⁺ channels regulates mandibular development. *J Clin Invest* 2013; **123**:1638–46.
55. Li H, Pink MD, Murphy JG, Stein A, Dell'Acqua ML, Hogan PG. Balanced interactions of calcineurin with AKAP79 regulate Ca²⁺-calcineurin-NFAT signaling. *Nat Struct Mol Biol* 2012; **19**:337–45.
56. Sun L, Youn HD, Loh C, Stolow M, He W, Liu JO. Cabin 1, a negative regulator for calcineurin signaling in T lymphocytes. *Immunity* 1998; **8**:703–711.
57. Aubareda A, Mulero MC, Pérez-Riba M. Functional characterization of the calcipressin 1 motif that suppresses calcineurin-mediated NFAT-dependent cytokine gene expression in human T cells. *Cell Signal* 2006; **18**:1430–1438.
58. Zhu J, Shibasaki F, Price R, *et al.* Intramolecular masking of nuclear import signal on NF-AT4 by casein kinase I and MEKK1. *Cell* 1998; **93**:851–861.
59. Beals CR, Sheridan CM, Turck CW, Gardner P, Crabtree GR. Nuclear export of NF-

- ATc enhanced by glycogen synthase kinase-3. *Science* (80-) 1997; **275**:1930–1933.
60. Gwack Y, Sharma S, Nardone J, *et al.* A genome-wide *Drosophila* RNAi screen identifies DYRK-family kinases as regulators of NFAT. *Nature* 2006; **441**:646–650.
61. Klee CB, Draetta GF, Hubbard MJ. Calcineurin. *Adv Enzymol Relat Areas Mol Biol* 1988; **61**:149–200.
62. Serrano-Pérez MC, Fernández M, Neria F, *et al.* NFAT transcription factors regulate survival, proliferation, migration, and differentiation of neural precursor cells. *Glia* 2015; **63**:987–1004.
63. Cho A, Tang Y, Davila J, *et al.* Calcineurin signaling regulates neural induction through antagonizing the BMP pathway. *Neuron* 2014; **82**:109–124.
64. Graef I a, Wang F, Charron F, *et al.* Neurotrophins and netrins require calcineurin/NFAT signaling to stimulate outgrowth of embryonic axons. *Cell* 2003; **113**:657–70.
65. Hui KKW, Liadis N, Robertson J, Kanungo A, Henderson JT. Calcineurin inhibition enhances motor neuron survival following injury. *J Cell Mol Med* 2010; **14**:671–86.
66. Baumgärtel K, Mansuy IM. Neural functions of calcineurin in synaptic plasticity and memory. *Learn Mem* 2012; **19**:375–84.
67. Arron JR, Winslow MM, Polleri A, *et al.* NFAT dysregulation by increased dosage of DSCR1 and DYRK1A on chromosome 21. *Nature* 2006; **441**:595–600.
68. Kurabayashi N, Sanada K. Increased dosage of DYRK1A and DSCR1 delays neuronal differentiation in neocortical progenitor cells. *Genes Dev* 2013; **27**:2708–21.
69. Martínez-Martínez S, Genescà L, Rodríguez A, *et al.* The RCAN carboxyl end mediates calcineurin docking-dependent inhibition via a site that dictates binding to substrates and regulators. *Proc Natl Acad Sci U S A* 2009; **106**:6117–22.
70. Kefalov VJ. Rod and cone visual pigments and phototransduction through pharmacological, genetic, and physiological approaches. *J Biol Chem* 2012; **287**:1635–1641.
71. Kawamura S, Tachibanaki S. Rod and cone photoreceptors: Molecular basis of the difference in their physiology. *Comp Biochem Physiol - A Mol Integr Physiol* 2008; **150**:369–377.
72. Bowmaker JK, Dartnall HJ. Visual pigments of rods and cones in a human retina. *J Physiol* 1980; **298**:501–511.
73. Pascolini D, Mariotti SP. Global estimates of visual impairment: 2010. *Br J Ophthalmol* 2012; **96**:614–618.
74. Voleti VB, Hubschman JP. Age-related eye disease. *Maturitas* 2013; **75**:29–33.
75. da Cruz L, Fynes K, Georgiadis O, *et al.* Phase 1 clinical study of an embryonic stem cell-derived retinal pigment epithelium patch in age-related macular degeneration. *Nat Biotechnol* 2018.
76. Fimbel SM, Montgomery JE, Burket CT, Hyde DR. Regeneration of Inner Retinal Neurons after Intravitreal Injection of Ouabain in Zebrafish. *J Neurosci* 2007; **27**:1712–1724.
77. Bernardos RL, Barthel LK, Meyers JR, Raymond PA. Late-Stage Neuronal Progenitors in the Retina Are Radial Muller Glia That Function as Retinal Stem Cells. *J Neurosci* 2007; **27**:7028–7040.
78. Morrow EM, Furukawa T, Cepko CL. Vertebrate photoreceptor cell development and disease. *Trends Cell Biol* 1998; **8**:353–358.

79. Bilotta J, Saszik S, Sutherland SE. Rod contributions to the electroretinogram of the dark-adapted developing zebrafish. *Dev Dyn* 2001; **222**:564–70.
80. Bibliowicz J, Tittle RK, Gross JM. *Toward a better understanding of human eye disease: Insights from the zebrafish, Danio rerio*. 1st ed. Elsevier Inc.; 2011.
81. Hoon M, Okawa H, Della Santina L, Wong ROL. Functional architecture of the retina: development and disease. *Prog Retin Eye Res* 2014; **42**:44–84.
82. Gestri G, Link BA, Neuhauss SC. The Visual System of Zebrafish and its Use to Model Human Ocular Diseases. *Dev Neurobiol* 2013; **72**:302–327.
83. Chhetri J, Jacobson G, Gueven N. Zebrafish-on the move towards ophthalmological research. *Eye* 2014; **28**:367–380.
84. Easter SS, Nicola GN. The development of vision in the zebrafish (*Danio rerio*). *Dev Biol* 1996; **180**:646–663.
85. Neuhauss SC, Biehlmaier O, Seeliger MW, *et al*. Genetic disorders of vision revealed by a behavioral screen of 400 essential loci in zebrafish. *J Neurosci* 1999; **19**:8603–8615.
86. Orger MB, Baier H. Channeling of red and green cone inputs to the zebrafish optomotor response. *Vis Neurosci* 2005; **22**:275–281.
87. Emran F, Rihel J, Dowling JE. A Behavioral Assay to Measure Responsiveness of Zebrafish to Changes in Light Intensities. *J Vis Exp* 2008:1–6.

Figures:



Figure 1. Overview of zebrafish development. Scanning electron microscopy of zebrafish at 1dpf (a), 2dpf (b), 3dpf (c), 4dpf (d), 5dpf (e) and 7dpf (f).

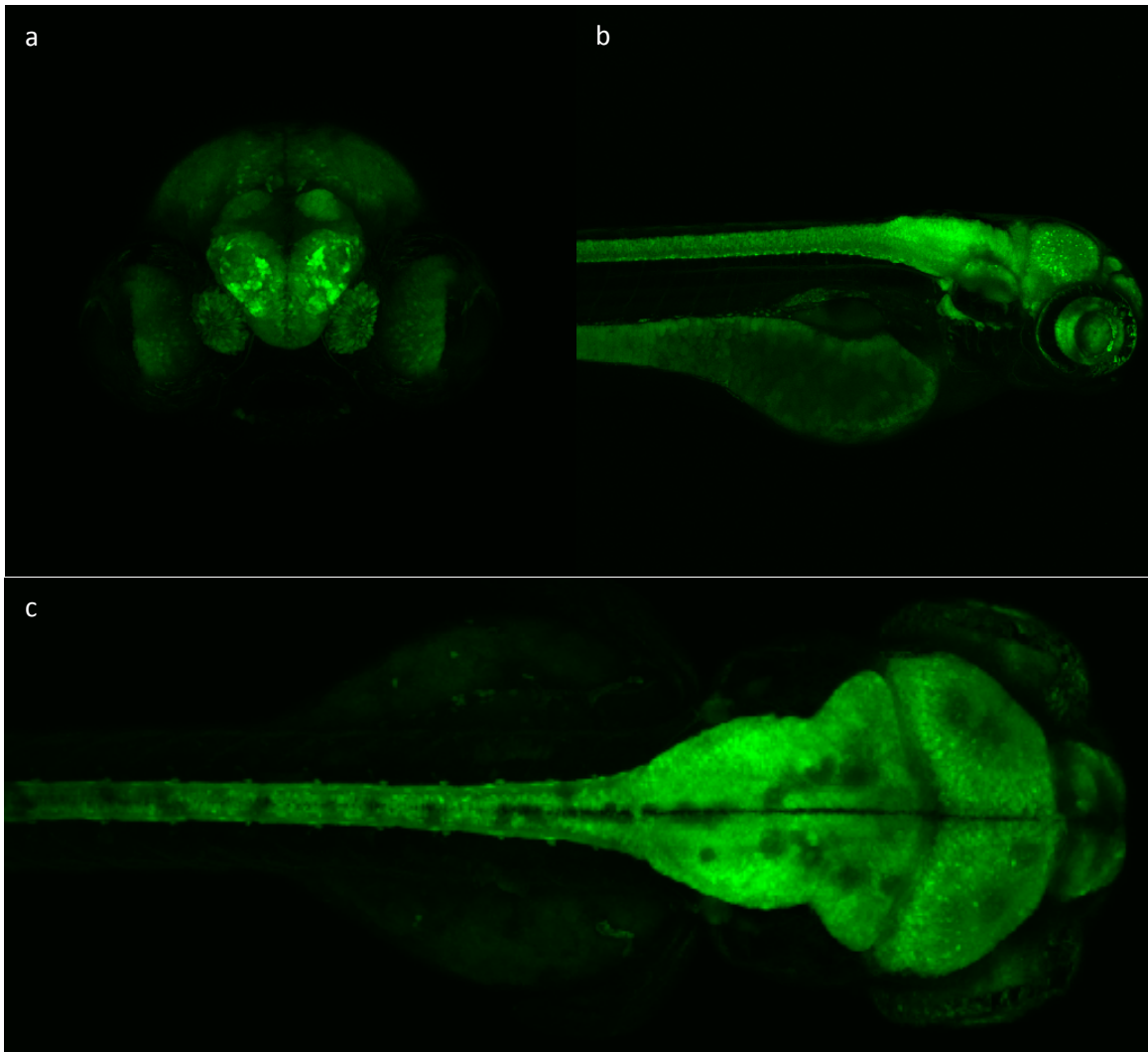


Figure 2. Zebrafish brain at 3 days post fertilization. Transgenic zebrafish expressing GFP under the *elavl3* promoter imaged at 3 dpf by confocal microscopy. Maximum z-projections shown for an anterior view (a), lateral view (b) and dorsal view (c). Adapted from Clift et al. (2015) [47].

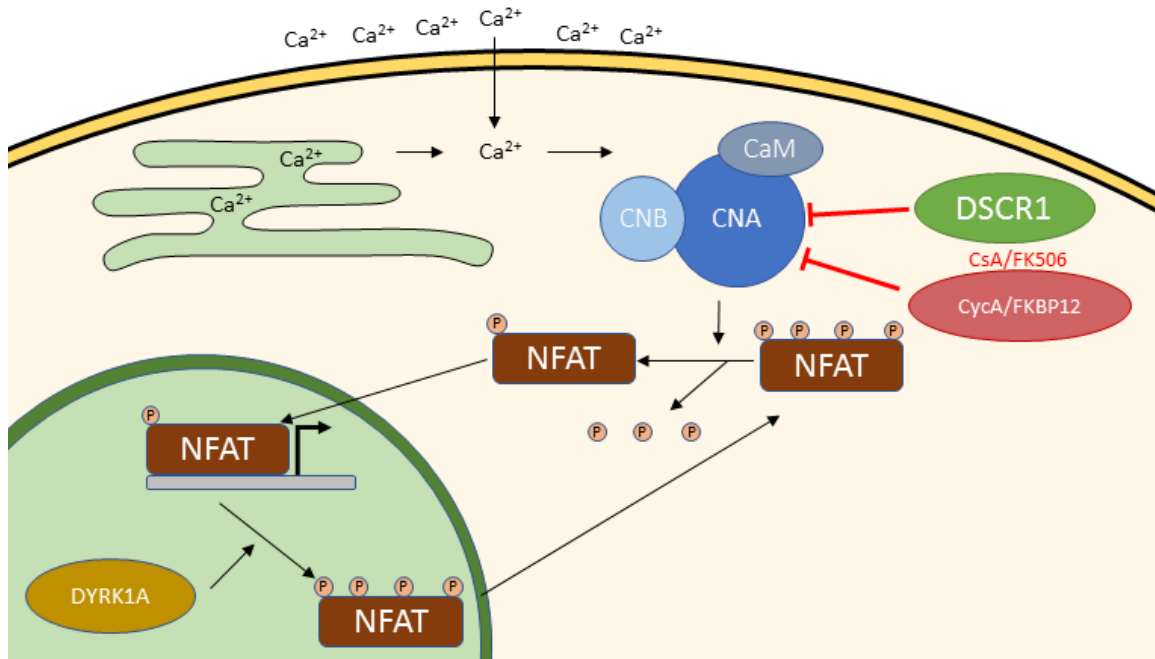


Figure 3. Model of the Calcineurin signaling pathway. Calcineurin is activated by intracellular free calcium (Ca^{2+}). Once activated Calcineurin dephosphorylates the nuclear factor of activated T cells (NFAT), which undergoes a conformation change, exposing a nuclear localization signal. NFAT then translocates into the nucleus where it acts as a transcription factor. Calcineurin can be inhibited by the regulator of Calcineurin, DSCR1, or by immunosuppressant drugs such as cyclosporine (CsA) or FK506 in complex with immunophilins (CyclophilinA [CycA] or FK506 binding protein 12 [FKBP12]). DYRK1A inhibits the Calcineurin-NFAT pathway by phosphorylating NFAT which leads to the nuclear export of p-NFAT. CNB= Regulatory subunit (ppp3r), CNA= Catalytic subunit (ppp3c).

Chapter 2: Effects of embryonic cyclosporine exposures on brain development and behavior

Clift, D. E., **Thorn, R. J.**, Passarelli, E. A., Kapoor, M., LoPiccolo, M. K., Richendrfer, H. A., Colwill, R.M., Creton, R. (2015). Effects of embryonic cyclosporine exposures on brain development and behavior. *Behavioural Brain Research*, 282, 117–124.
<https://doi.org/10.1016/j.bbr.2015.01.006>

I assisted in the design and performance of the cyclosporine and FK506 experiments, analyzed the results and wrote the results and discussion of the manuscript.

Abstract

Cyclosporine, a calcineurin inhibitor, is successfully used as an immunosuppressant in transplant medicine. However, the use of this pharmaceutical during pregnancy is concerning, since calcineurin is thought to play a role in neural development. The risk for human brain development is difficult to evaluate, because of a lack of basic information on the sensitive developmental times and the potentially pleiotropic effects on brain development and behavior. In the present study, we use zebrafish as a model system to examine the effects of embryonic cyclosporine exposures. Early embryonic exposures reduced the size of the eyes and brain. Late embryonic exposures did not affect the size of the eyes or brain but did lead to substantial behavioral defects at the larval stages. The cyclosporine-exposed larvae displayed a reduced avoidance response to visual stimuli, low swim speeds, increased resting, an increase in thigmotaxis, and changes in the average distance between larvae. Similar results were obtained with the calcineurin inhibitor FK506, suggesting that most, but not all, effects on brain development and behavior are mediated by calcineurin inhibition. Overall, the results show that cyclosporine can induce either structural or functional brain defects, depending on the exposure window. The observed functional brain defects highlight the importance of quantitative behavioral assays when evaluating the risk of developmental exposures.

Keywords: Zebrafish, brain, behavior, calcineurin, cyclosporine, cyclosporin

Introduction

The discovery of cyclosporine A as an immunosuppressive drug has revolutionized the field of transplant medicine, allowing allograft organ transplants to become commonplace [1]. Cyclosporine acts as an immunosuppressant by inhibiting calcineurin, a calcium-dependent protein phosphatase that plays a critical role in T-cell activation [2,3]. By inhibiting calcineurin and suppressing T-cell activation, cyclosporine effectively reduces the rate of transplant rejection. Following its success in transplant medicine, cyclosporine has been used for the treatment of a wide variety of autoimmune diseases, including psoriasis and rheumatoid arthritis [3].

Cyclosporine is classified as a pregnancy category C drug by the United States Food and Drug Administration [4]. In Pregnancy Category C, 'animal reproduction studies have shown an adverse effect on the fetus, there are no adequate and well-controlled studies in humans, and the benefits from the use of the drug in pregnant women may be acceptable despite its potential risks; or animal studies have not been conducted and there are no adequate and well-controlled studies in humans' [5,6]. The labeling of Category C pharmaceuticals must state that the drug 'should be used during pregnancy only if the potential benefit justifies the potential risk to the fetus' or 'should be given to a pregnant women only if clearly needed' [5]. Immunosuppressants are clearly needed in transplant medicine to prevent organ rejection and as a result cyclosporine treatment is continued during pregnancy despite the potential risk to the developing fetus [7]. The use of cyclosporine during pregnancy is concerning, since calcineurin is thought to play a role in

neural development and axonal growth [8]. However, the risk for human brain development is difficult to evaluate, because of a lack of basic information on the sensitive developmental times and the potentially pleiotropic effects on brain development and behavior. Models of ‘critical periods’ in human development predict that different types of defects may be induced depending on the exposure window [9], i.e. early developmental exposures can lead to major structural brain defects, while late developmental exposures are likely to induce more subtle or functional brain defects (Fig 1).

In the current study, we examine the effects of cyclosporine on brain development and behavior using zebrafish as a model system. The signaling pathways that regulate brain development and neural function are conserved in vertebrate species [10,11] and the zebrafish has emerged as a powerful model system in behavioral neuroscience [12–14]. Hundreds of synchronously developing embryos can be collected from the bottom of a tank on a daily basis and exposures can be carried out in a culture dish. The embryos are transparent, which makes it possible to image the developing brain in living embryos using various state-of-the-art molecular tools [15–17]. Zebrafish embryos develop rapidly. At 24 hours post-fertilization (hpf), the embryos have a beating heart, a moving tail, two large eyes, and a brain with distinct brain regions [18]. The embryos hatch from their chorion between 2 and 3 days post-fertilization (dpf). At 5 dpf, the free-swimming larvae are approximately 4 mm long, have inflated swim bladders, and display a broad range of behaviors, which can be examined in multiwell or multilane plates [19–25].

In the present study, zebrafish embryos were exposed to cyclosporine during different stages in embryonic development. We found that early embryonic exposures led to a reduction in eye and brain size. Late embryonic exposures did not affect the size of the eyes and brain, but did lead to significant behavioral defects.

Materials and Methods

Zebrafish embryos and exposures. Adult wild type zebrafish (*Danio rerio*) were originally obtained from Carolina Biological and have been maintained at Brown University as a genetically diverse outbred strain. For the analysis of structural brain defects, we used the *Tg(elavl3:EGFP)* line, which expresses the enhanced green fluorescent protein under control of a ubiquitous neuronal promoter [26]. Zebrafish embryos were collected within one hour after spawning and raised at 28.5°C in egg water, containing 60 mg/L sea salt (Instant Ocean) in deionized water and 0.25 mg/L methylene blue as a fungal inhibitor. Cyclosporine (cyclosporin A, Enzo Life Sciences) and FK506 (tacrolimus, Enzo Life Sciences) were diluted in egg water from 1000x stocks dissolved in dimethylsulfoxide (DMSO). The corresponding DMSO concentration (0.1% DMSO) was used as a control. Embryos were exposed from 2-26 hours post-fertilization (hpf), 26-50 hpf, or 50-74 hpf, washed four times in egg water, and grown in egg water for up to 5 days post-fertilization (dpf). The developing zebrafish are referred to as ‘embryos’ from 0-3 dpf and as ‘larvae’ afterwards [27].

Analysis of eye and brain defects. To examine eye size, wild type embryos were imaged at 3 dpf in a ventral view by standard bright-field microscopy on a Zeiss Axiovert 200M microscope, using a 10x objective. The eye length was measured in ImageJ, which can be downloaded at <http://imagej.nih.gov/ij/download.html>. Measurements of the left and right eyes were averaged in Microsoft Excel. These values were subsequently averaged over the number of embryos (n = number of embryos). To examine brain structure, *Tg(elavl3:EGFP)* embryos were imaged at 3 dpf by confocal or wide-field fluorescence microscopy. For confocal microscopy, the embryos were grown from 22-72 hpf in 0.003% 1-phenyl-2-thiourea (PTU) in egg water to suppress pigmentation. The 3 dpf embryos were oriented in 0.8% low-gelling temperature agarose. Neural patterns were imaged on a Leica SP2 AOBS confocal microscope using a 20x objective for a frontal view (transverse sections) or a 10x objective for a dorsal view (coronal sections). Z-stacks of 125 slices were acquired through 150 μ m of the brain using a 2 Airy unit pinhole, a 488 nm laser for excitation, and a 510-600 nm filter. The data sets were examined by collapsing the stacks as maximum projections and by FluidVis 3D visualization [28]. For wide-field fluorescence microscopy, *Tg(elavl3:EGFP)* embryos were imaged at 3 dpf in a dorsal view on a Zeiss Axiovert 200M microscope, using 10x objective and a Hamamatsu ORCA-ER monochrome camera. Larvae were oriented in 2% methyl cellulose in egg water. Forebrain, midbrain, and hindbrain length, width and area were measured in ImageJ.

Head-trunk angles. To examine if embryos display developmental delays, we measured the head-trunk angle as described previously [18]. Embryos were oriented in 2% methyl

cellulose in egg water and imaged in a side view. The angles were measured in ImageJ by drawing a line from the center of the eye to the center of the ear and a second line parallel to the notochord in the mid-trunk region.

Larval morphology. At 5 dpf, wild type larvae were oriented in 2% methyl cellulose in egg water and were imaged by standard bright-field microscopy on a Zeiss Axiovert 200M microscope, using a 5x objective and an AxioCam MRc5 color camera. A white reference image was acquired to avoid gradients in the background. Images from the anterior and posterior halves of the larvae were stitched with Fiji software [29], which can be downloaded at <http://fiji.sc/>. We used a linear blending method developed by Stephan Preibisch [30], which is available in the Fiji software under plugins, stitching, deprecated, 2D stitching by linear blending.

Analysis of behavior. The behavior of wild type zebrafish larvae was analyzed at 5 dpf. The 5 dpf larvae receive nutrients from their yolk sac and effects of feeding can be avoided at this time [21]. The larvae were imaged with a custom-built imaging system, as described previously [24,25]. In summary, the system includes a 15 megapixel Canon EOS Rebel T1i digital camera and an Acer Aspire 5517 laptop with a 15.6 inch screen to provide visual stimuli to the larvae. Larval behavior was examined in a ‘five-lane’ plate, with 5 larvae per lane (25 larvae per plate). The five-lane plate is made using a Nunc 1-well rectangular plate (Fisher 12-565-493), 50 ml of 0.8% agarose in egg water, and a CNC-milled plastic mold [25]. Each lane is 18 mm wide, 70 mm long and 3.5 mm deep

and has 60° sloping edges to avoid shadows and blind spots along the perimeter of the swimming area. The lanes have ample space to examine larval interactions and measure avoidance of aversive visual stimuli. Larvae were first imaged for 15 minutes without visual stimuli and then for 15 minutes in the presence of a moving red bar, which is 1.3 cm wide and moves up and down at a speed of 17 mm/sec in the upper half of the lanes. Images were acquired every 6 seconds for a 30 minute period and were analyzed in ImageJ. We developed an ImageJ macro (version 25k) that automatically separates the color channels, subtracts the background, applies a threshold, identifies larvae based on particle size, and repeats these steps for subsequent images in a series. This macro can be downloaded from Clift et al. 2014 [21]. The macro generates a long list of X,Y coordinates indicating the location and orientation of the larvae over time. The list of X,Y coordinates is copied in a Microsoft Excel template, which calculates: a) the percentage of time that the larvae are located in the lower half of the lane, away from the visual stimuli, b) the swim speed, c) the percentage of time that the larvae rest, which is defined as the percentage of time the larvae move less than 1 mm in a 6 second interval, d) the average distance between larvae, e) the percentage of time that larvae are together, which is defined as less than 5 mm apart from the nearest neighbor, and f) the percentage of time that larvae are located along the edge of the lane, which is defined as the outer 3 mm perimeter of the swimming area.

Statistical Analyses. The averages and standard errors of the mean (\pm SEM) were calculated and graphed in MS Excel. The eye and brain defects were averaged on a per-embryo basis (N= number of embryos). To assure independence of measurements in the

behavioral analyses, larval behavior was averaged on a per-lane basis (N= number of lanes). Differences between the treated groups and the corresponding DMSO controls were tested for significance with a t-test (two-tailed, unequal variance). For the initial dose-response studies, the data were analyzed with a one-way ANOVA ($p < 0.01$) using a post-hoc Bonferroni correction for multiple comparisons (four cyclosporine concentrations vs. a single DMSO control).

Results

Cyclosporine exposures affect eye size. Since calcineurin subunits are expressed in the developing brain and eye [31], we first examined if cyclosporine induces morphological defects in these organ systems. To examine the effects of cyclosporine on eye development, wild type embryos were exposed to 1, 2, 5 and 10 μM cyclosporine from 2-26 hpf and imaged at 3 dpf by standard bright-field microscopy. The length of the eyes was 331 μm (± 2) in the controls vs. 326 μm (± 3), 317 μm (± 3), 300 μm (± 4) and 270 μm (± 5) in embryos treated with 1, 2, 5, and 10 μM cyclosporine, respectively (Fig. 2). The ANOVA was < 0.01 and the post-hoc analysis revealed that embryos exposed to 2, 5, or 10 μM cyclosporine have significantly smaller eyes than the DMSO-treated controls (8×10^{-4} , 2×10^{-8} , 8×10^{-13} , $N=25$ embryos per group). In contrast, the 1 μM cyclosporine exposure did not affect eye size ($p=0.15$, $N=25$). The smaller eye size with 2, 5 and 10 μM cyclosporine (compared to the DMSO controls), corresponds to a 4%, 9% and 19% change, which can be reliably detected due to the low variability in the measurements of eye size. The 10 μM cyclosporine concentration was used in subsequent experiments.

Cyclosporine exposures affect brain size. The effect of cyclosporine on the developing brain was examined in *Tg(elavl3:EGFP)* embryos, exposed to 10 μ M cyclosporine from 2-26 hpf and imaged at 3 dpf by confocal and wide-field fluorescence microscopy. Confocal microscopy, combined with 3D visualization of the resulting data sets, is ideally suited for exploratory analyses of neural patterns [28] and revealed a cyclosporine-induced reduction in brain size (Fig. 3). Once identified, this effect was efficiently quantified by wide-field fluorescence microscopy (Fig 3C,F,G,H). The length of the forebrain was 139 μ m (\pm 3) in the DMSO-treated controls vs. 109 μ m (\pm 4) in the cyclosporine-treated embryos ($p=1\times 10^{-5}$, $N_{\text{DMSO}}=16$, $N_{\text{CsA}}=10$). The width of the forebrain, measured at the broadest forebrain region, was 204 μ m (\pm 2) in the DMSO-treated controls vs. 180 μ m (\pm 3) in the cyclosporine-treated embryos ($p=2\times 10^{-5}$, $N_{\text{DMSO}}=16$, $N_{\text{CsA}}=10$). The length of the midbrain was 214 μ m (\pm 6) in the DMSO-treated controls vs. 169 μ m (\pm 5) in the cyclosporine-treated embryos ($p=5\times 10^{-6}$, $N_{\text{DMSO}}=16$, $N_{\text{CsA}}=10$). The width of the midbrain, measured at the broadest midbrain region, was 413 μ m (\pm 3) in the DMSO-treated controls vs. 338 μ m (\pm 7) in the cyclosporine-treated embryos ($p=1\times 10^{-7}$, $N_{\text{DMSO}}=16$, $N_{\text{CsA}}=10$). The width of the hindbrain, measured at the boundary between the cerebellum and medulla, was 244 μ m (\pm 2) in the DMSO-treated controls vs. 221 μ m (\pm 2) in the cyclosporine-treated embryos ($p=1\times 10^{-6}$, $N_{\text{DMSO}}=16$, $N_{\text{CsA}}=10$). In summary, cyclosporine induced a significant decrease in eye size (Fig 2) and induced a significant decrease in all measured lengths and widths of the brain (Fig 3G). To examine if these effects could be attributed to a general delay in development, we measured the embryonic head-trunk angles, which is a standard method for staging zebrafish embryos [18]. We found that embryos exposed to 10 μ M cyclosporine from 2-26 hpf do not

display significant differences in the head-trunk angle compared to untreated or DMSO-treated controls (Fig 3H). Based on these results, we conclude that early embryonic cyclosporine exposures cause a reduction in eye size and a reduction in brain size that cannot be explained by a general developmental delay.

Sensitive periods. To determine if there is a sensitive period for the eye and brain defects, embryos were exposed to 10 μ M cyclosporine from 0-1 dpf (day 1), 1-2 dpf (day 2), or 2-3 dpf (day 3). We measured the eye length at 3 dpf (Fig 4A). In addition, since prior analyses showed effects on brain length and width, we measured the area of the forebrain (Fig 4B), area of the midbrain (Fig 4C) and the area of the cerebellum in the anterior-dorsal region of the hindbrain (Fig 4D). Day 1 exposures induced a significant decrease in the size of the eyes, forebrain, and midbrain. The eye length was 327 μ m (\pm 4) in the DMSO-treated controls vs. 266 μ m (\pm 3) in the cyclosporine-treated embryos ($p=2 \times 10^{-14}$, $N_{\text{DMSO}}=20$, $N_{\text{CsA}}=20$). The forebrain area was 24,864 μm^2 (\pm 534) in the DMSO-treated controls vs. 16,870 μm^2 (\pm 865) in the cyclosporine-treated embryos ($p=8 \times 10^{-7}$, $N_{\text{DMSO}}=16$, $N_{\text{CsA}}=10$). The midbrain area was 73,465 μm^2 (\pm 1,331) in the DMSO-treated controls vs. 51,128 μm^2 (\pm 1852) in the cyclosporine-treated embryos ($p=1 \times 10^{-8}$, $N_{\text{DMSO}}=16$, $N_{\text{CsA}}=10$). Day 2 exposures induced a significant decrease in the size of the eyes, forebrain, midbrain and hindbrain (cerebellum). The eye length was 328 μ m (\pm 2) in the DMSO-treated controls vs. 275 μ m (\pm 6) in the cyclosporine-treated embryos ($p=4 \times 10^{-9}$, $N_{\text{DMSO}}=20$, $N_{\text{CsA}}=20$). The forebrain area was 25,936 μm^2 (\pm 801) in the DMSO-treated controls vs. 16,637 μm^2 (\pm 917) in the cyclosporine-treated embryos ($p=1 \times 10^{-7}$, $N_{\text{DMSO}}=13$, $N_{\text{CsA}}=12$). The midbrain area was 73,651 μm^2 (\pm 1,434) in the

DMSO-treated controls and vs. $52,723 \mu\text{m}^2 (\pm 1,564)$ in the cyclosporine-treated embryos ($p=1 \times 10^{-9}$, $N_{\text{DMSO}}=13$, $N_{\text{CsA}}=12$). The area of the cerebellum was $43,824 \mu\text{m}^2 (\pm 1,917)$ in the DMSO-treated controls vs. $38,722 \mu\text{m}^2 (\pm 837)$ in the cyclosporine-treated embryos ($p=0.03$, $N_{\text{DMSO}}=13$, $N_{\text{CsA}}=12$). In summary, day 1 cyclosporine exposures led to a significant 19%, 32% and 30% decrease in the size of the eyes, forebrain and midbrain and day 2 cyclosporine exposures led to a significant 16%, 36%, 28%, and 12% decrease in the size of the eyes, forebrain, midbrain and cerebellum, respectively. In contrast, day 3 cyclosporine exposures did not induce significant changes in the size of the eyes, forebrain, midbrain, or cerebellum. Based on these results, we conclude that the size of eyes and the size of the brain are sensitive to cyclosporine exposures during early embryonic development (day 1 and 2), but not during late embryonic development (day 3).

Late embryonic exposures lead to changes in behavior. To examine if day 3 cyclosporine exposures induce functional brain defects, we grew DMSO and cyclosporine-exposed larvae to 5 dpf for behavioral analyses. At 5 dpf, the DMSO-treated and cyclosporine-treated larvae are indistinguishable by morphological criteria (Fig 5). However, the cyclosporine-exposed larvae displayed various behavioral defects in a 5-lane moving bar assay (Fig 6). This assay has two components. During the first 15 minutes, behaviors are analyzed without visual stimuli. During the subsequent 15 minutes, behaviors are analyzed in the presence of an aversive visual stimulus, a red moving bar, which the larvae avoid [21,25]. We found that day 3 cyclosporine exposures affected the avoidance response (Fig 7A), swim speed (Fig 7B), resting (Fig 7C), the

average distance between larvae (Fig 7D), the percentage of time that larvae are close together (Fig 7E), and the percentage of time the larvae spend on the edge of the swimming area (Fig 7F). Specifically, the time that larvae spent down in the lane, away from the visual stimulus, was 82% (± 3) in the DMSO-treated controls vs. 67% (± 3) in the cyclosporine-treated embryos ($p=2 \times 10^{-4}$, $N_{\text{DMSO}}=40$, $N_{\text{CsA}}=37$). The swim speed without visual stimuli was 29 mm/min (± 2) in the DMSO-treated controls vs. 22 mm/min (± 2) in the cyclosporine-treated embryos ($p=0.001$, $N_{\text{DMSO}}=40$, $N_{\text{CsA}}=37$). Similarly, the swim speed with visual stimuli was 27 mm/min (± 1) in the DMSO-treated controls vs. 21 mm/min (± 2) in the cyclosporine-treated embryos ($p=0.005$, $N_{\text{DMSO}}=40$, $N_{\text{CsA}}=37$). The percentage of time that larvae rest without visual stimuli was 44% (± 2) in the DMSO-treated controls vs. 61% (± 3) in the cyclosporine-treated embryos ($p=3 \times 10^{-6}$, $N_{\text{DMSO}}=40$, $N_{\text{CsA}}=37$). Similarly, the percentage of time that larvae rest with visual stimuli was 46% (± 2) in the DMSO-treated controls vs. 62% (± 3) in the cyclosporine-treated embryos ($p=2 \times 10^{-5}$, $N_{\text{DMSO}}=40$, $N_{\text{CsA}}=37$). The larval distance in the presence of visual stimuli was 26 mm (± 1) in the DMSO-treated controls vs. 32 mm (± 1) in the cyclosporine-treated embryos ($p=8 \times 10^{-4}$, $N_{\text{DMSO}}=40$, $N_{\text{CsA}}=37$). The percentage of time that larvae were together (<5 mm apart), without visual stimuli, was 11% (± 1) in the DMSO-treated controls vs. 25% (± 3) in the cyclosporine-treated embryos ($p=2 \times 10^{-4}$, $N_{\text{DMSO}}=40$, $N_{\text{CsA}}=37$). The percentage of time that the larvae were located on the outer edge of the swimming area, without visual stimuli was 67% (± 1) in the DMSO-treated controls vs. 82% (± 2) in the cyclosporine-treated embryos ($p=1 \times 10^{-7}$, $N_{\text{DMSO}}=40$, $N_{\text{CsA}}=37$). Similarly, the percentage of time that the larvae were located on the outer edge of the swimming area, with visual stimuli was 74% (± 1) in the DMSO-treated controls vs. 81%

(± 2) in the cyclosporine-treated embryos ($p=0.001$, $N_{\text{DMSO}}=40$, $N_{\text{CsA}}=37$). We conclude that cyclosporine exposures during late embryonic development lead to significant behavioral changes in free-swimming zebrafish larvae.

The calcineurin inhibitor FK506 induces similar defects. We examined whether similar developmental defects may be induced by FK506, another calcineurin inhibitor that is used as an immunosuppressant in transplant medicine [2,3]. We found that embryos exposed to 1 μM FK506 from 2-26 hpf displayed a similar decrease in eye size as embryos exposed to 10 μM cyclosporine. The length of the eyes was 327 μm (± 2) in the DMSO-treated controls vs. 279 μm (± 7) in the FK506-treated embryos ($p=2 \times 10^{-6}$, $N_{\text{DMSO}}=18$, $N_{\text{FK506}}=18$ embryos). Embryos exposed to 1 μM FK506 from 2-26 hpf displayed a reduction in brain size, similar to the reduction in brain size observed in cyclosporine-exposed embryos. The area of the forebrain was 21,908 μm^2 (± 480) in the DMSO-treated controls vs. 17,575 μm^2 (± 739) in the FK506-treated embryos ($p=2 \times 10^{-4}$, $N_{\text{DMSO}}=10$, $N_{\text{FK506}}=10$). The area of the midbrain was 67,347 μm^2 ($\pm 1,683$) in the DMSO-treated controls vs. 57,530 μm^2 ($\pm 2,006$) in the FK506-treated embryos ($p=0.002$, $N_{\text{DMSO}}=10$, $N_{\text{FK506}}=10$). The area of the hindbrain (cerebellum) was not significantly reduced in the FK506-treated embryos. In summary, FK506 induces a significant 15% reduction in eye length, 20% reduction in forebrain area, and 15% reduction in midbrain area.

Embryos exposed to 1 μ M FK506 during day 3 displayed similar behavioral defects as embryos exposed to 10 μ M cyclosporine during day 3. Specifically, the percentage of time that larvae avoid the visual stimulus was 79% (± 3) in the DMSO-treated controls vs. 63% (± 2) in the FK506-treated embryos ($p=7 \times 10^{-5}$, $N_{\text{DMSO}}=33$, $N_{\text{FK506}}=30$). The percentage of time that the larvae were located on the outer edge of the swimming area, without visual stimuli was 71% (± 2) in the DMSO-treated controls vs. 83% (± 1) in the FK506-treated embryos ($p=1 \times 10^{-6}$, $N_{\text{DMSO}}=33$, $N_{\text{FK506}}=30$). Similarly, the percentage of time that the larvae were located on the outer edge of the swimming area, with visual stimuli, was 73% (± 2) in the DMSO-treated controls vs. 80% (± 1) in the FK506-treated embryos ($p=0.002$, $N_{\text{DMSO}}=33$, $N_{\text{FK506}}=30$). The larval distance in the presence of visual stimuli was 26 mm (± 1) in the DMSO-treated controls vs. 33 mm (± 1) in the FK506-treated embryos ($p=2 \times 10^{-5}$, $N_{\text{DMSO}}=33$, $N_{\text{FK506}}=30$). While the FK506-induced changes in behavior are similar to the cyclosporine-induced changes in behavior, the behavioral profiles of FK506 and cyclosporine are not identical. The swim speed without visual stimuli was 22 mm/min (± 2) in the DMSO-treated controls vs. 27 mm/min (± 2) in the FK506-treated embryos ($p=0.052$, $N_{\text{DMSO}}=33$, $N_{\text{CSA}}=30$). The percentage of time that larvae rest without visual stimuli was 56% (± 3) in the DMSO-treated controls vs. 53% (± 3) in the FK506-treated embryos ($p=0.5$, $N_{\text{DMSO}}=33$, $N_{\text{CSA}}=30$). Thus, the effects of FK506 on swim speed and resting are not significant and show a trend in the opposite direction compared to the effects of cyclosporine on swim speed and resting. In summary, FK506 induced a significant decrease in avoidance of visual stimuli, increase in thigmotaxis, and increase in larval distance in the presence of visual stimuli, similar to the behavioral defects induced by cyclosporine exposures. However, the cyclosporine-

induced decrease in swim speed and increase in resting were not observed after FK506 exposure.

Discussion

The results of this study show that cyclosporine exposures during embryonic development can induce structural or behavioral defects, depending on the exposure window (Fig 8). Early embryonic cyclosporine exposures (day 1 or day 2) led to a reduction in eye size and brain size. Late embryonic exposures (day 3) did not affect eye and brain size, but did lead to significant behavioral defects in free-swimming zebrafish larvae.

Eye and brain defects were induced by early exposures to either cyclosporine or FK506. Both calcineurin inhibitors are immunosuppressants, but act through different mechanisms: cyclosporine inhibits calcineurin via cyclophilin and FK506 inhibits calcineurin via FKBP [2]. The similar defects induced by different calcineurin inhibitors, suggests that the observed effects are mediated by an inhibition of calcineurin signaling. It remains to be established if these effects are cell autonomous or if calcineurin signaling in other embryonic tissues influence development of the eye and brain. Calcineurin subunits are expressed in the developing brain and in the retina of the eye [31], suggesting that cell-autonomous processes might be important.

The late embryonic cyclosporine exposures led to various behavioral defects in free-swimming zebrafish larvae. The cyclosporine-exposed larvae displayed a reduced avoidance response, lower swim speeds, increased resting, and an increased preference for the edge of the swimming area. In addition, cyclosporine exposure affected larval interactions. The cyclosporine-exposed larvae remain further apart in the presence of visual stimuli, but spent more time close together without visual stimuli. It is possible that this broad range of behavioral defects is caused by an overarching syndrome. Previous studies have shown that thigmotaxis, a preference for the edge of a swimming area, is an anxiety-related behavior in zebrafish larvae [32,33]. In addition, the observed increase in immobility or ‘resting’ and low swim speed may reflect an increase in ‘freezing’ behavior, similar to larval freezing induced by a novel visual stimulus [34] and anxiety-related freezing behaviors in adult zebrafish [35]. Thus, the cyclosporine-induced increase in thigmotaxis and immobility could be indicative of an anxiety-related syndrome. However, it is also possible that the various behavioral defects are not linked by an overarching mechanism. For example, the organophosphate pesticide chlorpyrifos induces low swim speeds and decreased thigmotaxis [36], showing that the low swim speed and elevated thigmotaxis observed in the present study are not necessarily linked. In addition, the observed changes in larval interactions suggest that cyclosporine may induce a multifaceted syndrome.

Since day 3 cyclosporine and FK506 exposures induce similar behavioral defects, these defects are likely caused by calcineurin inhibition. The underlying mechanisms may include calcineurin-dependent axonal growth and guidance or calcineurin-dependent

neuronal apoptosis in the developing brain, similar to the roles of calcineurin in other systems [8,37]. A better understanding of these basic developmental mechanisms could provide novel insights in various neurodevelopmental disorders. For example, in Down syndrome, calcineurin/NFAT signaling is thought to be suppressed by RCAN1 and DYRK1A located on chromosome 21 [38,39], but little is known about the neural mechanisms that are affected by this suppression of calcineurin/NFAT signaling. In addition to the behavioral defects induced by both cyclosporine and FK506, we found that cyclosporine induced a few behavioral defects that were not observed with FK506. The reduced swim speeds and increased resting were observed after cyclosporine exposure, but not after FK506 exposure. Possibly, this subset of behavioral defects is caused by off-target effects, i.e. effects that are not mediated by calcineurin inhibition. Since the behavioral assays may be used to identify both calcineurin-mediated effects and off-target effects, the assays could be valuable for the development novel pharmaceuticals with minimal off-target effects.

Cyclosporine is used to prevent organ rejection in transplant medicine and has been successfully used during pregnancy [7]. These pregnancies are considered high risk and close maternal and fetal surveillance is vital. The results of our study raise the question if cyclosporine induces developmental brain disorders when used during pregnancy. However, to what extent can our results in zebrafish be translated to developmental disorders in humans? On one hand, there are substantial differences between zebrafish and human embryos, for example in the speed of development and the environment surrounding the embryo. In addition, it is unclear how the 1-10 μ M (1.2-12 mg/L)

cyclosporine concentrations used in this study relate to the 0.8-2 mg/L in the serum of patients who take cyclosporine for immunosuppression [40] and the unknown cyclosporine concentrations in developing human embryos. On the other hand, the conserved signaling pathways that regulate brain development [10,11][10-11] and the substantial structural and functional brain defects that were observed in the current study suggest that there is reason for concern. Data from clinical studies and data from studies using various model systems can be taken into account when advising patients who have transplants or autoimmune diseases. In addition, if calcineurin inhibitors are used during pregnancy, it is prudent to carry out health assessment not only during pregnancy, but also during childhood and adolescence. Finally, our results highlight the importance of studying different exposure windows in zebrafish and other animal model systems. The different exposure windows, combined with quantitative analyses of behavior, provide a better basic understanding of the factors that can induce functional brain defects during specific sensitive periods in development.

Acknowledgements. This work was supported by the Eunice Kennedy Shriver National Institute of Child Health and Human Development (R01 HD060647). Holly Richendrfer, Ruth Colwill and Robbert Creton received funding from the National Institute of Environmental Health Sciences (F32 ES021342, R03ES017755, P42 ES013660) and Robert Thorn received funding from a NIH training grant in molecular biology, cell biology and biochemistry (T32 GM007601). We thank Dr. Bonkowsky for the transgenic zebrafish line and thank Sean Pelkowski for contributing to the eye size experiments.

References:

1. Kahan BD. Forty years of publication of transplantation proceedings--the second decade: the cyclosporine revolution. *Transpl Proc* 2009; **41**:1423–1437.
2. Liu JO. Calmodulin-dependent phosphatase, kinases, and transcriptional corepressors involved in T-cell activation. *Immunol Rev* 2009; **228**:184–198.
3. Azzi JR, Sayegh MH, Mallat SG. Calcineurin inhibitors: 40 years later, can't live without. *J Immunol* 2013; **191**:5785–5791.
4. Babalola O, Strober BE. Management of psoriasis in pregnancy. *Dermatol Ther* 2013; **26**:285–292.
5. FDA. U.S. Food and Drug Administration. CFR - Code of Federal Regulations Title 21. <http://www.accessdata.fda.gov/scripts/cdrh/cfdocs/cfcfr/CFRSearch.cfm?fr=20157> 2014; (retrieved Nov 2014).
6. Ramoz LL, Patel-Shori NM. Recent changes in pregnancy and lactation labeling: retirement of risk categories. *Pharmacotherapy* 2014; **34**:389–395.
7. Armenti VT, Constantinescu S, Moritz MJ, Davison JM. Pregnancy after transplantation. *Transplant Rev (Orlando)* 2008; **22**:223–40.
8. Nguyen T, Di Giovanni S. NFAT signaling in neural development and axon growth. *Int J Dev Neurosci* 2008; **26**:141–145.
9. Moore KL, Persaud TVN, Torchia MG. The Developing Human: Clinically Oriented Embryology. Elsevier, 9th edition. Philadelphia, PA. 2013.
10. Cavodeassi F, Houart C. Brain regionalization: of signaling centers and boundaries. *Dev Neurobiol* 2012; **72**:218–233.
11. Rinkwitz S, Mourrain P, Becker TS. Zebrafish: an integrative system for neurogenomics and neurosciences. *Prog Neurobiol* 2011; **93**:231–243.
12. Gerlai R. Fish in behavior research: unique tools with a great promise! *J Neurosci Methods* 2014; **234**:54–58.
13. Kalueff A V, Stewart AM, Gerlai R. Zebrafish as an emerging model for studying complex brain disorders. *Trends Pharmacol Sci* 2014; **35**:63–75.
14. Stewart AM, Braubach O, Spitsbergen J, Gerlai R, Kalueff A V. Zebrafish models for translational neuroscience research: from tank to bedside. *Trends Neurosci* 2014; **37**:264–278.
15. Del Bene F, Wyart C. Optogenetics: a new enlightenment age for zebrafish neurobiology. *Dev Neurobiol* 2012; **72**:404–414.
16. Simmich J, Staykov E, Scott E. Zebrafish as an appealing model for optogenetic studies. *Prog Brain Res* 2012; **196**:145–162.
17. Weber T, Koster R. Genetic tools for multicolor imaging in zebrafish larvae. *Methods* 2013; **62**:279–291.
18. Kimmel CB, Ballard WW, Kimmel SR, Ullmann B, Schilling TF. Stages of embryonic development of the zebrafish. *Dev Dyn* 1995; **203**:253–310.
19. Kokel D, Bryan J, Laggner C, et al. Rapid behavior-based identification of neuroactive small molecules in the zebrafish. *Nat Chem Biol* 2010; **6**:231–237.
20. Rihel J, Prober D a, Arvanites A, et al. Zebrafish behavioral profiling links drugs to biological targets and rest/wake regulation. *Science* 2010; **327**:348–51.
21. Clift D, Richendrfer H, Thorn RJ, Colwill RM, Creton R. High-Throughput Analysis of Behavior in Zebrafish Larvae: Effects of Feeding. *Zebrafish* 2014; **11**:455–461.

22. Colwill RM, Creton R. Imaging escape and avoidance behavior in zebrafish larvae. *Rev Neurosci* 2011; **22**:63–73.
23. Creton R. Automated analysis of behavior in zebrafish larvae. *Behav Brain Res* 2009; **203**:127–36.
24. Pelkowski SD, Kapoor M, Richendrfer H a, Wang X, Colwill RM, Creton R. A novel high-throughput imaging system for automated analyses of avoidance behavior in zebrafish larvae. *Behav Brain Res* 2011; **223**:135–44.
25. Richendrfer H, Créton R. Automated high-throughput behavioral analyses in zebrafish larvae. *J Vis Exp* 2013:e50622.
26. Park HC, Kim CH, Bae YK, *et al.* Analysis of upstream elements in the HuC promoter leads to the establishment of transgenic zebrafish with fluorescent neurons. *Dev Biol* 2000; **227**:279–293.
27. Anon. No Title.
28. Lewis D. The CAVE artists. *Nat Med* 2014; **20**:228–230.
29. Schindelin J, Arganda-Carreras I, Frise E, *et al.* Fiji: an open-source platform for biological-image analysis. *Nat Methods* 2012; **9**:676–682.
30. Preibisch S, Saalfeld S, Tomancak P. Globally optimal stitching of tiled 3D microscopic image acquisitions. *Bioinformatics* 2009; **25**:1463–1465.
31. Hammond DR, Udvardia AJ. Cabin1 expression suggests roles in neuronal development. *Dev Dyn* 2010; **239**:2443–51.
32. Richendrfer H, Pelkowski SD, Colwill RM, Creton R. On the edge: pharmacological evidence for anxiety-related behavior in zebrafish larvae. *Behav Brain Res* 2012; **228**:99–106.
33. Schnorr SJ, Steenbergen PJ, Richardson MK, Champagne DL. Measuring thigmotaxis in larval zebrafish. *Behav Brain Res* 2012; **228**:367–374.
34. O’Neale A, Ellis J, Creton R, Colwill RM. Single stimulus learning in zebrafish larvae. *Neurobiol Learn Mem* 2013; **108**:145–154.
35. Cachat J, Stewart A, Grossman L, *et al.* Measuring behavioral and endocrine responses to novelty stress in adult zebrafish. *Nat Protoc* 2010; **5**:1786–1799.
36. Richendrfer H, Pelkowski SD, Colwill RM, Créton R. Developmental sub-chronic exposure to chlorpyrifos reduces anxiety-related behavior in zebrafish larvae. *Neurotoxicol Teratol* 2012; **34**:458–65.
37. Hara MR, Snyder SH. Cell signaling and neuronal death. *Annu Rev Pharmacol Toxicol* 2007; **47**:117–141.
38. Arron JR, Winslow MM, Polleri A, *et al.* NFAT dysregulation by increased dosage of DSCR1 and DYRK1A on chromosome 21. *Nature* 2006; **441**:595–600.
39. Park J, Oh Y, Chung KC. Two key genes closely implicated with the neuropathological characteristics in Down syndrome: DYRK1A and RCAN1. *BMB Rep* 2009; **42**:6–15.
40. Keown PA. New concepts in cyclosporine monitoring. *Curr Opin Nephrol Hypertens* 2002; **11**:619–626.

Figures:

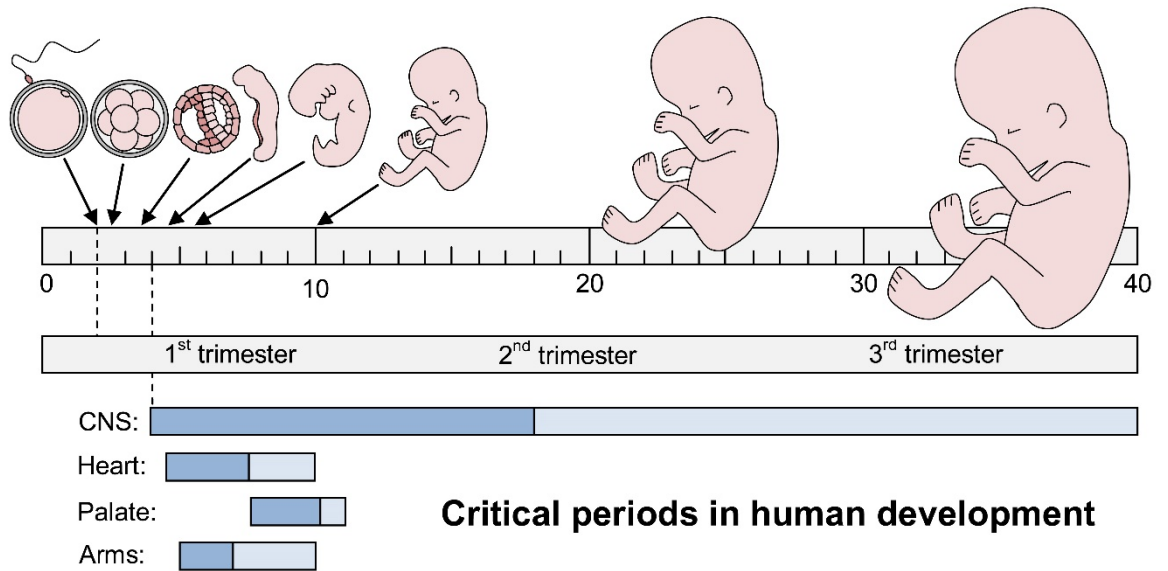


Figure 1. Critical or sensitive periods in human development. Most developing organs are sensitive to teratogens during the embryonic period from 4-10 weeks of gestation. A notable exception is the central nervous system (CNS), which remains sensitive throughout the fetal period from 10-40 weeks of gestation. To illustrate the extended period of sensitivity of the CNS, we redrew the textbook model from Moore et al. 2013 [9] on a linear 40-week scale (with permission). Dark blue = major structural defects, light blue = minor structural or functional defects. 40 weeks of gestation = 38 weeks of development.

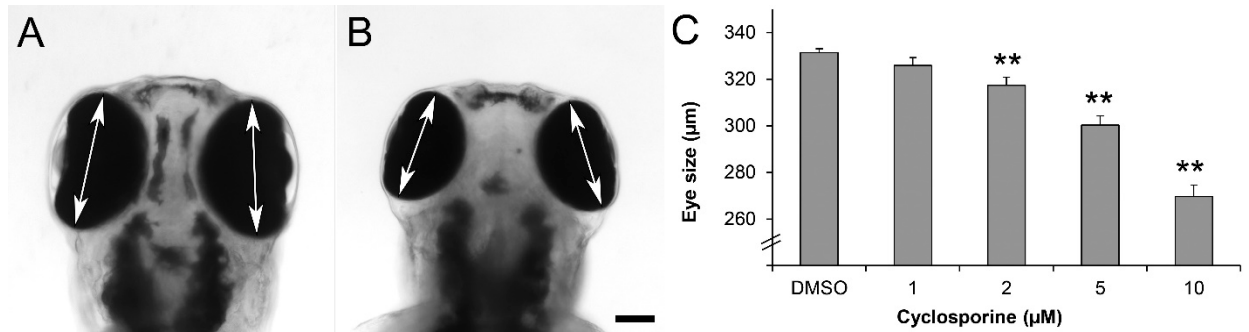


Figure 2. Cyclosporine exposures affect eye size. A) Control embryo, exposed to 0.1% DMSO from 2-26 hpf and imaged at 3 dpf. B) Embryo exposed to 10 μM cyclosporine from 2-26 hpf and imaged at 3 dpf. C) Measurements of eye size in embryos exposed to various concentrations of cyclosporine. Arrows indicate the maximum eye diameter, which was used as a measure of eye size. ** = $p < 0.01 / 4$ (two-tailed t-test with Bonferroni correction for multiple comparisons). Scale bar = 100 μm .

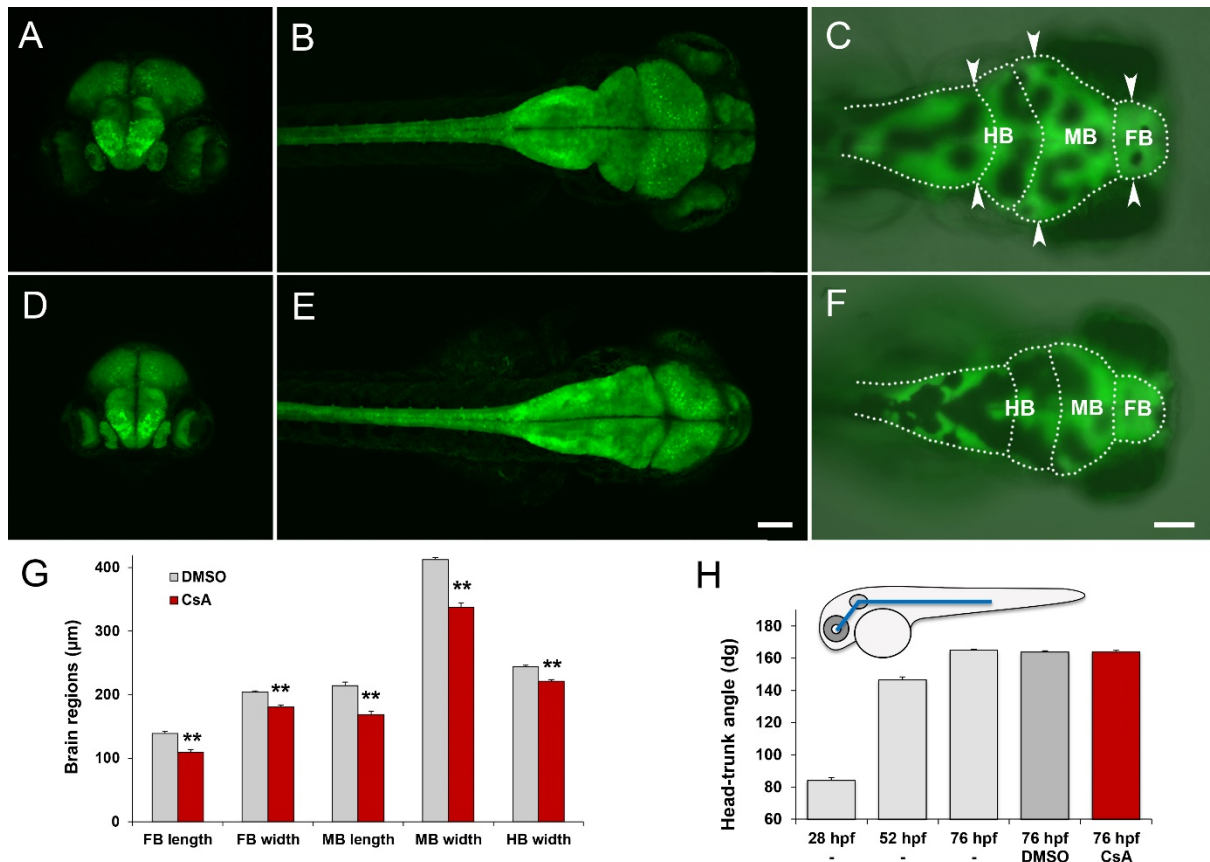


Figure 3. Cyclosporine exposures affect brain size. A-C) Control embryos exposed to 0.1% DMSO from 2-26 hpf and imaged at 3 dpf. D-F) Embryos exposed to 10 μ M cyclosporine from 2-26 hpf and imaged at 3 dpf. A,D) frontal view by confocal microscopy. B,E) dorsal view by confocal microscopy. C,F) dorsal view by fluorescence microscopy, with outlines of the forebrain (FB), midbrain (MB) and hindbrain (HB). G) Length and width of forebrain, midbrain and hindbrain. H) Measurements of the head-trunk angle. The cyclosporine-treated embryos do not display a significant developmental delay compared to the DMSO-treated or untreated controls. For imaging brain size, we used *elav:GFP* embryos, which express GFP in the brain and spinal cord. Arrow heads = measurements of brain width. CsA=cyclosporine exposure. Scale bars = 100 μ m. ** $p < 0.01$ (two-tailed t-test).

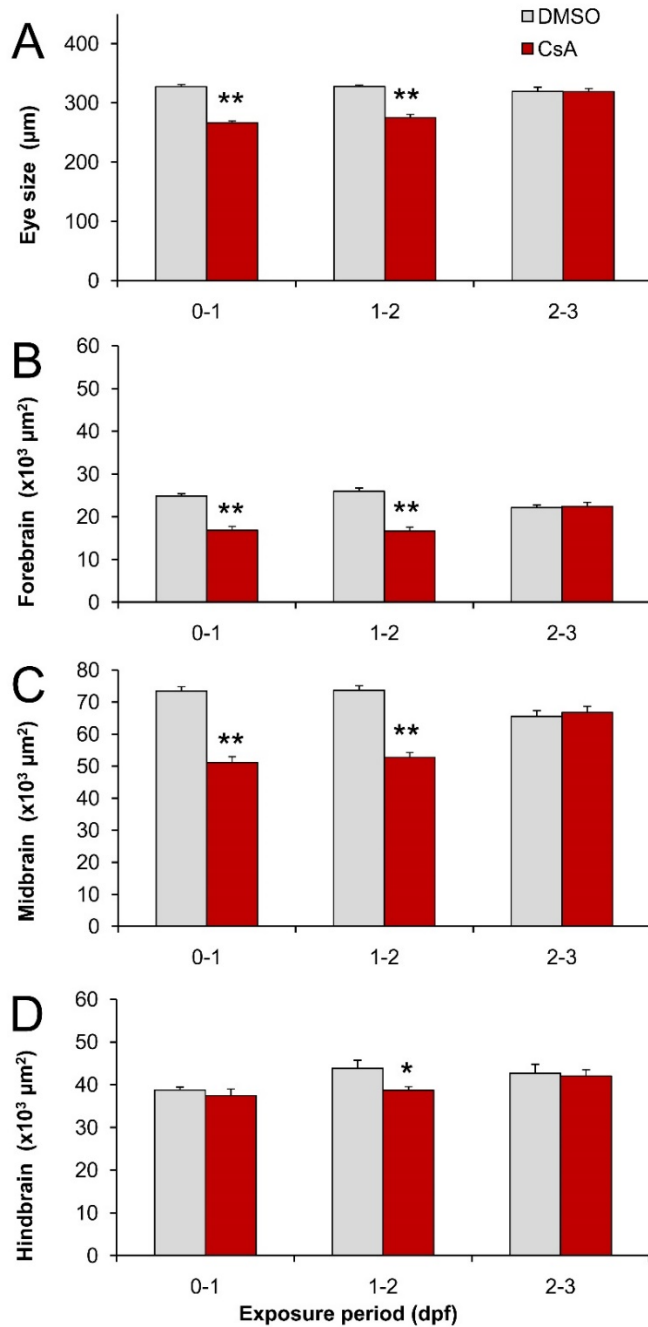


Figure 4. Sensitive periods for eye and brain defects. A) Eye size. B) Forebrain area. C) Midbrain area. D) Anterior hindbrain area (cerebellum). Embryos exposed to 10 μM cyclosporine (CsA) from 0-1 and 1-2 dpf display a reduction in eye and brain size. In contrast, embryos exposed from 2-3 dpf do not display a reduction in eye and brain size. The wild type (A) and *elav:GFP* embryos (B-D) were imaged at 3 dpf. * $p < 0.05$, ** $p < 0.01$ (two tailed t-test).

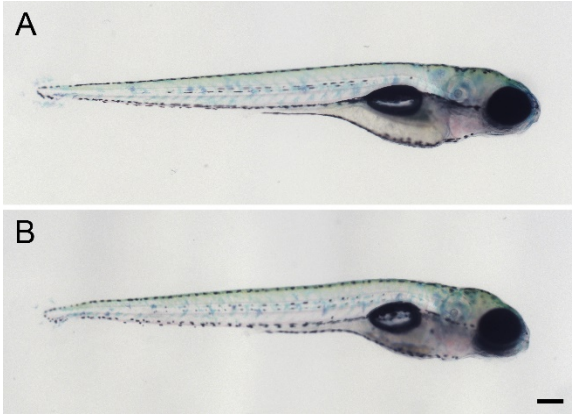


Figure 5. Larval morphology at 5 dpf. A) Control larva, exposed to 0.1% DMSO from 2-3 dpf. B) Larva exposed to 10 μ M cyclosporine from 2-3 dpf. These late embryonic cyclosporine exposures do not induce gross morphological defects. Scale bar = 200 μ m.

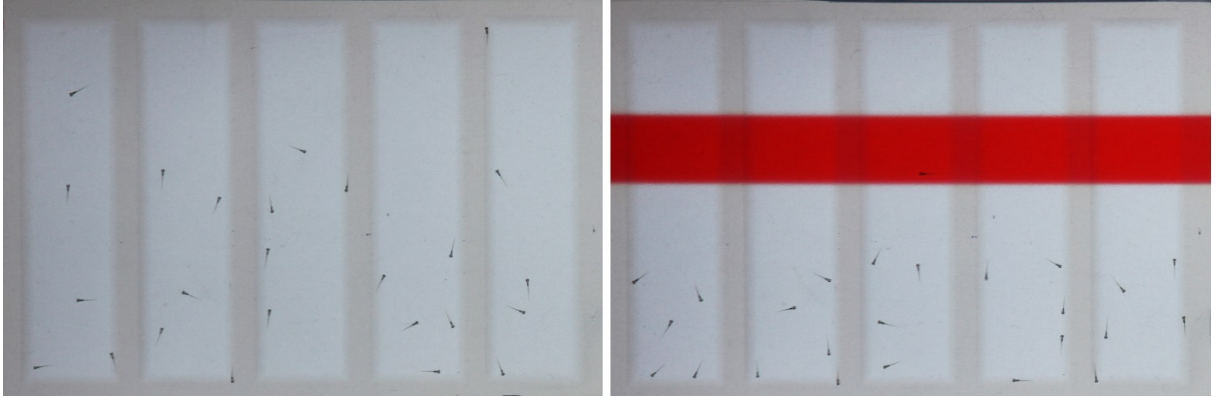


Figure 6. Automated analysis of behavior in a five-lane plate. Five-day-old larvae are imaged for 15 minutes without visual stimuli (left panel) and then for 15 minutes in the presence of a red bar, which moves up and down in the upper half of the lanes (right panel). The larvae swim towards the lower half of the lanes, away from the visual stimulus.

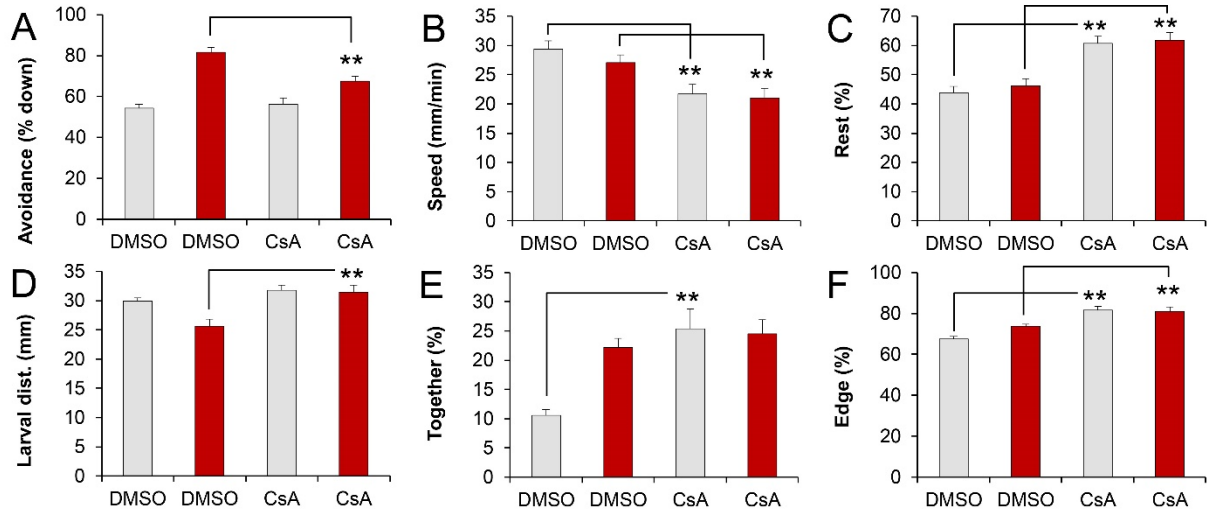


Figure 7. Behavioral defects at 5 dpf. A) Avoidance of visual stimuli. B) Swim speed. C) Resting (larvae move less than 1 mm / 6 sec interval). D) Average distance between larvae. E) Together (larvae are less than 5 mm apart). F) Edge preference or thigmotaxis (larvae are less than 3 mm from the perimeter). The cyclosporine-exposed embryos display significant behavioral defects, as compared to the DMSO-treated controls (** p < 0.01, t-test). DMSO = Control embryos were exposed to 0.1% DMSO from 2-3 dpf. CsA = Embryos were exposed to 10 μ M cyclosporine from 2-3 dpf. Gray bars = without visual stimuli. Red bars = with visual stimuli.

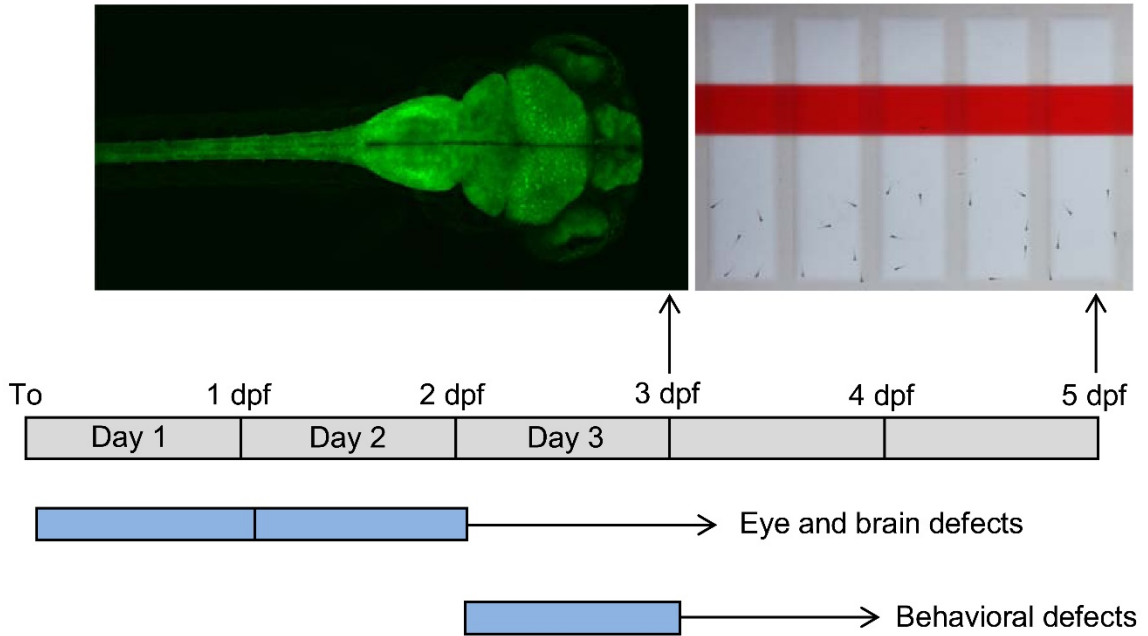


Figure 8. Summary of sensitive periods in zebrafish development. Early embryonic exposures to cyclosporine lead to structural brain defects. Late embryonic exposures to cyclosporine lead to behavioral defects. Blue = window of cyclosporine exposure.

Chapter 3: Examining Calcineurin Inhibition in the Developing Zebrafish Brain

Thorn R.J., Clift D.E., Seto R.J., Creton R. (in preparation)

I performed a majority of the experiments with assistance from DEC and RJS and performed all analysis and wrote the manuscript with RC.

Abstract

Calcineurin, a serine/threonine phosphatase, is best known for its role in the immune system but is also thought to play a critical role in brain development. Various studies suggest that suppressed calcineurin signaling contributes to cognitive disability in Down syndrome, through regulators of calcineurin signaling on chromosome 21, and questions have been raised about the use of Calcineurin inhibitors during pregnancy. However, little is known about the underlying calcineurin-dependent mechanisms that regulate brain development and function. The current studies make use of zebrafish as a model system to examine specific roles of calcineurin in the developing brain. Zebrafish embryos were injected with varying levels of morpholinos against two regulatory or B subunits of calcineurin. We found that calcineurin inhibition during early brain development led to microcephaly and specific behavioral defects, in a subunit dependent manner. Additionally, we found an increase in apoptosis in calcineurin B morphants. These results suggest that inhibition of calcineurin signaling during early development leads to apoptosis and subsequent structural and functional brain defects, and that the different calcineurin regulatory subunits have different developmental roles.

Introduction

Calcineurin is a calcium dependent serine/threonine phosphatase that is composed of two subunits: a catalytic (or A) and regulatory (or B) subunit [1]. Calcineurin is activated by increases in Ca^{2+} , which is mediated by calmodulin [1]. The catalytic pocket of calcineurin has been shown to have nonspecific phosphatase activity, and yet calcineurin

only activates specific signaling pathways [2]. There are two binding motifs located on calcineurin substrates that allow these substrates to dock to calcineurin and be dephosphorylated. The motifs are the PxIxIT motif, which docks on the catalytic subunit, and the LxVP motif, which docks at the interface between the catalytic and regulatory subunits. [2,3].

Calcineurin has been a focus of research due to its importance in T-cell activation. Calcineurin dephosphorylates the transcription factor, nuclear factor of activated T-cells (NFAT) leading to the activation of T-cells [4,5]. Cyclosporine and Tacrolimus are two examples of calcineurin inhibitors that have been used extensively as immunosuppressant drugs given to patients after solid organ transplant [6]. Both drugs bind with an adapter immunophilins (Cyclophilin A or FKBP12) to inhibit substrate docking to calcineurin, effectively inhibiting calcineurin activity. Immunosuppressive-immunophilin complexes have been shown to block the LxVP motif binding pocket on calcineurin, exemplifying the importance of this binding pockets for activity [7–10]. Since the regulatory subunit is involved in the LxVP motif binding pocket, the regulatory subunit may be important for substrate specificity of calcineurin.

In addition to the importance of calcineurin in the immune system, studies have shown links between Down syndrome and calcineurin signaling [11,12]. In Down syndrome there is an extra copy of the 21st chromosome which can lead to an approximately 1.5-fold increase in expression of genes on the 21st chromosome. Two genes that are located on the 21st chromosome, DSCR1 (also called RCAN [regulator of calcineurin]) and

DYRK1A are known to inhibit calcineurin signaling. DSCR1 inhibits calcineurin directly through the PxIxIT motif binding pocket and DYRK1A is a kinase that has been shown to phosphorylate NFAT, which is a known substrate of calcineurin [11]. An increase in both DSCR1 and DYRK1A expression is thought to lead to inhibition of calcineurin signaling both directly and through downstream phosphorylation [11,13]. During mammalian development, calcineurin has been shown to play roles in corticogenesis, synaptogenesis and neuritogenesis [14] which suggests that inhibition of the calcineurin signaling pathway could lead to the nervous system phenotypes in Down syndrome. Additionally, previous research in zebrafish has shown that use of the calcineurin inhibitor cyclosporine during development leads to gross morphological brain defects and behavioral abnormalities [15].

In the current study, we have taken advantage of zebrafish as a model for calcineurin signaling inhibition during brain development. Zebrafish allow for *in vivo* imaging of the brain and they exhibit stereotyped behaviors which can be examined during development. We have used antisense oligo morpholinos to inhibit calcineurin during early development and have examined the effects on brain and behavioral development. We have shown that calcineurin inhibition leads to an overall decrease in brain size and behavioral defects, in a regulatory subunit dependent manner. Additionally, the zebrafish with suppressed calcineurin signaling provide an effective model to test potential treatments to alleviate the symptoms of calcineurin-dependent disorders.

Materials and Methods

Zebrafish. Adult wild type zebrafish (*Danio rerio*) were originally obtained from Carolina Biological and maintained at Brown University as a genetically diverse outbred strain. Zebrafish spawn in the morning when kept on a 14 hr light, 10 hr dark cycle in a mixed male and female population. A few tanks with adult fish will produce hundreds of embryos on a daily basis. Zebrafish embryos from 0-3 days post-fertilization (dpf) and zebrafish larvae from 3-7 dpf were grown at 28.5°C on a 12 hour light / 12 hour dark cycle in egg water, containing 60 mg/l sea salt (Instant Ocean) and 0.25 mg/l methylene blue in deionized water. The embryos and larvae were grown in 2L culture trays and were assigned randomly to different experimental groups prior to experimental manipulation or imaging. The sex of embryos and larvae cannot be determined at these early stages, since zebrafish use elusive polygenic factors for sex determination and both males and females have juvenile ovaries between 2.5 and 4 weeks of development [16]. Zebrafish larvae were imaged at 5 dpf when the larvae use nutrients that are available in their yolk sac and display a range of locomotor behaviors. The larvae are approximately 4 mm long during this period. The use of zebrafish in our studies is in compliance with federal (PHS, USDA) and international (AAALAC) guidelines and has been approved by our Institutional Animal Care and Use Committee (IACUC).

Embryo immunolabeling. Calcineurin localization was visualized by immunolabeling of zebrafish embryos. At 3dpf, embryos were fixed in 4% paraformaldehyde in phosphate buffered saline overnight at 4°C. After fixation, embryos were dehydrated in a methanol

series and stored in 100% methanol at -20°C until needed. Embryos were rehydrated through a series into 100% PBS and then washed in PBS with 0.1% Tween (PBST) 3 times for 5 minutes each at room temperature. Embryos were then permeabilized by rinsing in distilled water at room temperature and in prechilled acetone at -20°C for 1 hour. The embryos were then rinsed in distilled water and PBS. The PBS was removed and the embryos were incubated in Invitrogen Image iT FX Signal Enhancer for 30 minutes at room temperature. The embryos were washed 3 times with PBS and then blocked in PBS with 2% DMSO, 0.2% TritonX-100, 2% Normal Goat Serum and 1% Bovine Serum Albumin for 1 hour at room temperature. Embryos were incubated in an anti-calcineurin B antibody (Abcam ab210093) overnight at 4°C. The embryos were washed in PBST with 2% DMSO over 4 hours at room temperature. Embryos were incubated in goat anti rabbit secondary antibody conjugated with alexa Fluor488 (molecular probes A11008) in block overnight at 4°C. Embryos were then washed in PBST with 2% DMSO over 4 hours at room temperature and flat mounted in DABCO and imaged on an Olympus FV3000 confocal microscope. For paraffin sectioning, 7dpf embryos were fixed in 4% paraformaldehyde overnight, and then mounted in paraffin and sectioned. Slides were deparaffinized in xylene and then rehydrated through ethanol series. Antigen retrieval was performed by heating the slides in 0.01 sodium citrate. The slides were treated for endogenous peroxidase by incubating in 0.3% hydrogen peroxide and then blocked with 2.5% NHS from the ImmPACT DAB Peroxidase (HRP) Substrate Kit (Vector SK-4105). Slides were incubated in calcineurin primary antibody overnight at 4°C. Slides were washed and Impress reagent from kit (Vector #MP-7500). Slides were washed and developed using Impact DAB for 2 minutes, which stains calcineurin-

positive cells brown. The slides were then washed in water and counterstained with hematoxylin, a blue nuclear stain. Slides were mounted in cytooseal60 and imaged on a Zeiss Axiovert 200M Light Microscope.

Morpholino injections. To specifically suppress calcineurin regulatory subunits, ppp3r1a and ppp3r1b were knocked down by morpholino injection. Two morpholinos were designed by GeneTools (ppp3r1a: TAACTTGCCTCATTTCCCATTTTGC, ppp3r1b: CTCGCCTCATTTCCCATTTGTGTGGC) to target the translational start site of the transcripts in zebrafish (ppp3r1a: ENSDART00000139560.2 and ppp3r1b:ENSDART00000100869.3). The morpholinos were dissolved in ultrapure water at a 1mM stock concentration and stored in the dark at room temperature. The ppp3r1 morpholinos or GeneTools standard control morpholino (CCTCTTACCTCAGTTACAATTTATA) were diluted into an injection solution containing 0.4 or 0.8 mM morpholino and 0.5 mM fluorescent dextrans (either fluorescein dextran (MW 10,000) or texas red dextran (MW 10,000)) in ultrapure water. Zebrafish embryos were injected at the 1 to 4 cell stages with 1-2 nl of the control, ppp3r1a, ppp3r1b morpholino. After injection, embryos were raised in a 50 ml Petri dish at 28.5°C. Embryos were screened at 1 dpf for fluorescein dextran fluorescence using a NightSea fluorescence system attached to a dissection scope.

Western blotting. Larvae were deyolked in batches as described by Link et al. [17]. Briefly, 15–20 larvae were placed in a 1.5ml Eppendorf tube. Egg water was removed

and 1 ml deyolk buffer (55 mM NaCl, 1.8 mM KCl, 1.25 mM NaHCO₃) was added. Larvae were pipetted through a p200 pipette tip to disrupt the yolk, and then agitated at 1100 RPM for 5 minutes. They were then centrifuged at 300xg for 30 seconds. The larvae were then washed twice by removing the deyolk buffer, adding 1mL wash buffer (110 mM NaCl, 3.5 mM KCl, 2.7 mM CaCl₂, 10 mM Tris-Cl pH8.5), agitating at 1100 RPM for for 2 minutes, and centrifuging at 300xg for 1 minute. After washes, all liquid was removed, and 4 µl 1x SDS buffer (5% 2-Mercapto Ethanol, 2% SDS, 5% glycerol, 0.05 mM Tris pH 6.8, 0.017% Bromophenol Blue in water) per larva was added. The samples were homogenized and 6 larval equivalents of protein isolate was assayed. The blots were labeled with a rabbit-anti-calcineurin B polyclonal antibody (Abcam ab154650) and a mouse-anti-alpha tubulin monoclonal antibody (Sigma T6199). A HRP-conjugated goat-anti-rabbit polyclonal antibody (Abcam ab6721) and a HRP-conjugated goat-anti-mouse polyclonal antibody (Abcam ab97265) were used as secondary antibodies. The chemiluminescence signal was detected using film. Relative amounts of protein were calculated in ImageJ by measuring the intensity of the actin and calcineurin B bands. Each well was normalized to the tubulin band and the control was set at “1.0” for comparison.

Acridine orange staining. Acridine orange fluorescence was used to measure apoptosis in zebrafish as described [18]. Briefly, zebrafish were injected at the 1-4 cell stage with morpholino and at 1dpf were immersed in 2µg/mL solution of acridine orange dye in water. Embryos were immersed for 30 minutes and washed with fresh egg water 3 times.

Embryos were immobilized in low gel temperature agarose in a glass bottom dish and imaged by confocal microscopy.

The zebrafish imaging system. Visually-guided behaviors were recorded using a zebrafish imaging system described previously [19–21]. Briefly, the imaging system is housed in a $180 \times 40 \times 40$ cm cabinet. The top shelf of the cabinet holds an 18 megapixel Canon EOS Rebel T6 digital camera with an EF-S 55–250 mm f/4.0–5.6 IS zoom lens. The camera is connected to a continuous power supply (Canon ACK-E10 AC Adapter) and is controlled by a laptop computer using Canon's Remote Capture software, which is included with the camera. The software is set to interval mode to acquire high-resolution images every 6 sec. The bottom shelf of the cabinet holds a second laptop (Acer Aspire 5517) with a 15.6 inch LCD screen, which is used to provide visual stimuli to the larvae. The 15.6 inch LCD screen has a 1366×768 pixel resolution and a brightness of 220 cd/m^2 . To avoid moiré patterns in the images, a plastic diffuser (Pendaflex 52345) is placed between the LCD screen and the microplates containing the larvae.

Assays for visually-guided behaviors in 5-lane plates. The 5-lane plates were created as described previously [20,22]. Briefly, a one-well plate (ThermoFisher Scientific, Cat. No. 267060) is filled with 50 ml liquid agarose (0.8% agarose in deionized water at 70–80°C). A custom-designed 5-lane mold is placed on top of the agarose, which gels as it cools down to room temperature. After removing the mold, the plate has 5 lanes that are each 70 mm long \times 18 mm wide with 60° sloping edges to reach a 66 mm \times 14 mm

bottom at a 3.5 mm depth. The optics of the plate is optimal when each lane is filled precisely to the rim with egg water. Zebrafish larvae are transferred to the plates 20 min prior to imaging. In the imaging system, visual stimuli are shown to the larvae as PowerPoint presentations. Our previous studies have shown that 5-7 dpf larvae avoid a red bar that moves up and down in the upper half of a 5-lane plate [20,22]. Larvae were imaged at 5 dpf, first for 15 min without visual stimuli and then for 15 min with a moving red bar.

Image Analysis. Acquired images were analyzed in ImageJ using a custom-developed macro. The latest version of this macro (version 26c) can analyze four plates, with multiple treatment groups and changing visual stimuli over time. The software asks the user to enter information about the wells and the periods with different visual stimuli. It opens the first image, splits the color channels, and selects a channel in which the visual stimuli and background have similar intensities. It then subtracts the background, applies an auto-threshold for individual wells, carries out a particle analysis on individual wells, and logs various parameters of the larvae in a 'Results' file. This process is automatically repeated for all subsequent images in a series. The Results file is then sorted based on well number and imported into a MS Excel template. This template compares the larval centroids with the center of the lane to determine if a larva is located 'up' or 'down' in the lane. Similarly, the centroids are used to examine swim speed, together, and edge. Together is defined as the percentage of time that larvae are less than 5 mm apart. Edge is defined as the percentage of time that larvae are less than 3 mm away from the end of the lane or less than 3 mm away from the side of the lane. The ImageJ macro and MS Excel

template are available in Thorn et al. 2017 [21] and future updates will be posted on Brown University's zebrafish website:

<https://www.brown.edu/research/projects/zebrafish/> The automated image analysis contributes to an unbiased approach in studying visually-guided behavior. For example, effects of observer bias and observer fatigue can be avoided. In addition, we took the following two steps avoid other potential causes of bias: 1) we did not discard data from wells or lanes that showed unexpected results and 2) we did not sample at lower frequencies. In future experiments, using preset criteria and predetermined sampling methods, it may be possible to reduce variability in behavior by excluding wells with larvae that show little movement and to reduce file size by analyzing only one in five images. Preliminary results suggest that similar results can be obtained using this lower sampling frequency.

Statistical analysis. Differences were examined for statistical significance using a two-tailed t-test. In most cases, comparisons were made between a single treatment group and a control (two samples with unequal variance). Differences were considered significant when $p < 0.05$. For the behavioral experiments we performed a one-way analysis of variance (ANOVA) with a Tukey post-hoc test to test the difference between groups. Differences were considered significant with a $p < 0.05$

Results

Expression of calcineurin regulatory subunits in Zebrafish

Expression of the calcineurin regulatory subunit was examined by immunolabeling whole mount and paraffin sectioned zebrafish embryos. We found that at 3 dpf calcineurin is widely expressed in the nervous system (Fig 1). In the brain there is wide expression of calcineurin B, with especially notable expression in the optic tectum neuropil (Fig 1a), the pallium (Fig 1b) and the optic chiasm (Fig 1c). Within the cells we see that calcineurin regulatory subunit is excluded from nuclei (Fig 1d,e), and there is high expression within axonal areas such as the optic tectum neuropil in the midbrain (Fig 1a) and the plexiform layers of the eye (Fig 1c,e). There is also expression, albeit lower, in soma layers (Fig 1b). These results show that calcineurin regulatory subunits are widely expressed within the zebrafish brain. The calcineurin regulatory subunit is excluded from nuclei when counterstained with a nuclear stain (not shown), which is consistent with the function of calcineurin in the cytoplasm.

Calcineurin Knockdown by Morpholino Injection

Calcineurin B protein synthesis was knocked down using antisense morpholinos. Zebrafish have two genes coding for regulatory subunits, *ppp3r1a* and *ppp3r1b* (both code for the regulatory B subunit) and morpholinos were designed to target the translation start sites of each subunit. We tested the effectiveness of both morpholinos by western blotting 3 days after morpholino injection. We found that coinjection of both morpholinos was effective at knocking down the regulatory subunit at 3 dpf by 10 fold

when compared to uninjected embryos and 7 fold when compared to standard control injected embryos (Fig 2). Additionally, when separately injected we measured an approximate 50% decrease in calcineurin regulatory subunit expression in either morphants (Fig 2). These results show that our morpholino targeting of calcineurin B is effective method of calcineurin inhibition.

Effects of calcineurin knockdown on brain size

To examine the effect of calcineurin knockdown in the developing zebrafish brain, we injected zebrafish embryos with a 1:1 mixture of both calcineurin regulatory subunit morpholinos. The regulatory subunit is required for calcineurin catalytic activity, by knocking down both calcineurin subunits we will greatly decrease calcineurin catalytic activity. We used an *elav:GFP* transgenic line of fish to measure the brain areas in live embryos, as described in Clift et al. 2015. At 3dpf we measured the cross-sectional area of the forebrain, midbrain and hindbrain as well as the length of the eyes. We injected a lower (3 ng) and higher (6 ng) dose of the morpholino mixture. Using a low dose, we found a significant decrease in the length of the eye (330 μm vs 318 μm ; $p=0.024$), the forebrain area (27,883 μm^2 vs 24,429 μm^2 ; $p=0.030$) and midbrain area (70,994 μm^2 vs 60,594 μm^2 ; $p=0.0045$) in calcineurin regulatory subunit morphants compared to standard control injected (Fig 2). At high levels, we found a significant decrease in eye length (316 μm vs 283 μm ; $p=0.039$), forebrain area (25,861 μm^2 vs 20,491 μm^2 ; $p=0.033$), midbrain area (65,343 μm^2 vs 50,889 μm^2 , $p=0.013$) and hindbrain area (36,565 μm^2 vs 27,747 μm^2 ; $p=0.0039$) in calcineurin regulatory subunit morphants when compared to standard

control morphants (Fig 2). Based on these results, we conclude that calcineurin is critical for brain development.

Effect of calcineurin knockdown on apoptosis

We examined apoptosis in response to calcineurin knockdown, as a potential mechanism affecting brain size. We used acridine orange staining to quantify apoptosis in live zebrafish larvae at 1dpf (Fig 3a). Embryos were injected with a 1:1 mix of both morpholinos or with the standard control morpholino and were assayed at 1dpf for apoptosis in the head region. We found a significant, over 2-fold increase in apoptosis in the r1ab morphants when compared to standard control morphants (100 puncti vs 215 puncti; $p=0.026$) (Fig 3b). These results suggest that calcineurin knockdown increases apoptosis, although further studies are needed to identify the affected cells.

Regulatory Subunit Phenotypes

It has been previously reported that the regulatory subunits of calcineurin may be involved in substrate specificity [2,23]. To test this in zebrafish, we examined brain development after separately knocking down the two calcineurin regulatory subunits (r1a and r1b). We again injected low (1.5ng) and high (3ng) doses of the morpholino into elav:GFP embryos. When injecting the morpholinos separately at low doses, no significant differences were observed in any measured areas of the eyes and brain (Fig 4). At high levels, r1a morphants displayed decreases in eye length (314 μm vs 282 μm ;

p=0.0059), forebrain area (26,222 μm^2 vs 22,029 μm^2 ; p=0.011), midbrain area (67,143 μm^2 vs. 56,344 μm^2 ; p=0.0012) and hindbrain area (36,906 μm^2 vs 31,023 μm^2 ; p=0.0054) compared to standard control morphants (Fig 4). R1b morphants displayed only a decrease in the midbrain (67,143 μm^2 vs 60,434 μm^2 ; p=0.0046). This subunit dependent difference in brain size suggests that there are specific roles for each subunit during brain development.

Effect on Knockdown on Behavior

Calcineurin morphants were examined by automated analysis of behavior. We focused on low doses of morpholinos that do not induce changes in brain size. We injected wild type zebrafish embryos with low levels of r1a, r1b or standard control morpholino, grew the embryos to larval stages, and assayed avoidance behavior at 5dpf. In the avoidance behavior assay [15,20,22], we examine the larvae are examined in two different phases. The first is a baseline phase without stimuli for 15 minutes, followed by presentation of a moving red bar in the top half of the lanes only for the next 15 minutes. We assayed the larva's avoidance (percent down), activity (swim speed), social interaction (percent together) and thigmotaxis (percent edge). In all cases, there was a statistically significant difference between groups as determined by one-way ANOVA (percent Down: $F(5,194)=60.706$, $p=7.5 \times 10^{-38}$, Swim Speed: $F(5,194) = 4.134$, $p=1.4 \times 10^{-3}$, percent Together: $F(5,194) = 28.007$, $p=2.6 \times 10^{-21}$ and percent Edge: $F(5,194) = 3.167$, $p=9.0 \times 10^{-3}$). To compare differences between groups we used Tukey post hoc tests. We found that all 3 morphant groups showed normal avoidance of the bar, with a significant

increase in the percent down, comparing the period without visual stimuli to the period with visual stimuli (control morpholino 55% vs 85%; $p=5.3 \times 10^{-13}$, r1a 63% vs 87%; $p=5.3 \times 10^{-13}$, r1b 60% vs 82%, $p=5.5 \times 10^{-13}$) (Fig 5). Overall, the r1b morphants showed decreased activity with a significant decrease in swim speed with no stimulus present compared to the standard control (36mm/min vs 28mm/min; $p=0.038$) and r1a morphants. (37mm/min vs 28mm/min; $p=0.011$) (Fig 5). The r1a morphant group displayed a significant increase in the percent together in the moving bar phase compared to the standard control morphant (22% vs 29%; $p=0.018$) (Fig 5). Based on these results, we can conclude that even though there are no discernable brain differences in these low dose injected embryos, there is an observable behavioral difference indicating an effect on development even at low levels of calcineurin inhibition.

Discussion

In the current study, we introduce and characterize a new model for studying the inhibition of calcineurin during brain development. We show that calcineurin inhibition leads to microcephaly at 3 dpf and behavioral abnormalities at 5 dpf in a regulatory subunit dependent manner. By examining the alternative knockdowns of each regulator subunit, we can observe effects of each subunit and test whether there are redundant roles of the subunits. Our results show that calcineurin is localized in the embryonic zebrafish brain and plays a role in brain development.

Prior to this work, the expression of the calcineurin regulatory subunit had only been examined through RNA *in situ* hybridization at 1dpf [24]. These experiments showed a broad expression of both subunits within the developing brain. Since we were targeting the regulatory subunit of calcineurin for knockdown, we immunolabeled for the calcineurin regulatory subunits. In both whole mount immunolabeling (Fig 1a,b,c) and immunolabeling of paraffin sections (Fig 1d,e) we found that the calcineurin regulatory subunit is widely expressed throughout the brain and eye. Although it is widely expressed, it is enriched in the axonal layers of the eye. As seen in Figure 1, the calcineurin regulatory subunit is enriched in the inner and outer plexiform layers of the eye, which are known to be axonal layers [25]. Additionally, in Fig 1a there is expression of calcineurin in the optic tectum neuropil and there is calcineurin regulatory subunit expression in the cell bodies of photoreceptors. The high levels of expression in the axons is interesting and has been previously unreported. In our calcineurin regulatory subunit morphants, we found a decrease in brain and eye sizes (Fig 2), indicating that calcineurin is important for brain and eye development. We propose that the decrease in brain size is caused by the increase in apoptosis we observe in our morphants (Fig 3). This increase in apoptosis with inhibited calcineurin signaling is in opposition to previous studies that calcineurin inhibition limits apoptosis after injury [26]. This difference is likely as a result of differences in the brain during development, such as the natural pruning of axons and neuronal apoptosis pathways that are present during development [27].

To better understand the specific roles of the calcineurin subunits, we assayed the regulatory subunits of calcineurin separately to examine their effect on brain

development. R1a and r1b seem to have separate but overlapping roles during development. We found that calcineurin r1a morphants displayed decreases in eye length, and forebrain, midbrain and hindbrain areas, but calcineurin r1b morphants displayed only a decrease in midbrain area. Additionally, each morphant displays differing profiles of behavior. Specifically, the calcineurin r1b morphants displayed a decreased swim speed, which was not observed in the r1a morphants and the r1ab morphants showed an increased percent together, that was not observed in the r1b morphants. This increased percent together could be considered a change in ‘social’ behavior and is unlikely to be caused by visual defects, since both morphants respond well to visual stimuli. Overall, the changes in brain structure and function, point to the importance of the separate subunits in different parts of brain development. These differences may be caused by differences in substrate specificity between holoenzymes with the r1a or r1b subunits, or there may be separate expression patterns of each regulatory subunit. Since the antibody we used in the study recognizes both subunits and the morpholinos don’t fully knockout protein expression (Fig 1c), the immunolabeling experiments did not answer that question.

Our results suggest that calcineurin is indeed integral for brain development and behavior. Additionally, the fact that our results show differing rolls for the two calcineurin subunits in zebrafish adds weight to the idea that regulatory subunits are not redundant and may be important in substrate specificity of the holoenzyme.

In addition to showing the importance of the regulatory subunits in calcineurin activity, we have developed a useful *in vivo* model for assessing calcineurin modulation in zebrafish. Previously, we have shown that zebrafish treated with cyclosporine A, a calcineurin inhibiting drug, during development have brain and behavioral defects [15]. While we knew that this drug, and by association calcineurin, was important during development, the current model more closely replicates the inhibition of calcineurin in disorders such as Down syndrome. The inhibition of calcineurin signaling in Down syndrome may be responsible for some of the phenotypes of Down syndrome, both developmentally and throughout life [11,12]. Studies are examining the potential usefulness of DYRK1A inhibitors (such as INDY and CX-4945) in alleviating some phenotypes of Down syndrome [28,29]. Our model of calcineurin inhibition could be useful in testing current pharmaceutical remedies, as well testing potential candidates for future treatments. Behavioral profiling and cluster analysis are commonly used in zebrafish as a way to evaluate different pharmacological treatments with similar targets in the developing brain [30,31], cluster analysis would be an effective method for screening large libraries for potential Down syndrome therapies and make the drug discovery process more efficient. Our model is a definitive step forward in studying calcineurin modulation and will be useful in testing future therapies.

References:

1. Hoffman A, Taleski G, Sontag E. The protein serine/threonine phosphatases PP2A, PP1 and calcineurin: A triple threat in the regulation of the neuronal cytoskeleton. *Mol Cell Neurosci* 2017; **84**:119–131.
2. Rodríguez A, Roy J, Martínez-Martínez S, *et al.* A conserved docking surface on calcineurin mediates interaction with substrates and immunosuppressants. *Mol Cell* 2009; **33**:616–26.
3. Aramburu J, Garcia-Cózar F, Raghavan A, Okamura H, Rao A, Hogan PG. Selective inhibition of NFAT activation by a peptide spanning the calcineurin targeting site of NFAT. *Mol Cell* 1998; **1**:627–37.
4. Loh C, Shaw KT, Carew J, *et al.* Calcineurin binds the transcription factor NFAT1 and reversibly regulates its activity. *J Biol Chem* 1996; **271**:10884–91.
5. Luo C, Burgeon E, Carew JA, *et al.* Recombinant NFAT1 (NFATp) is regulated by calcineurin in T cells and mediates transcription of several cytokine genes. *Mol Cell Biol* 1996; **16**:3955–66.
6. Flanagan WM, Corthésy B, Bram RJ, Crabtree GR. Nuclear association of a T-cell transcription factor blocked by FK-506 and cyclosporin A. *Nature* 1991; **352**:803–7.
7. Liu J, Farmer JD, Lane WS, Friedman J, Weissman I, Schreiber SL. Calcineurin is a common target of cyclophilin-cyclosporin A and FKBP-FK506 complexes. *Cell* 1991; **66**:807–15.
8. Friedman J, Weissman I. Two cytoplasmic candidates for immunophilin action are revealed by affinity for a new cyclophilin: one in the presence and one in the absence of CsA. *Cell* 1991; **66**:799–806.
9. Grigoriu S, Bond R, Cossio P, *et al.* The molecular mechanism of substrate engagement and immunosuppressant inhibition of calcineurin. *PLoS Biol* 2013; **11**:e1001492.
10. Peti W, Page R. Strategies to make protein serine/threonine (PP1, calcineurin) and tyrosine phosphatases (PTP1B) druggable: Achieving specificity by targeting substrate and regulatory protein interaction sites. *Bioorganic Med Chem* 2015; **23**:2781–2785.
11. Arron JR, Winslow MM, Polleri A, *et al.* NFAT dysregulation by increased dosage of DSCR1 and DYRK1A on chromosome 21. *Nature* 2006; **441**:595–600.
12. Kurabayashi N, Sanada K. Increased dosage of DYRK1A and DSCR1 delays neuronal differentiation in neocortical progenitor cells. *Genes Dev* 2013; **27**:2708–21.
13. Ryoo S-R, Cho H-J, Lee H-W, *et al.* Dual-specificity tyrosine(Y)-phosphorylation regulated kinase 1A-mediated phosphorylation of amyloid precursor protein: evidence for a functional link between Down syndrome and Alzheimer's disease. *J Neurochem* 2008; **104**:1333–44.
14. Kipanyula MJ, Kimaro WH, Etet PFS. The Emerging Roles of the Calcineurin-Nuclear Factor of Activated T-Lymphocytes Pathway in Nervous System Functions and Diseases. *J Aging Res* 2016; **2016**.
15. Clift DE, Thorn RJ, Passarelli EA, *et al.* Effects of embryonic cyclosporine exposures on brain development and behavior. *Behav Brain Res* 2015; **282**:117–24.
16. Liew WC, Orbán L. Zebrafish sex: a complicated affair. *Brief Funct Genomics* 2014; **13**:172–87.
17. Link V, Shevchenko A, Heisenberg C-P. Proteomics of early zebrafish embryos.

BMC Dev Biol 2006; **6**:1.

18. Tucker B, Lardelli M. A rapid apoptosis assay measuring relative acridine orange fluorescence in zebrafish embryos. *Zebrafish* 2007; **4**:113–116.
19. Pelkowski SD, Kapoor M, Richendrfer H a, Wang X, Colwill RM, Creton R. A novel high-throughput imaging system for automated analyses of avoidance behavior in zebrafish larvae. *Behav Brain Res* 2011; **223**:135–44.
20. Richendrfer H, Créton R. Automated high-throughput behavioral analyses in zebrafish larvae. *J Vis Exp* 2013:e50622.
21. Thorn RJ, Clift DE, Ojo O, Colwill RM, Creton R. The loss and recovery of vertebrate vision examined in microplates. *PLoS One* 2017; **12**:e0183414.
22. Clift D, Richendrfer H, Thorn RJ, Colwill RM, Creton R. High-Throughput Analysis of Behavior in Zebrafish Larvae: Effects of Feeding. *Zebrafish* 2014; **11**:455–461.
23. Liu J, Masuda ES, Tsuruta L, Arai N, Arai K. Two independent calcineurin-binding regions in the N-terminal domain of murine NF-ATx1 recruit calcineurin to murine NF-ATx1. *J Immunol* 1999; **162**:4755–61.
24. Hammond DR, Udvardia AJ. Cabin1 expression suggests roles in neuronal development. *Dev Dyn* 2010; **239**:2443–51.
25. Zucker CL, Dowling JE. Centrifugal fibres synapse on dopaminergic interplexiform cells in the teleost retina. *Nature* 1987; **300**.
26. Hui KKW, Liadis N, Robertson J, Kanungo A, Henderson JT. Calcineurin inhibition enhances motor neuron survival following injury. *J Cell Mol Med* 2010; **14**:671–86.
27. Harrington AW, Ginty DD. Long-distance retrograde neurotrophic factor signalling in neurons. 2013; **14**:177–187.
28. Kim H, Lee K-S, Kim A-K, *et al.* A chemical with proven clinical safety rescues Down-syndrome-related phenotypes in through DYRK1A inhibition. *Dis Model Mech* 2016; **9**:839–848.
29. Ogawa Y, Nonaka Y, Goto T, *et al.* Development of a novel selective inhibitor of the Down syndrome-related kinase Dyrk1A. *Nat Commun* 2010; **1**:1–9.
30. Bruni G, Rennekamp AJ, Velenich A, *et al.* Zebrafish behavioral profiling identifies multitarget antipsychotic-like compounds. *Nat Chem Biol* 2016; **12**:559–566.
31. Richendrfer H, Creton R. Cluster analysis profiling of behaviors in zebrafish larvae treated with antidepressants and pesticides. *Neurotoxicol Teratol* 2017.

Figures:

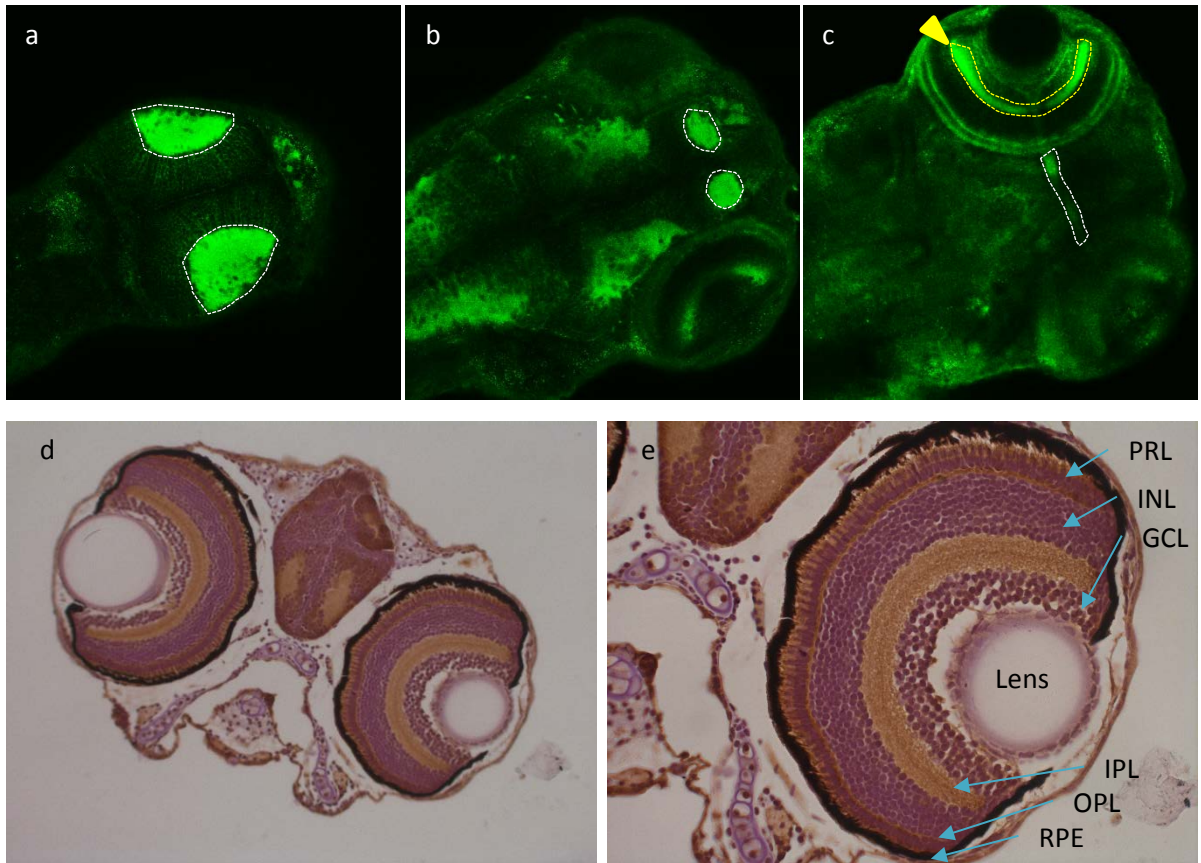


Figure 1. Immunolabeling for Calcineurin B in Zebrafish. Whole mount (a-c) and paraffin sections (d-e) immunolabeled for calcineurin B. a-c) z-sections of 3dpf zebrafish fluorescently labelled for calcineurin B with notable structures encircled. a) Optic tectum neuropil encircled. b) Pallium encircled. c) Optic chiasm encircled in white and inner plexiform layer of the eye encircled in yellow with arrowhead. d-e) 7dpf zebrafish larvae were paraffin sectioned and immunolabeled for calcineurin B (brown) and counterstained with hematoxylin for nuclei (blue). d) Overview of the brain and eyes using a 20x objective. e) Image of the left eye taken with a 40x objective and eye layers labeled. GCL = Ganglion Cell Layer IPL = Inner Plexiform Layer INL = Inner Nuclear Layer OPL = Outer Plexiform Layer PRL = Photoreceptor Layer RPE = Retinal Pigment Epithelium

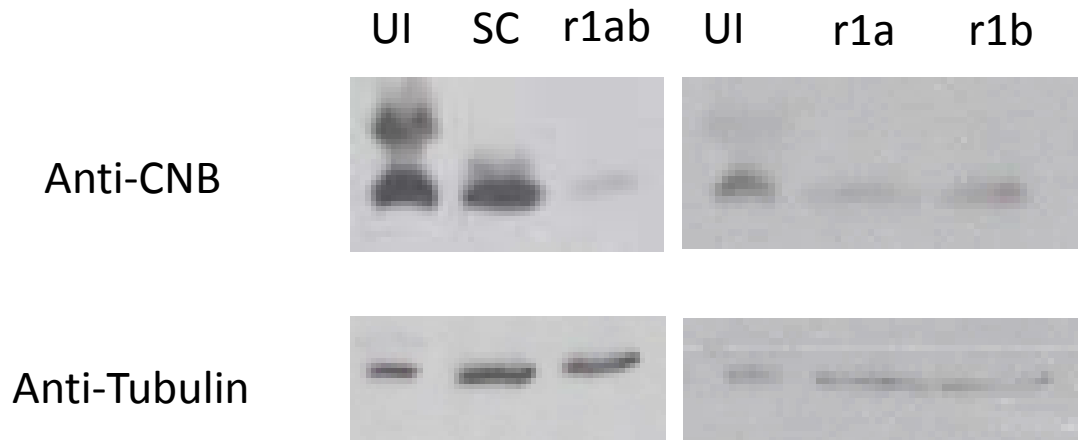


Figure 2. Western Blot for Calcineurin B in Zebrafish. Western blots were performed on 3dpf embryos that were uninjected (UI), injected with a standard control morpholino (SC), coinjected with the ppp3r1a and ppp3r1b morpholino (r1ab), separately injected with the ppp3r1a (r1a) or the ppp3r1b morpholino (r1b). Top row shows blotting with an anti-calcineurin B (Anti-CNB) antibody and the bottom row shows blotting with an anti-tubulin antibody as a loading control. Standard control morpholino is targeted to an intron in human beta globin gene and ordered premade from Genetools. SC and r1ab were injected with 6 ng morpholino total (3ng each morpholino for r1ab) and the r1a and r1b groups were injected with 3 ng morpholino total.

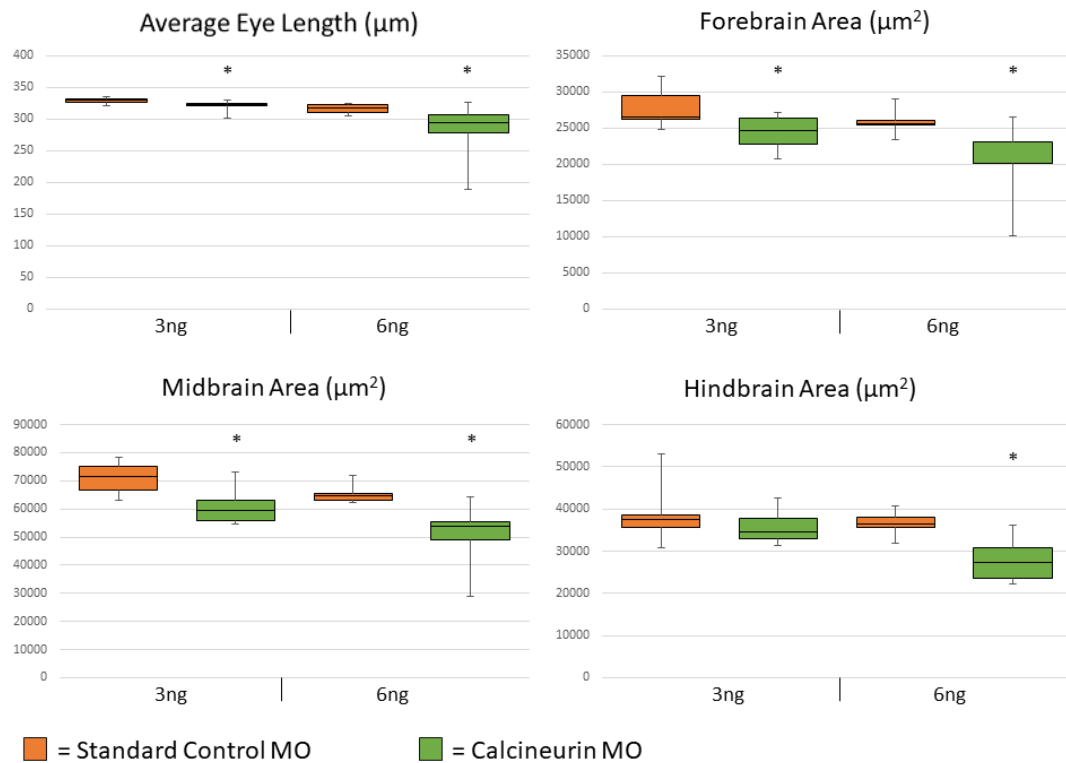


Figure 3. Effects of Calcineurin B knockdown in zebrafish. Elavl3:GFP zebrafish embryos were injected with a combination of the ppp3r1a and ppp3r1b MO or standard control MO totaling 3ng or 6ng of morpholino at the 1-4 cell stage. Results show length for average eye length in μm or cross-sectional area for forebrain, midbrain and hindbrain areas in μm^2 as measured at 3dpf. Two-tailed t-tests was performed and asterisks represent $p < 0.05$ when compared to embryos injected with standard control morpholino. $n = 7$ (3ng SC), 6 (6ng SC), 7 (3ng r1ab), 8 (6ng r1ab)

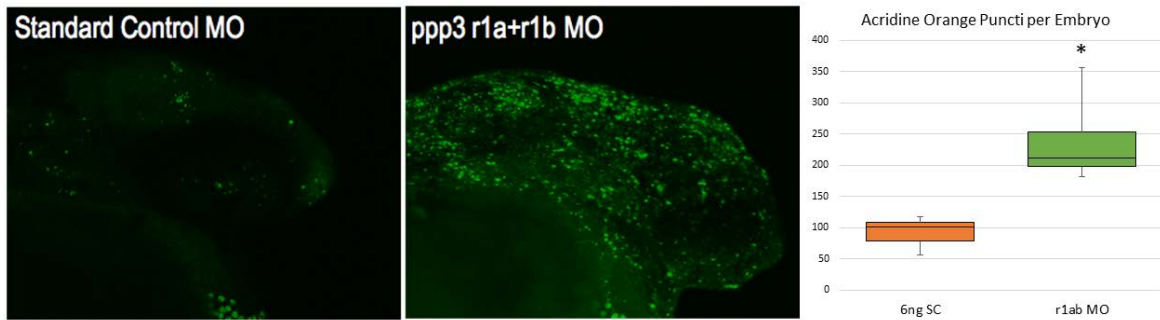


Figure 4. Effect of Calcineurin B knockdown on apoptosis. Wild-type zebrafish embryos were injected with a combination of the ppp3r1a and ppp3r1b MO or standard control MO totaling 6ng of morpholino. At 1dpf, acridine orange was used to label apoptotic cells. Zebrafish embryos were imaged by confocal microscopy and representative maximal z-projections are shown for the standard control and ppp3r1a+r1b injected groups. Apoptosis was measured as the average number of puncti per embryo. Asterisks represents $p < 0.05$ when means were compared by a two-tailed t-test. $n = 3$ (SC) or 4 (r1ab).

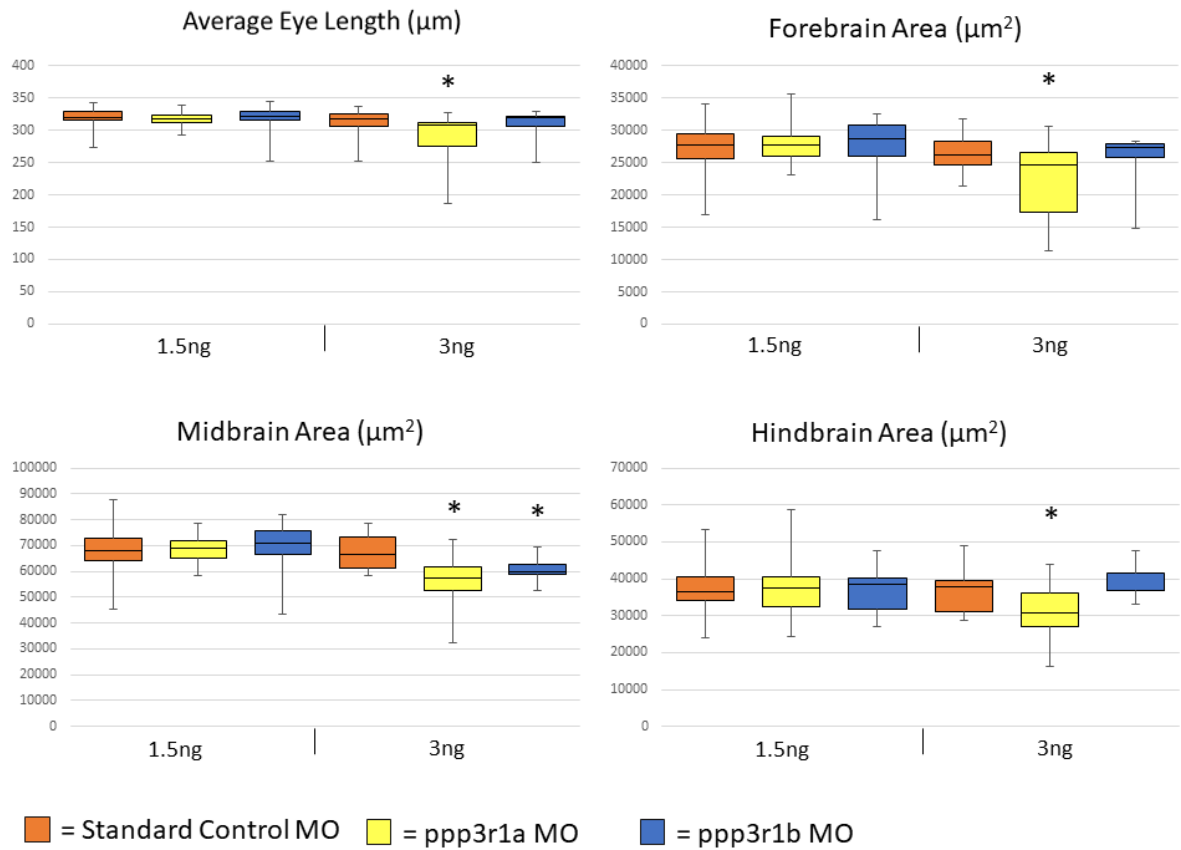


Figure 5. Effects of separate knockdown of Calcineurin B subunits on zebrafish. Elavl3:GFP zebrafish embryos were injected with a ppp3r1a MO, ppp3r1b MO or standard control MO totaling 1.5ng or 3ng of morpholino. Results show average eye length in μm or cross-sectional area for forebrain, midbrain and hindbrain areas in μm^2 as measured at 3dpf. Two-tailed t-tests were performed and asterisks represent $p < 0.05$ when compared to embryos injected with standard control morpholino. N = 36 (1.5ng SC), 25 (3ng SC), 35 (1.5ng r1a), 17 (3ng r1ab), 31 (1.5ng r1b), 9 (3ng r1b)

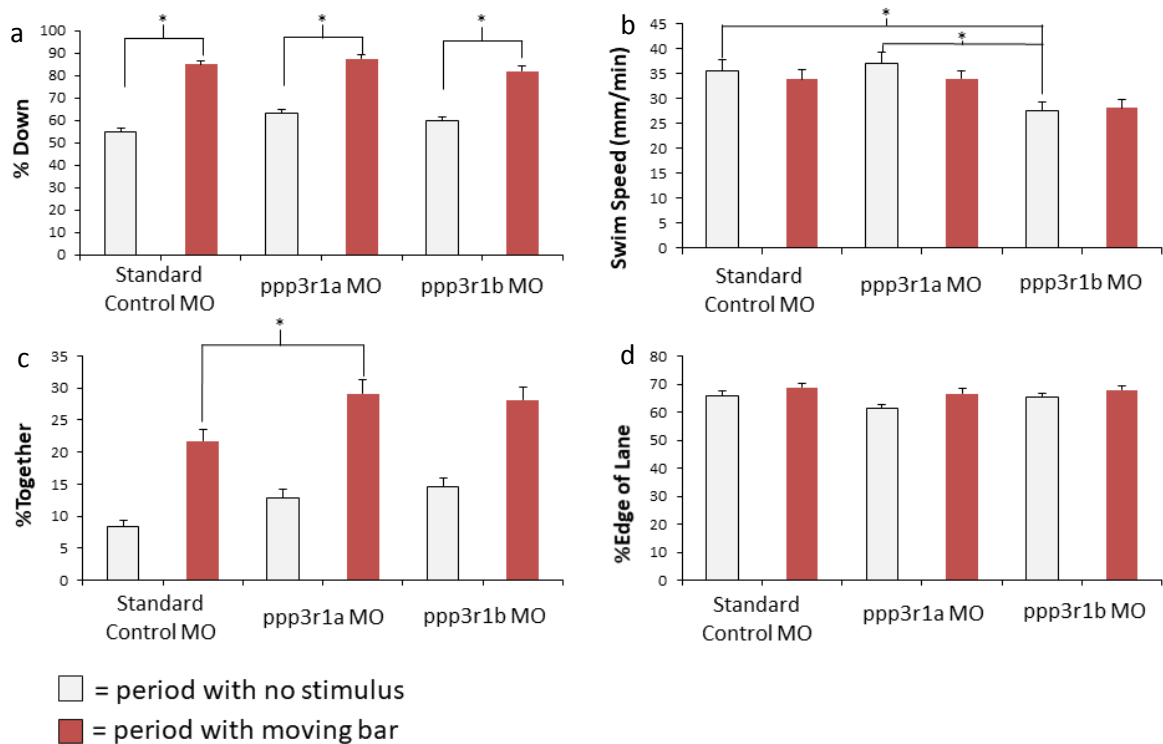


Figure 6. Effects of separate knockdown of Calcineurin B subunits on zebrafish behavior. Wildtype zebrafish embryos were injected with a ppp3r1a MO, ppp3r1b MO or standard control MO totaling 1.5ng of morpholino. Zebrafish were assayed in our 5-lane assay of avoidance behavior for the avoidance of the red bar (a), swim speed (b), percent together (c) and thigmotaxis (d). Two-tailed t-tests were performed and $p < 0.05$ for relevant comparisons are represented by asterisks on the graphs. $n = 34$ wells (SC and r1b) or 32 wells (r1a)

Chapter 4: The loss and recovery of vertebrate vision examined in microplates

Thorn, R. J., Clift, D. E., Ojo, O., Colwill, R. M., & Creton, R. (2017). The loss and recovery of vertebrate vision examined in microplates. *PloS One*, 12(8), e0183414. <https://doi.org/10.1371/journal.pone.0183414>

I designed and performed the experiments in collaboration with DEC and OO, analyzed the results, performed statistical analysis of all data and wrote the manuscript with RC.

Abstract

Regenerative medicine offers potentially ground-breaking treatments of blindness and low vision. However, as new methodologies are developed, a critical question will need to be addressed: how do we monitor *in vivo* for functional success? In the present study, we developed novel behavioral assays to examine vision in a vertebrate model system. In the assays, zebrafish larvae are imaged in multiwell or multilane plates while various red, green, blue, yellow or cyan objects are presented to the larvae on a computer screen. The assays were used to examine a loss of vision at 4 or 5 days post-fertilization and a gradual recovery of vision in subsequent days. The developed assays are the first to measure the loss and recovery of vertebrate vision in microplates and provide an efficient platform to evaluate novel treatments of visual impairment.

Introduction

Visual impairment has been estimated to affect 285 million people worldwide; 246 million people have low vision and 39 million people are blind [1]. While visual impairment is generally irreversible, it may be possible to treat blindness and low vision using novel methodologies in regenerative medicine. Phase I and Phase II clinical trials are in progress using stem cell-based therapies to treat retinal disease [2]. In addition, comparative studies in vertebrate model systems have provided a better understanding of the signaling pathways that regulate regenerative neurogenesis and these signaling pathways may be used to stimulate endogenous regeneration of the visual system [3,4].

However, as novel methodologies are developed, a critical question will need to be addressed: how do we monitor *in vivo* for functional success?

The analysis of visually-guided behaviors in zebrafish larvae provides an effective approach to examine visual function. The development, anatomy and physiology of the visual system is highly conserved in vertebrate species and zebrafish larvae have a cone-dominated retina for full-color vision [5,6]. Hundreds of embryos can be collected from the bottom of a tank on a daily basis. The larvae hatch from their chorion around 3 days post-fertilization (dpf) and have a functional visual system at 5 dpf [6]. By analyzing visually-guided behaviors in zebrafish larvae, it is possible to detect functional defects, even when the visual system appears normal by morphological criteria. For example, specific visual defects have been identified by measuring the optokinetic response (OKR) and optomotor response (OMR). In the OKR assay, zebrafish larvae are immobilized inside a cylindrical drum with rotating black and white stripes. The eyes of the larvae follow the stripes, a response that gradually develops between 3-4 dpf and can be reliably measured at 4-5 dpf [7,8]. OKR assays have been used in zebrafish mutagenesis screens to identify a broad range of genes important for vision [7,9–11]. In OMR assays, zebrafish larvae are placed in elongated swimming tracks and are then presented with moving black and white or colored stripes [11–13]. The larvae swim in the same direction as the moving stripes, a response that can be reliably measured at 6-7 dpf [11,13]. Similar to OKR assays, OMR assays have been used in mutagenesis screens to identify a wide variety of genes important for vision [10,11]. The behavior of zebrafish larvae can be examined in microplates with commercially available imaging systems,

providing unique opportunities for high-throughput applications. Imaging systems such as the ZebraBox from ViewPoint and DanioVision from Noldus are equipped with infrared lights for imaging zebrafish larvae and white lights for studying light-dependent locomotor responses [14–17]. However, these microplate imaging systems are not equipped for a display of more complex visual stimuli.

In the current study, we present several novel assays for measuring visually-guided behaviors in microplates. In the assays, zebrafish larvae are imaged in multiwell or multilane plates while moving objects are presented to the larvae on a computer screen. The developed assays were used for measuring a loss and recovery of visual function in zebrafish larvae. The developed assays are the first to measure the loss and recovery of vertebrate vision in microplates and provide an efficient platform to evaluate novel treatments of visual impairment.

Materials and methods

Ethics Statement

Zebrafish larvae were anesthetized with Tricaine (also known as MS-222) during the UV exposure at 5 days post-fertilization. The use of zebrafish in our studies is in compliance with federal (PHS, USDA) and international (AAALAC) guidelines and has been approved by Brown University's Institutional Animal Care and Use Committee (IACUC).

Zebrafish

Adult wild type zebrafish (*Danio rerio*) were originally obtained from Carolina Biological and have been maintained at Brown University as a genetically diverse outbred strain. Zebrafish spawn in the morning when kept on a 14 hr light, 10 hr dark cycle in a mixed male and female population. A few tanks with adult fish will produce hundreds of embryos on a daily basis. Zebrafish embryos from 0-3 days post-fertilization (dpf) and zebrafish larvae from 3-7 dpf were grown at 28.5°C on a 12 hour light / 12 hour dark cycle in egg water, containing 60 mg/l sea salt (Instant Ocean) and 0.25 mg/l methylene blue in deionized water. The embryos and larvae were grown in 2L culture trays and were assigned randomly to different experimental groups prior to experimental manipulation or imaging. The sex of embryos and larvae cannot be determined at these early stages, since zebrafish use elusive polygenic factors for sex determination and both males and females have juvenile ovaries between 2.5 and 4 weeks of development [18]. Zebrafish larvae were imaged at 4-7 dpf when the larvae use nutrients that are available in their yolk sac and display a range of locomotor behaviors. The larvae are approximately 4 mm long during this period. The larvae are euthanized using an overdose of tricaine (0.04% w/v, pH7). After 20 minutes, the euthanized larvae are transferred to a container with bleach (sodium hypochlorite 6.15%, diluted 1:5 in egg water).

UV illumination

Visual defects were induced by UV illumination using a protocol adapted from Meyers et al. 2012 [19]. In short, 5 dpf zebrafish larvae were anesthetized with 0.012% tricaine

(also known as MS-222) pH7 and transferred to a GeneTools light box containing a cooled LED array, which emits 900 mW of 365 nm light. After 5 min UV illumination, larvae were washed in egg water and were allowed to recover from the anesthesia for 2 hours prior to the analysis of visually-guided behaviors. As controls, larvae were left untreated or were exposed to 0.012% tricaine, without UV-illumination, washed in egg water and were again allowed to recover from the anesthesia for 2 hours prior to the analysis of visually-guided behaviors. The protocol for UV illumination was modified for the rotating-cross assays. We increased the period of UV illumination to 5½ minutes to further reduce visual responses at 5 dpf. In addition, we reduced the tricaine concentration to 0.00025%, since preliminary experiments revealed effects of higher tricaine concentrations in the behavioral assays.

Morpholino injections

To specifically suppress photoreceptor function, Pde6c signaling was knocked down by morpholino injection. A *pde6c* morpholino designed by GeneTools (GCTATCCTTGTCTGCCATGTTTGAA) targets the translational start site of both *pde6c* transcripts in zebrafish (ENSDART0000016224.7 and ENSDART00000169073.1). The GeneTools standard control morpholino (CCTCTTACCTCAGTTACAATTTATA) was injected as a negative control. The morpholinos were dissolved in ultrapure water at a 1mM stock concentration and stored in the dark at room temperature. Prior to injection, the morpholinos were diluted into an injection solution containing 0.6 mM morpholino and 0.5 mM fluorescein dextran (MW

10,000) in ultrapure water. Zebrafish embryos were injected at the 1 to 4 cell stage with 1-2 nl of the control or pde6c morpholino. After injection, embryos were raised in a 50 ml Petri dish at 28.5°C. All embryos were screened at 1 dpf for fluorescein dextran fluorescence using a NightSea fluorescence system attached to a dissection scope.

Western blots

Embryos were deyolked in batches as outlined in Link et al. [20]. Briefly, 15-20 larvae were placed in a 1.5ml Eppendorf tube. Egg water was removed and 1 ml deyolk buffer (55 mM NaCl, 1.8 mM KCl, 1.25 mM NaHCO₃) was added. Larvae were pipetted through a p200 pipette tip to disrupt the yolk, and then agitated at 1100 RPM for 5 minutes. They were then centrifuged at 300xg for 30 seconds. The larvae were then washed twice by removing the deyolk buffer, adding 1mL wash buffer (110 mM NaCl, 3.5 mM KCl, 2.7 mM CaCl₂, 10 mM Tris-Cl pH8.5), agitating at 1100 RPM for 2 minutes, and centrifuging at 300xg for 1 minute. After washes, all liquid was removed, and 4 ul 1x SDS buffer (5% 2-Mercapto Ethanol, 2% SDS, 5% glycerol, 0.05 mM Tris pH 6.8, 0.017% Bromophenol Blue in water) per larva was added. The samples were homogenized and 6 larval equivalents of protein isolate was assayed. The blots were labeled with a rabbit-anti-pde6c polyclonal antibody (Abcam ab198744) and a mouse-anti-alpha tubulin monoclonal antibody (Sigma T6199). A HRP-conjugated goat-anti-rabbit polyclonal antibody (Abcam ab6721) and a HRP-conjugated goat-anti-mouse polyclonal antibody (Abcam ab97265) were used as secondary antibodies. The HRP label

was imaged using a SuperSignal (TM) West Pico PLUS Chemiluminiscent Substrate (Thermo Scientific 34579) and an Azure c600 imaging system (Azure Biosystems).

The zebrafish imaging system

Visually-guided behaviors were recorded using a zebrafish imaging system described previously [21,22], with minor modifications. The imaging system is housed in a $180 \times 40 \times 40$ cm cabinet. The top shelf of the cabinet holds an 18 megapixel Canon EOS Rebel T6 digital camera with an EF-S 55–250 mm f/4.0–5.6 IS zoom lens. The camera is connected to a continuous power supply (Canon ACK-E10 AC Adapter) and is controlled by a laptop computer using Canon's Remote Capture software, which is included with the camera. The software is set to interval mode to acquire high-resolution images every 6 sec. The bottom shelf of the cabinet holds a second laptop (Acer Aspire 5517) with a 15.6 inch LCD screen, which is used to provide visual stimuli to the larvae. The 15.6 inch LCD screen has a 1366×768 pixel resolution and a brightness of 220 cd/m^2 . To avoid moiré patterns in the images, a plastic diffuser (Pendaflex 52345) is placed on the LCD screen. The plates with the larvae are placed on top of the diffuser approximately 10 minutes prior to imaging and the LCD screen warms the plates to 26°C (4°C above ambient). The zebrafish imaging system can be duplicated on a limited budget and can image 4 microplates simultaneously, while retaining sufficient resolution to identify the location and orientation of zebrafish larvae. Brown University currently has 8 zebrafish imaging systems set up in two laboratories, with a combined capacity of imaging 32 microplates simultaneously. The scalable capacity of the system makes it possible to

examine subtle visual defects in more detail or initiate medium- to high-throughput applications. The imaging system is unique in the display of complex visual stimuli in microplates.

Assays for visually-guided behaviors in 5-lane plates

The 5-lane plates were created as described previously [22,23]. Briefly, a one-well plate (ThermoFisher Scientific, Cat. No. 267060) is filled with 50 ml liquid agarose (0.8% agarose in deionized water at 70-80°C). A custom-designed 5-lane mold is placed on top of the agarose, which gels as it cools down to room temperature. After removing the mold, the plate has 5 lanes that are each 70 mm long \times 18 mm wide with 60° sloping edges to reach a 66 mm \times 14 mm bottom at a 3.5 mm depth. The optics of the plate is optimal when each lane is filled precisely to the rim with egg water. Zebrafish larvae are transferred to the plates 20 min prior to imaging. In the imaging system, visual stimuli are shown to the larvae as PowerPoint presentations. Our previous studies have shown that 5-7 dpf larvae avoid a red bar that moves up and down in the upper half of a 5-lane plate [22,23]. The current study introduces the following new assays for 5-lane plates. 1) The bar-dots assay: in this assay larvae are imaged for 15 min on a white background, 15 min with a moving red bar in the upper half of a lane, and 15 min with 0.5 mm red dots moving up in a lane (S1 File). 2) The two-bar assay: in this assay larvae are imaged for 15 min on a white background, 15 min with a moving red bar in the upper half of a lane, and 15 min with a moving red bar in the lower half of a lane (S2 File). 3) The 4x repeated two-bar assay: in this assay larvae are imaged for 20 min on a white background, 10 min

with a moving red bar in the upper half of a lane, and 10 min with a moving red bar in the lower half of a lane. The two-bar sequence is shown to the larvae four times in a row (S3 File). 4) The bar-dots RGBY assay: in this assay larvae are imaged for 10 min on a white background, 10 min with a moving bar in the upper half of a lane, and 10 min with 1 mm dots moving up in a lane. The blank-bar-dots sequence is shown to the larvae in red, green, blue and yellow (S4 File).

Assays for visually-guided behaviors in 6-well plates

The 6-well plates were created as described previously [21]. In summary, the wells of a 6-well plate are filled with 5 ml liquid agarose (0.8% agarose in deionized water at 70-80°C). After the agarose solidifies, a plastic vial is used to stamp a 27 mm diameter × 5 mm deep hole in the agarose. The optics of the plate is optimal when each well is filled with egg water precisely to the rim of the agarose. Zebrafish larvae are transferred to the wells 20 min prior to imaging. The current study introduces the following new assays for 6-well plates. 1) Rotating spectral cross assay: larvae are imaged for 20 min on a light background, 10 min with a cross that rotates in a clockwise direction, and 10 min with a cross that rotates in a counter-clockwise direction. The pair of rotating crosses are shown to the larvae in red, green, blue, yellow, and cyan and rotate at $90^\circ/5$ sec which corresponds to 3 rounds per minute. The background is set to a light gray for optimal color separation during the image analysis (S5 File). 2) The 4x repeated red cross assay: larvae are imaged for 20 min on a light gray background, 10 min with a red cross that rotates in a clockwise direction, and 10 min with a red cross that rotates in a counter-

clockwise direction. The two-cross sequence is shown to the larvae four times in a row and crosses rotate at 3 rounds per minute (S6 File).

Image analysis

Acquired images were analyzed in ImageJ using a custom-developed macro. This macro (version 26bc) can analyze four microplates, with multiple treatment groups and changing visual stimuli over time. The software asks the user to enter information about the wells and the periods with different visual stimuli. It opens the first image, splits the color channels, and selects a channel in which the visual stimuli and background have similar intensities. It then subtracts the background, applies an auto-threshold for individual wells, carries out a particle analysis on individual wells, and logs various parameters of the larvae in a 'Results' file. This process is automatically repeated for all subsequent images in a series. The Results file is then sorted based on well number and imported into a MS Excel template. This template compares the larval centroids with the center of the lane to determine if a larva is located 'up' or 'down' in the lane. The template also compares the larval centroids with the larval center of the 'bounding box' to determine the larval orientation in specific quadrants of the well. For example, a larva is considered to have a clockwise orientation if it faces up ($\pm 45^\circ$) or right ($\pm 45^\circ$) in the top-left quarter of a well. The ImageJ macro (S7 File) and MS Excel template (S8 File) are available in the supplementary information and future updates will be posted on Brown University's zebrafish website:

<https://www.brown.edu/research/projects/zebrafish/> The automated image analysis

contributes to an unbiased approach in studying visually-guided behavior. For example, effects of observer bias and observer fatigue can be avoided.

Statistical analysis

The obtained results were averaged in MS Excel. To assure that all data points are independent, even in wells with multiple larvae, we analyzed the data on a per well basis (n=number of wells). Within each well, we consider all 'larval measurements' equally. For example, a well with 5 larvae imaged for 10 minutes at 10 frames per minute, will provide 500 larval measurements, which are averaged as a whole. The averaging over a 10 minute period reduces variability between wells and makes it possible to obtain reliable data with a relatively low number of larvae. However, it is possible to analyze the data at shorter intervals, which could provide additional information on changes within the 10 minute period. The percentage of larval measurements in the upper half of the lane (% up) and the percentage of larval measurements with a clockwise orientation (% cw) have a normal distribution. Differences in % up and % cw were tested for significance using a two-tailed t-test with unequal variance. The calculated p-values were adjusted with a Bonferroni correction for multiple comparisons. Differences in behavior were considered significant when $p < 0.01$. When differences in behavior were significant at a 95% confidence limit ($p < 0.05$), the results were described in the text, but not indicated with an asterisk in the graphs. The conservative Bonferroni correction and stringent p-value help to avoid type I errors (false positives), which is important in assay development. For repeated measures over time, we used a one-way repeated measures

analysis of variance (ANOVA) with stimulus acting as the independent variable and %up or %cw as dependent variables, with a Greenhouse-Geisser correction when sphericity was violated. All ANOVAs were carried out using IBM SPSS Statistics 24.

Code availability

The ImageJ macro and MS Excel template for automated analyses of behavior are included in the supplementary information.

Data availability

The original imaging data is available upon request. The PowerPoint files with visual stimuli are included in the supplementary information.

Results

Automated analysis of behavior

Visually-guided behaviors were measured using a custom-built imaging system for automated analyses of behavior [21,22]. This imaging system is easy to use, can be built on a limited budget and makes use of open-source software for image analysis (Fig 1). Images are acquired using an 18 megapixel Canon camera and visual stimuli are shown to zebrafish larvae as PowerPoint presentations on a computer screen. In the current study, we developed a new ImageJ macro and MS Excel template for automated analyses

of microplates with changing visual stimuli over time. The macro includes dialog boxes and algorithms for the identification of experimental groups and periods with different visual stimuli. The imaging system and software make it possible to measure the location and orientation of larvae in a set of four microplates, while moving objects with different colors are presented to the larvae.

Assays for visually-guided behaviors in 5-lane plates

Several new assays were developed to examine vision of 5 day-old zebrafish larvae in 5-lane plates (Fig 2). These assays expand on previous studies, which showed that zebrafish larvae avoid a moving red bar [22,23]. We first developed a ‘bar-dots assay’, which combines a red bar that moves up and down in the upper half of the plate with an array of red dots that move continuously up in the plate (Fig 2a). We found that the larvae avoid the area with the moving bar and swim in the same direction as the moving red dots (Fig 2c). The responses to the two visual stimuli differ significantly and this difference may be used as a robust measure of vision ($p=5 \times 10^{-11}$, $n=10$ lanes). In a second assay, called the ‘two-bar assay’, we showed a moving red bar in the upper half of the plate followed by a moving red bar in the lower half of the plate (Fig 2b). In this assay, larvae avoid the areas with the moving bars (Fig 2d) and larval locations differ significantly in response to the first and second bar ($p=4 \times 10^{-6}$, $n=10$ lanes). The bar-dots and two-bar assays described above were carried out using two 5-lane plates with 5 larvae per lane (50 larvae total). To examine if reliable results can be obtained with a lower number of larvae, we imaged two 5-lane plates with one larva per lane (10 larvae total). The same experiment was carried

out twice without averaging the results, which allowed for an evaluation of the assay with only 10 larvae. Visual responses were examined in a '4x repeated two-bar assay', which includes a moving red bar in the upper half of the plate (bar 1) and a moving red bar in the lower half of the plate (bar 2), shown to the larvae four times in a row (Fig 2e). We tested the effect of stimulus on percent up in experiment 1 and experiment 2 by performing a repeated measures ANOVA. We found that in both cases the stimulus had a significant effect on % up at a critical value of $p=0.05$ with a Greenhouse-Geisser correction for sphericity (experiment 1: $F(2.955,26.594)=11.667$, $p=4.9 \times 10^{-5}$ and experiment 2: $F(3.655,32.893) = 3.622$, $p=0.017$). The measurements with 1 larva per lane are not as robust as the measurements with 5 larvae per lane, which may be expected since the experiments with 1 larva per lane contain 5x fewer observations than the experiments with 5 larvae per lane. Group effects with 5 larvae per lane are unlikely, since robust shoaling behaviors are only observed later in development [24,25]. S1 Table provides a summary of the assays at 5 dpf. In addition, we examined if the 4x repeated two-bar assay could be used to detect visual responses in younger larvae, at 4 dpf. In this experiment, two 5-lane plates were imaged using 5 larvae per lane and significant differences were observed when comparing the average of all bar 1 and bar 2 periods ($p=4 \times 10^{-8}$, $n=10$ lanes). Overall, the results in the 5-lane plates suggest that robust measurements of vision can be obtained at 4 and 5 dpf.

Assays for visually-guided behaviors in 6-well plates

Novel ‘rotating cross’ assays were developed to examine vision of zebrafish larvae in 6-well plates (Fig 3). As a visual stimulus, we created a cross, which first rotates in a clockwise direction and then in a counter-clockwise direction. The rotating cross was colored red, green, blue, yellow, or cyan (Fig 3a) and is shown on a light gray background for optimal color separation during the image analysis. We found that 5 day-old zebrafish larvae display a clockwise orientation when the cross rotates clockwise and display a counter-clockwise orientation when the cross rotates counter-clockwise (Fig 3b). This change in larval orientation is robust in all colors (e.g. $p=1 \times 10^{-15}$ in red, $p=1 \times 10^{-12}$ in green, $p=1 \times 10^{-11}$ in blue). To examine if reliable results can be obtained with a lower number of larvae, we imaged two 6-well plates with one larva per well (12 larvae total). The same experiment was carried out twice without averaging the results, which allowed for an evaluation of the assay with only 12 larvae. In these experiments, we showed a red cross rotating clockwise followed by a red cross rotating counter-clockwise and repeated this sequence four times (Fig 3c). We tested the effect of stimulus on clockwise orientation in experiment 1 and experiment 2 by performing a repeated measures ANOVA. We found that in both cases the stimulus had a significant effect on the percent clockwise at a critical value of $p=0.05$ with a Greenhouse-Geisser correction for sphericity in experiment 2 (experiment 1: $F(8,88)=4.843$, $p=5.4 \times 10^{-5}$ and experiment 2: $F(4.258,46.833) = 8.480$, $p=2.2 \times 10^{-5}$). S1 Table provides a summary of all assays at 5 dpf, using 10-60 larvae per experimental group. In general, the table indicates that one needs 12 larvae per experimental group to measure significant visual responses. However, the assays become substantially more sensitive using 50-60 larvae per

experimental group. We also examined if a 4x repeated rotating red cross assay could be used to detect visual responses in younger larvae, at 4 dpf. In this experiment, two 6-well plates were imaged using 5 larvae per well and significant differences were observed when comparing the average of all clockwise and counter-clockwise periods ($p=4 \times 10^{-11}$, $n=12$ wells). Since the larvae are located only a few millimeters away from the computer screen, the larvae will view the visual stimuli differently than a distant observer. For example, an approaching arm of the rotating cross and an approaching bar in the multilane plates may look similar from the viewpoint of a larva. The main differences between the assays are the measurement of larval location (multilane plates) vs. larval orientation (6-well plates) and the shape of the swimming area. In multilane plates, larvae typically swim away from the moving bar until they reach a corner at the end of the lane. In contrast, larvae in 6-well plates do not have an endpoint, as they can continue to swim around in the well. Based on the results in 6-well plates, we conclude that robust measurements of vision can be obtained with the rotating cross assay using either 5 larvae per well or using 1 larva per well with repeated visual stimuli.

UV-induced visual defects examined in 5-lane plates

The 5-lane plates were used to examine visual defects and the recovery from these defects. Visual defects were induced at 5 dpf by UV illumination, using a protocol adapted from Meyers et al. (2012) [19]. The larvae were anesthetized with tricaine during a 5 min UV-illumination period and tricaine-treated larvae, without UV illumination, were used as controls. Larvae from both groups were washed in egg water and allowed to

recover from the anesthetic for 2 hours prior to the behavioral assays. Visual defects were first examined in 5-lane plates, with 5 larvae per lane, using a modified bar-dots assay carried out in red, green, blue and yellow (Fig 4). The tricaine-treated control larvae displayed clear visual responses in red, green, blue and yellow at 5, 6 and 7 days post-fertilization (dpf). In each of these cases, we confirmed that the response to the bar was significantly different from the response to the dots ($p < 0.01$, $n = 10$ lanes). UV-illuminated larvae did not respond to visual stimuli in any color at 5 dpf (Fig 4a), consistent with prior studies showing a destruction of photoreceptor cells by high-intensity light [19]. At 6 dpf, the UV-illuminated larvae showed a gradual recovery of vision, i.e. the larvae displayed a significant visual response in red, green and yellow (Fig 4b). These responses are lower than the responses observed in the controls ($p < 0.01$ in all colors), indicating that the recovery of vision is incomplete at 6 dpf. At 7 dpf, the UV-illuminated larvae show a significant visual response in red, blue and yellow (Fig 4c). The visual response in red, green and yellow is suppressed in the UV-illuminated larvae compared to the tricaine-treated controls ($p < 0.01$, $p < 0.05$, $p < 0.01$, respectively) indicating that the recovery of vision still incomplete at 7 dpf.

UV-induced visual defects examined in 6-well plates

We used the rotating-cross assay in 6-well plates to examine UV-induced visual defects and the recovery from these defects. The rotating cross assay was carried out with 5 larvae per well as shown in Figure 3b. Untreated and tricaine-treated control larvae showed a robust response to all colors at 5, 6, and 7 dpf (Fig 5). In each color, the

response to the cross rotating clockwise was significantly different from the response to the cross rotating counter-clockwise ($p < 0.01$, $n = 12$ wells). UV-illuminated larvae did not display a significant response to the visual stimuli in any color at 5 dpf (Fig 5a). To examine if UV illumination affects motor performance, we analyzed the average swim speed during the first 20 minutes of the experiment without visual stimuli. We found that UV illumination does not have a significant effect on swim speed (6 mm/min in the tricaine controls ($N = 11$ wells, 55 larvae, $SEM = 1.82$) vs. 5 mm/min in the UV exposure group ($N = 10$ wells, 50 larvae, $SEM = .814$), $p = .527$, two tailed t-test). Thus, the UV-treatment affects the response to visual stimuli, but does not affect swim speed in 5 dpf larvae. UV-treated larvae did not display a significant response to visual stimuli at 6 dpf. However, a partial recovery of vision was observed at 7 dpf. The 7 dpf larvae displayed a significant visual response in red, green, blue and cyan, but not in yellow (Fig 5c). The response in red, blue, yellow and cyan was reduced in the UV-illuminated larvae as compared to the tricaine-treated controls ($p < 0.01$, $p < 0.05$, $p < 0.05$, $p < 0.01$, respectively), indicating that the recovery of vision still incomplete at 7 dpf. Based on these results, we conclude that the rotating cross assay is an efficient tool to examine UV-induced visual defects and the gradual recovery from these defects.

Visual defects induced by pde6c knockdown

A specific defect in visual function was induced by morpholino-mediated knockdown of the phosphodiesterase Pde6c, a key signal transduction protein in retinal cone cells [26]. Previous studies have shown that low morpholino concentrations are effective in the

zebrafish retina at 4 dpf, but not at 5 dpf, which allows one to examine a loss and recovery of visual function [27]. We examined Pde6c protein levels in 4 dpf larvae by Western blotting (Fig 6a). We found Pde6c protein levels are reduced 49% in pde6c morpholino-injected larvae as compared to control morpholino-injected larvae (ratiometric measurements with Tubulin protein levels in the denominator). These results indicate that the pde6c morpholino is effective in knocking down Pde6c levels. Visual defects were examined using 1 larva per well and the 4x repeated rotating red cross assay, starting at 4 dpf. Larvae injected with control morpholinos displayed a robust response to each of the four pairs of rotating red crosses at 4 dpf [$F(4.468,151.914)=8.007$, $p=2.7 \times 10^{-6}$, with Greenhouse-Geisser correction for sphericity violation] and 5 dpf [$F(5.787,196.756)=37.813$, $p=1.1 \times 10^{-29}$, with Greenhouse-Geisser correction for sphericity violation] (Fig 6). In each pair of crosses, the response to the cross rotating clockwise was significantly different from the response to the cross rotating counter-clockwise ($p < 0.01$). The pde6c morpholino-injected larvae did not display a significant visual response at 4 dpf [$F(4.983,159.454)=1.665$, $p=0.146$, with Greenhouse-Geisser correction for sphericity violation]. To examine if pde6c morpholinos affect motor performance, we analyzed the average swim speed during the first 20 minutes of the experiment without visual stimuli. We found that the pde6c morpholino does not have a significant effect on swim speed (17 mm/min with the control morpholino (N=36 wells, 36 larvae, SEM = 3.00) vs. 18 mm/min with the pde6c morpholino (N=34 wells, 34 larvae, SEM = 3.64), $p=.763$, two-tailed ttest). Thus, pde6c morpholino-injected larvae display normal swim speeds at 4 dpf, but don't respond to visual stimuli. At 5 dpf, the pde6c morpholino-injected larvae display a near complete recovery of vision

[$F(4.925,157.589)=21.992$, $p=1.6 \times 10^{-16}$]. Based on these results, we conclude that the 4x repeated rotating red cross assay can be used to examine morpholino-induced visual defects and the recovery from these defects.

Discussion

In the current study, we introduce new software and algorithms for automated analyses of visually-guided behaviors and present novel assays for measuring vertebrate vision in microplates. In addition, we used the developed methodologies to detect visual defects and the gradual recovery from these defects.

The software was written as an open-source ImageJ macro and was designed for automated analyses of microplates with multiple visual stimuli that change over time. With this macro, it is possible to measure the location and orientation of larvae in a large field of view (4 microplates per image), while various red, green, blue, yellow or cyan objects are presented to the larvae. The developed software builds on a previously developed ImageJ macro that we developed for automated analyses of zebrafish behavior in microplates [22,23]. However, the previously developed macro was not suitable for automated analyses of multi-color experiments. Both the previously developed macro and the new macro presented in this study allow for the analysis of microplates while objects are displayed to zebrafish larvae, which is not feasible using any commercially-available imaging system.

The developed assays in 5-lane plates build on our previous studies showing that zebrafish larvae avoid a moving red bar [22,23]. We found that the red bar assay can be substantially improved by including additional visual stimuli. In the ‘bar-dots’ assay, 5 dpf larvae first swim away from the moving bar into the lower half of the lane, and then swim in the same direction as the moving dots into the upper half of the lane. These changes in larval location are robust and provide a reliable measure of vision. Similarly, the two-bar assay and 4x repeated two-bar assay can be used to drive 5 dpf larvae up and down a lane. In the ‘rotating cross’ assay in 6-well plates, larvae display a clockwise orientation when the cross rotates clockwise, and a counter-clockwise orientation when the cross rotates counter-clockwise. In this assay, larvae respond well to all colors tested, including red, green, blue, yellow and cyan on a light background. The rotating cross assay is robust and can be used to evaluate vision when a limited number of larvae are available. The response of zebrafish larvae to moving objects may be used in nature to avoid predators and capture prey, depending on the size of the object [28]. Thus, the larvae may view the moving bar as a looming predator and the moving dots as prey. Zebrafish larvae are also known to maintain a fixed location in a water stream, which is the basis of an orienting behavior in the optomotor response [29]. Similarly, the observed response to the rotating cross may reflect an optomotor-related orienting behavior. The 4x repeated two-bar assay and the 4x repeated rotating cross assays were used to reliably measure visual responses early in development, at 4 dpf. Thus, larvae displayed a visual response to the moving bar and rotating cross at same developmental stage as the optokinetic response, which can be reliably measured at 4 dpf [7,8] and 2-3 days earlier than the optomotor response, which can be reliably measured at 6-7 dpf [11,13].

The developed methodologies were used to measure a loss and recovery of vision. Visual defects were induced at 5 dpf by UV-illumination, using an adapted protocol from Meyers et al. [19]. These UV-illuminated larvae did not display a significant response to visual stimuli in a multicolor bar-dots assay or a multicolor rotating cross assay. However, vision gradually recovers in 1-2 days after UV-illumination. This rapid recovery of vision is consistent with previous studies showing retinal regeneration following light-induced ablation of photoreceptor cells [19] and a rapid recovery of vision after cone photoreceptor ablation using a nitroreductase system [30]. In the rotating cross assay, 7dpf larvae displayed a recovery of visual responses in red, green, blue and cyan, but not in yellow. The suppressed response in yellow could indicate a persistent UV-induced defect in blue photoreceptor cells, i.e. the yellow stimuli and light background are likely indistinguishable without seeing blue. Apart from the UV illumination, we also used *pde6c* morpholinos to temporarily block photoreceptor function.

Pde6c is a signaling protein in cone photoreceptors and mutations in the *pde6c* gene lead to visual defects in both zebrafish and humans [26]. Zebrafish larvae express *pde6c* in cone photoreceptors and homozygous *pde6c* mutant larvae display a rapid degeneration of cone photoreceptors during early larval stages [26,31]. Electroretinograms and optokinetic assays revealed that the *pde6c* mutant larvae are blind, consistent with the idea that early larval vision depends on cone photoreceptors. Rods do not degenerate in *pde6c* mutant fish and an optokinetic response can be observed at 3 weeks post-fertilization in low-light conditions [31]. We chose to use morpholinos, instead of mutant

fish lines, based on previous studies showing that morpholino concentrations can be adjusted to affect the zebrafish retina at 4 dpf, but not at 5 dpf [27]. While morpholinos can have off-target effects [32], the *pde6c* morpholinos effectively suppressed Pde6c protein levels, did not affect baseline motor performance, and induced visual defects at 4 dpf consistent with the mutant phenotype. In addition, we found that visual responses recover at 5 dpf, suggesting that *pde6c* morpholinos may be used to examine both the loss and recovery of visual function.

Based on the obtained results, we conclude that the developed assays are efficient in measuring the loss and recovery of visual function. The developed assays are the first to measure the loss and recovery of vertebrate vision in microplates and provide an efficient platform to evaluate novel treatments of visual impairment.

Acknowledgments

We thank Emily Passarelli for her contributions to the development of the behavioral assays.

Author contribution

RJT, RMC and RC planned the project and experiments. RJT, DEC, OO and RC performed the experiments and analyzed the results. RMC contributed to the

interpretation of the results. RJT and RC created the ImageJ macro and wrote the manuscript. All authors reviewed the manuscript.

References:

1. Pascolini D, Mariotti SP (2012) Global estimates of visual impairment: 2010. *Br J Ophthalmol* 96: 614-618.
2. Zarbin M (2016) Cell-Based Therapy for Degenerative Retinal Disease. *Trends Mol Med* 22: 115-134.
3. Brockerhoff SE, Fadool JM (2011) Genetics of photoreceptor degeneration and regeneration in zebrafish. *Cell Mol Life Sci* 68: 651-659.
4. Alunni A, Bally-Cuif L (2016) A comparative view of regenerative neurogenesis in vertebrates. *Development* 143: 741-753.
5. Gestri G, Link BA, Neuhauss SC (2012) The visual system of zebrafish and its use to model human ocular diseases. *Dev Neurobiol* 72: 302-327.
6. Chhetri J, Jacobson G, Gueven N (2014) Zebrafish--on the move towards ophthalmological research. *Eye (Lond)* 28: 367-380.
7. Brockerhoff SE, Hurley JB, Janssen-Bienhold U, Neuhauss SC, Driever W, et al. (1995) A behavioral screen for isolating zebrafish mutants with visual system defects. *Proc Natl Acad Sci U S A* 92: 10545-10549.
8. Easter SS, Jr., Nicola GN (1996) The development of vision in the zebrafish (*Danio rerio*). *Dev Biol* 180: 646-663.
9. Brockerhoff SE, Dowling JE, Hurley JB (1998) Zebrafish retinal mutants. *Vision Res* 38: 1335-1339.
10. Muto A, Orger MB, Wehman AM, Smear MC, Kay JN, et al. (2005) Forward genetic analysis of visual behavior in zebrafish. *PLoS Genet* 1: e66.
11. Neuhauss SC, Biehlmaier O, Seeliger MW, Das T, Kohler K, et al. (1999) Genetic disorders of vision revealed by a behavioral screen of 400 essential loci in zebrafish. *J Neurosci* 19: 8603-8615.
12. Orger MB, Baier H (2005) Channeling of red and green cone inputs to the zebrafish optomotor response. *Vis Neurosci* 22: 275-281.
13. Orger MB, Smear MC, Anstis SM, Baier H (2000) Perception of Fourier and non-Fourier motion by larval zebrafish. *Nat Neurosci* 3: 1128-1133.
14. Elbaz I, Yelin-Bekerman L, Nicenboim J, Vatine G, Appelbaum L (2012) Genetic ablation of hypocretin neurons alters behavioral state transitions in zebrafish. *J Neurosci* 32: 12961-12972.
15. Emran F, Rihel J, Dowling JE (2008) A behavioral assay to measure responsiveness of zebrafish to changes in light intensities. *J Vis Exp*.
16. Rihel J, Prober DA, Arvanites A, Lam K, Zimmerman S, et al. (2010) Zebrafish behavioral profiling links drugs to biological targets and rest/wake regulation. *Science* 327: 348-351.
17. Scott CA, Marsden AN, Slusarski DC (2016) Automated, high-throughput, in vivo analysis of visual function using the zebrafish. *Dev Dyn* 245: 605-613.
18. Liew WC, Orban L (2014) Zebrafish sex: a complicated affair. *Brief Funct Genomics* 13: 172-187.
19. Meyers JR, Hu L, Moses A, Kaboli K, Papandrea A, et al. (2012) beta-catenin/Wnt signaling controls progenitor fate in the developing and regenerating zebrafish retina. *Neural Dev* 7: 30.

20. Link V, Shevchenko A, Heisenberg CP (2006) Proteomics of early zebrafish embryos. *BMC Dev Biol* 6: 1.
21. Pelkowski SD, Kapoor M, Richendrfer HA, Wang X, Colwill RM, et al. (2011) A novel high-throughput imaging system for automated analyses of avoidance behavior in zebrafish larvae. *Behav Brain Res* 223: 135-144.
22. Richendrfer H, Creton R (2013) Automated high-throughput behavioral analyses in zebrafish larvae. *J Vis Exp*: e50622.
23. Clift D, Richendrfer H, Thorn RJ, Colwill RM, Creton R (2014) High-throughput analysis of behavior in zebrafish larvae: effects of feeding. *Zebrafish* 11: 455-461.
24. Buske C, Gerlai R (2011) Shoaling develops with age in Zebrafish (*Danio rerio*). *Prog Neuropsychopharmacol Biol Psychiatry* 35: 1409-1415.
25. Buske C, Gerlai R (2012) Maturation of shoaling behavior is accompanied by changes in the dopaminergic and serotonergic systems in zebrafish. *Dev Psychobiol* 54: 28-35.
26. Stearns G, Evangelista M, Fadool JM, Brockerhoff SE (2007) A mutation in the cone-specific *pde6* gene causes rapid cone photoreceptor degeneration in zebrafish. *J Neurosci* 27: 13866-13874.
27. Rinner O, Makhankov YV, Biehlmaier O, Neuhauss SC (2005) Knockdown of cone-specific kinase GRK7 in larval zebrafish leads to impaired cone response recovery and delayed dark adaptation. *Neuron* 47: 231-242.
28. Barker AJ, Baier H (2015) Sensorimotor decision making in the zebrafish tectum. *Curr Biol* 25: 2804-2814.
29. Naumann EA, Fitzgerald JE, Dunn TW, Rihel J, Sompolinsky H, et al. (2016) From Whole-Brain Data to Functional Circuit Models: The Zebrafish Optomotor Response. *Cell* 167: 947-960 e920.
30. Hagerman GF, Noel NC, Cao SY, DuVal MG, Oel AP, et al. (2016) Rapid Recovery of Visual Function Associated with Blue Cone Ablation in Zebrafish. *PLoS One* 11: e0166932.
31. Nishiwaki Y, Komori A, Sagara H, Suzuki E, Manabe T, et al. (2008) Mutation of cGMP phosphodiesterase 6 α '-subunit gene causes progressive degeneration of cone photoreceptors in zebrafish. *Mech Dev* 125: 932-946.
32. Housden BE, Muhar M, Gemberling M, Gersbach CA, Stainier DY, et al. (2017) Loss-of-function genetic tools for animal models: cross-species and cross-platform differences. *Nat Rev Genet* 18: 24-40.

Figures:

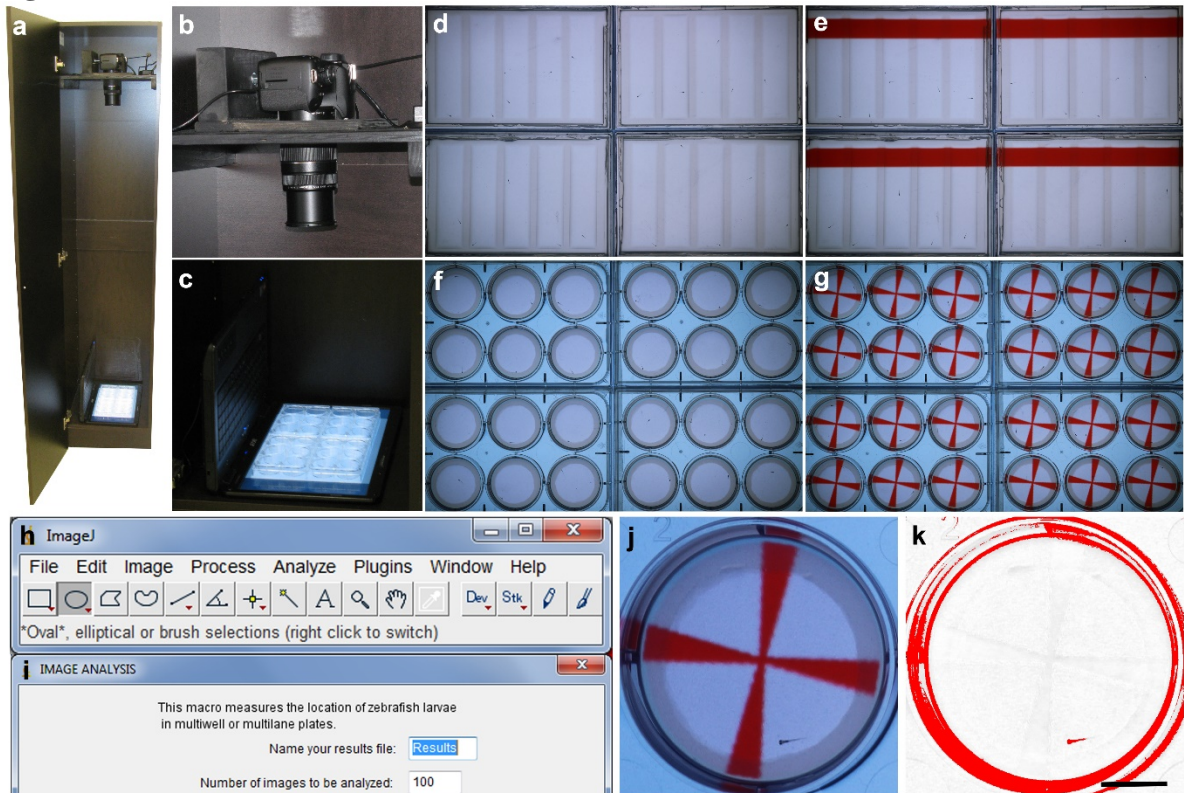


Figure 1. Imaging system for automated analyses of behavior. a) Imaging cabinet. b) Canon EOS Rebel T6 camera for acquisition of 18 megapixel color images. c) Four microplates with zebrafish larvae on the screen of a laptop. Visual stimuli are shown to the larvae using PowerPoint presentations. d) Four 5-lane plates without visual stimuli. e) Four 5-lane plates with a moving red bar. f) Four 6-well plates without visual stimuli. g) Four 6-well plates with a rotating red cross. h) The acquired images are analyzed in ImageJ. i) An ImageJ macro was developed for the automated analysis of large imaging files. The macro opens the first image, splits the color channels, selects a channel in which the visual stimuli and background have similar intensities, subtracts the background, applies a threshold, carries out a particle analysis, logs the measured coordinates, and automatically repeats this process for subsequent images in the series. j) Well with an agarose ring, a red cross and a 5 day-old zebrafish larva. k) The same well in the red channel after background subtraction and a threshold for dark objects. The acquired images showing four plates have sufficient resolution for measuring the location and the orientation of individual larvae. Scale bar = 1 cm.

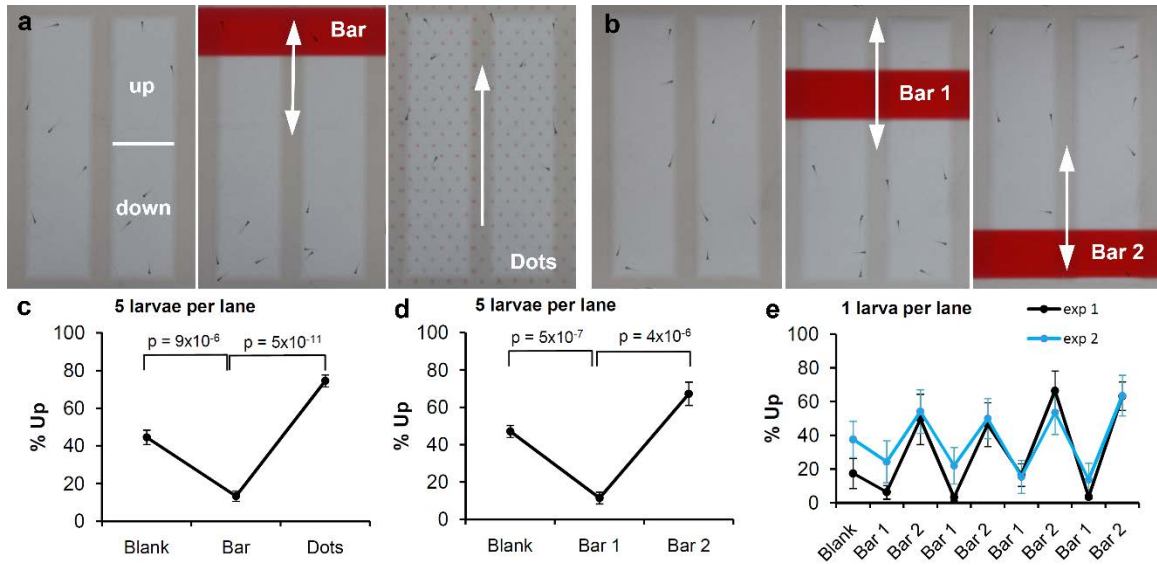


Figure 2. Visual stimuli in 5-lane plates. a) In the bar-dots assay, larvae are imaged for 15 min without visual stimuli, 15 min with a moving red bar and then 15 min with moving red dots. b) In the two-bar assay, larvae are imaged for 15 min without visual stimuli, 15 min with a moving red bar and then 15 min with a moving red bar in the opposite half of the plate. c) Measurements of larval location in the bar-dots assay. d) Measurements of larval location in the two-bar assay. e) Measurements of larval location using 1 larva per lane and a 4x repeated two-bar stimulus (10 min per bar). Differences in larval location were tested for significance using a two-tailed t-test with unequal variance and a Bonferroni correction for multiple comparisons when only pairwise comparisons were considered (c,d). A repeated measures ANOVA was performed to test the effect of stimulus on the % up for 4x repeated two-bar stimulus study. When sphericity was violated, a Greenhouse-Geisser correction was used (e). To assure that the data points are independent, even when using 5 larvae per lane, the data was analyzed on a per-lane basis (n=10 lanes). All larvae were imaged at 5 dpf. % up = percentage of larval measurements in the upper half of a lane. The arrows indicate the movement of the visual stimuli.

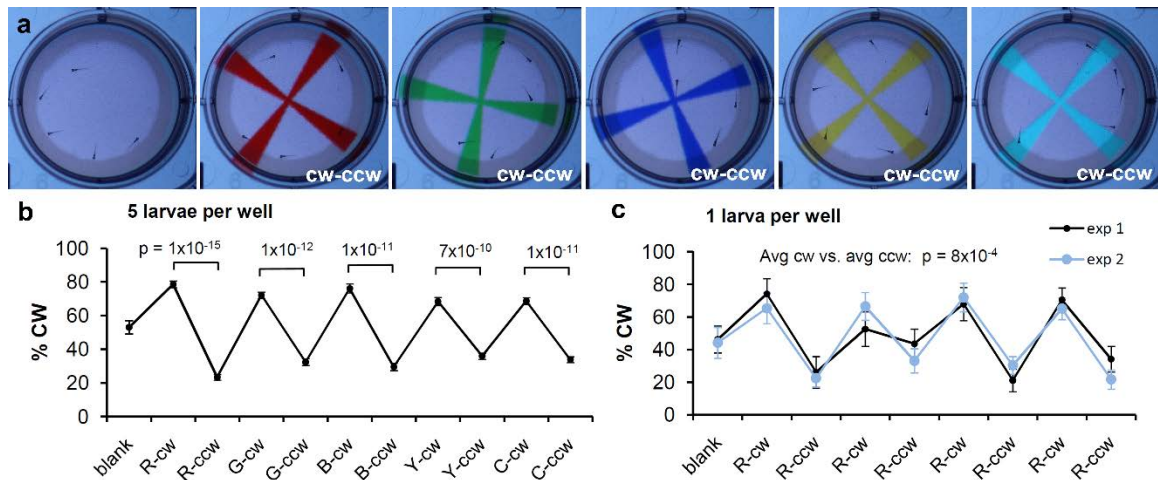


Figure 3. Visual stimuli in 6-well plates. a) View of a single well in a 6-well plate. b) Rotating cross assay using 5 larvae per well. c) Rotating red cross assay using 1 larva per well. In each color, the cross first rotates 10 minutes clockwise (cw) and then 10 minutes counter-clockwise (ccw). R, G, B, Y, C = red, green, blue, yellow, cyan. % CW = the percentage of measurements in which larvae display a clockwise orientation. Differences in the response to cw and ccw visual stimuli were tested for significance using a two-tailed t-test with unequal variance ($n=12$ wells) and a Bonferroni correction for multiple comparisons when only pairwise comparisons were considered (a,b) A repeated measures ANOVA was performed to test the effect of stimulus on the % CW for 4x repeated two-bar stimulus study. When sphericity was violated, a Greenhouse-Geisser correction was used (c).

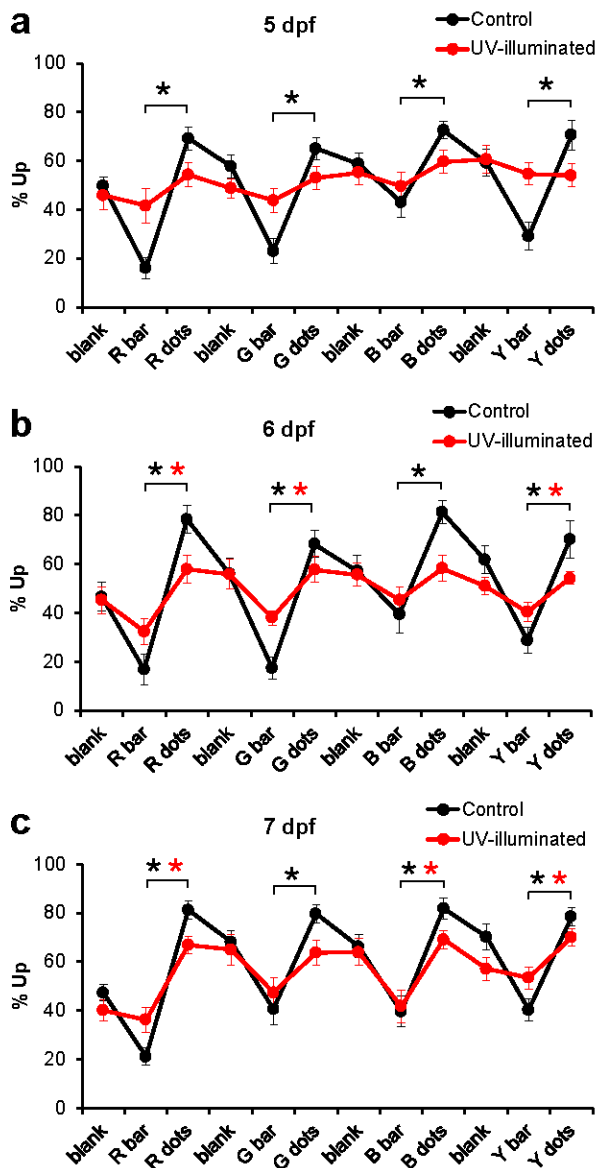


Figure 4. Effects of UV illumination examined in 5-lane plates. a) UV-illuminated larvae display a strongly reduced visual response at 5 dpf. b) Partial recovery of the response to visual stimuli at 6 dpf. c) Near complete recovery of the response to visual stimuli at 7 dpf. R, G, B, Y = red, green, blue, yellow. Black * = $p < 0.01$, bar vs. dots in control larvae (exposed to tricaine without UV illumination). Red * = $p < 0.01$ bar vs. dots in UV-illuminated larvae (two-tailed t-test with unequal variance, $n = 10$ lanes). The 5-lane plates contained 5 larvae per lane.

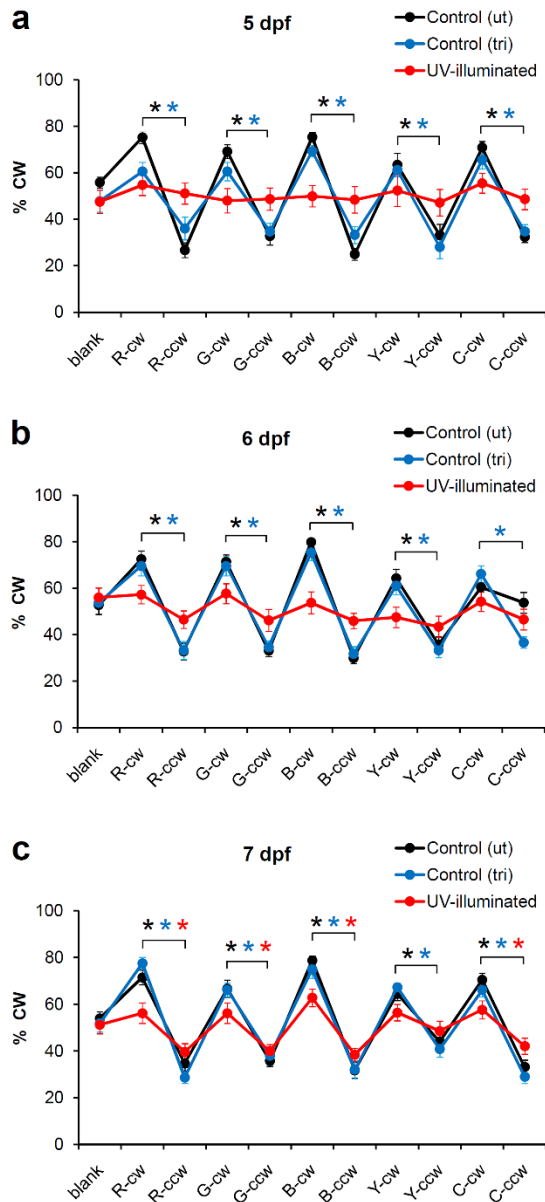


Figure 5. Effects of UV illumination examined in 6-well plates. a) UV-illuminated larvae do not show a significant response to visual stimuli at 5 dpf. b) Similarly, UV-illuminated larvae do not show a significant response to visual stimuli at 6 dpf. c) Near complete recovery of vision at 7 dpf. Black * = $p < 0.01$, cw vs. ccw in unexposed control larvae. Blue * = $p < 0.01$, cw vs. ccw in tricaine-exposed control larvae. Red * = $p < 0.01$, cw vs. ccw in UV-illuminated larvae (two-tailed t-test with unequal variance, $n = 12$ wells per experimental group). R,G,B,Y,C = rotating cross in red, green, blue, yellow and cyan. cw = clockwise rotation of cross. ccw = counter-clockwise rotation of cross. The 6-well plates contained 5 larvae per well.

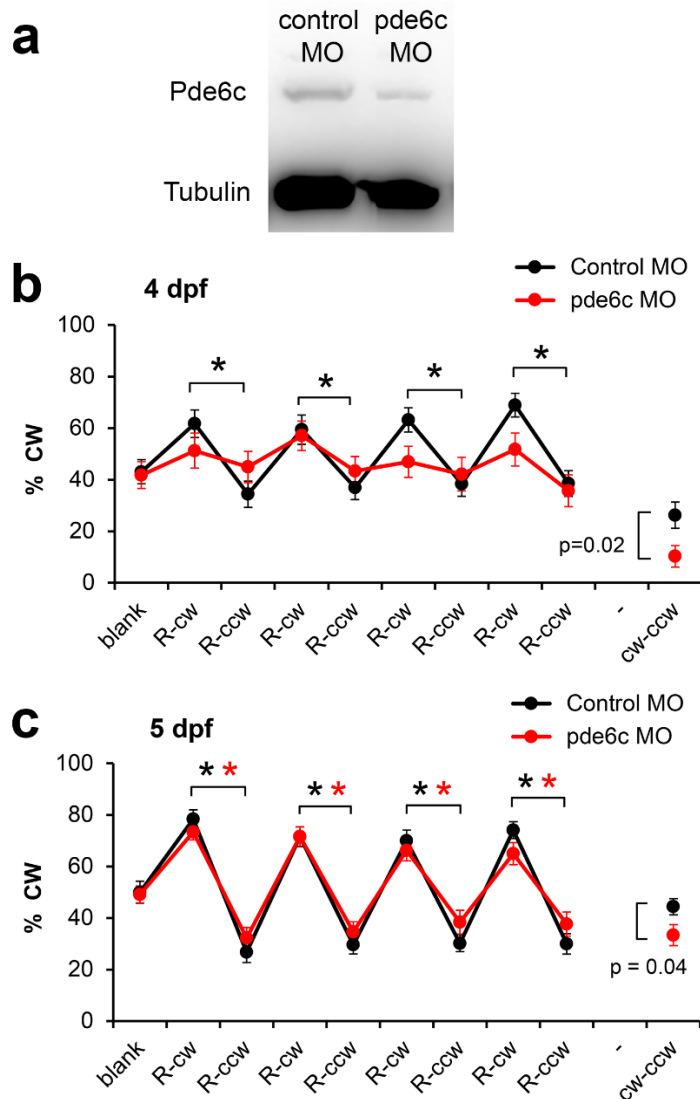


Figure 6. Visual defects after pde6c knockdown. a) Effects of pde6c knockdown at 4 dpf. Pde6c protein levels were suppressed by pde6c morpholino oligonucleotides (MO) as shown by Western blotting. b) The 4 dpf control larvae displayed a significant visual response to the 4x repeated rotating red cross. In contrast, the pde6c morpholino-injected larvae did not show a significant response to the visual stimuli. c) Effects of pde6c knockdown at 5 dpf. The control larvae and pde6c larvae display a robust response to the rotating red cross at 5 dpf. Black * = $p < 0.01$, cw vs. ccw in control larvae. Red * = $p < 0.01$, cw vs. ccw in pde6c larvae (two-tailed t-test with unequal variance for pairwise comparisons, $n=35$ wells in the control group, $n=33$ wells in the pde6c group). R = red cross, cw = clockwise rotation of cross, ccw = counter-clockwise rotation of cross. The average response to clockwise stimuli minus the average response to counter-clockwise stimuli is shown as a separate point in the graph (cw-ccw). These averages are significantly different between the control and pde6c groups at a 95% confidence limit ($p < 0.05$). The 6-well plates contained 1 larva per well.

Supporting Information

	Plate	# plates	Larvae per well	Visual stimuli	Color	Comparison	P (n=wells)	Total larvae
1.	5-lane	2	5	bar, dots	red	blank vs. bar	9×10^{-6} (10)	50
	"	2	5	"	red	bar vs. dots	5×10^{-11} (10)	50
2.	5-lane	2	5	bar 1, bar 2	red	blank vs. bar	5×10^{-7} (10)	50
	"	2	5	"	red	bar 1 vs. bar 2	4×10^{-6} (10)	50
3.	5-lane	2	1	bar 1, bar 2 (4x)	red	blank vs. bar	1 (10)	<u>10</u>
	"	2	1	"	red	bar 1 vs. bar 2	0.2 (10)	<u>10</u>
	"	2	1	"	red	bar vs. bar (4x)	0.0101 (10)	<u>10</u>
4.	6-well	2	5	cross cw, ccw	red	cw vs. ccw	1×10^{-15} (12)	60
	"	2	5	"	green	cw vs. ccw	1×10^{-12} (12)	60
	"	2	5	"	blue	cw vs. ccw	1×10^{-11} (12)	60
	"	2	5	"	yellow	cw vs. ccw	7×10^{-10} (12)	60
	"	2	5	"	cyan	cw vs. ccw	1×10^{-11} (12)	60
5.	6-well	2	1	cross cw, ccw (4x)	red	blank vs. cw	0.24 (12)	<u>12</u>
	"	2	1	"	red	cw vs. ccw	4×10^{-3} (12)	<u>12</u>
	"	2	1	"	red	cw vs. ccw (4x)	8×10^{-4} (12)	<u>12</u>

S1 Table. Assays for visually-guided behaviors in 5 day old zebrafish larvae.

Behavioral assays were compared using 2 plates per experiment. In experiments with 1 larva per lane or well, we examined 2 plates per experiment (n=10 lanes or 12 wells), repeated this in a second experiment, and presented the average p-values of the two experiments. P = two-tailed t-test, unequal variance, with a Bonferroni correction for multiple comparisons (2, 2, 3, 1, 3 in experiment 1-5). To maintain independence of measurements in lanes or wells containing multiple larvae, the statistical analyses were carried out on a per-well basis (n = number of wells or lanes). cw = clockwise, ccw = counter-clockwise.

Chapter 5: Discussion

Discussion

In the preceding chapters, I discussed my work using zebrafish to observe brain development (Chapter 2), neurodevelopmental disease (Chapter 3) and regeneration (Chapter 4). Overall, I have made progress in using zebrafish as a model to test disruptions during development and to model neurodevelopmental disease and regeneration. In Chapter 2, I discussed how we used zebrafish to test neurodevelopmental sensitivity to cyclosporine, a commonly used immunosuppressant drug. In Chapter 3, I discussed how we used zebrafish to model calcineurin inhibition as a proxy for the potential contributions of calcineurin inhibition to Down syndrome. Finally, in Chapter 4, I discussed our progress in using analysis of zebrafish behavior as a high throughput method to test the loss and recovery of zebrafish vision.

Zebrafish, what are they good for?

Scientists face many challenges when considering animal model use in developmental biology. Common mammalian models (e.g. mice, rats, rabbits, pigs, etc.) that are closely related to humans evolutionarily have embryos that develop within the mother, which makes it difficult to observe the development and complicates the process of experimentally altering gene expression. Common invertebrate models (e.g. flies, worms, etc.) are more accessible to genetic manipulation and observation, as they develop externally, but their organ systems can be difficult to compare to human organ systems. Externally developing vertebrates, such as zebrafish and the African clawed frog *Xenopus Laevis*, occupy a niche between these two groups. Zebrafish have similar early development to humans and can be used as an effective model for human disease. They

also spawn eggs, which are fertilized externally and the embryos can develop in a culture dish, allowing for easy access for imaging and genetic techniques. One tank of zebrafish can produce, on a daily basis, hundreds of fertilized eggs, which are well suited for use as a high-throughput modeling system.

In my research, I have taken advantage of the many benefits of zebrafish as a developmental model in several ways. I used their external development to easily treat embryos with cyclosporine during development to test developmental toxicity. The use of zebrafish allowed for precise temporal control of the treatments, which is technically challenging in most other vertebrate systems. In Chapters 3 and 4, I was able to inject morpholinos into many zebrafish embryos and observe their development because of their accessibility. Throughout all my research, I took advantage of the stereotyped behaviors of zebrafish to assess subtle brain defects (Chapters 2 and 3) and loss and recovery of vision (Chapter 4). These different approaches to assaying zebrafish during development showcase the power of zebrafish as a model.

Expanding toolbox, expanded results

In future experiments using zebrafish to test developmental neurotoxicity, additional genetic tools can be implemented to create a more complete picture of the disruption occurring during zebrafish brain development. For one, the genetically encoded calcineurin indicator, GCaMP, can be expressed in the zebrafish brain to gain information on the neural networks that are affected by environmental or genetic disruptions. GCaMPs are genetically encoded calcium indicators that allow for the visualization of neuronal pulses through flashes of green fluorescence that occur when

calcium increases in an activated neuron [1]. Since zebrafish embryos are transparent, we could image neural pulses through development in a minimally invasive way. To fit with our analysis, neural pulses of treated and untreated fish can be imaged and compiled to create heatmaps. By comparing the differences between the treated and untreated pulse heatmaps, we can determine the pathways or brain areas that are differentially affected by various compounds and add such information to brain size analysis and behavioral assays.

Our laboratory has also been creating a more efficient high-throughput system for analyzing behavior. In our current studies, we used a behavioral setup with 10-lane plates (Chapters 2 and 3) or 6-well plates (Chapter 4). In both cases, we used a moving visual stimulus to test avoidance or vision respectively. We have worked on expanding our behavioral assay in many ways to acquire a more complete view of subtle brain defects through behavior. We began using 96-well plates with an updated ImageJ macro to increase the throughput of our system. Once optimized, this will allow us to use more fish per experiment, or to test more conditions at a faster pace. Preliminary experiments have shown promising results using 96-well plates for overall activity assays (Appendix B).

I have also updated the 6-well plate assay to examine habituation in zebrafish. Habituation is a non-associative form of learning wherein an animal displays a decreased response to a stimulus after repeated presentations of the stimulus [2]. By training one group of fish in the behavioral assay and allowing others to remain untrained, we can measure the difference in response to “test” stimuli by measuring swim speed. Zebrafish are become hyperactive in response to a new stimulus, and this measurement allows us to determine when a zebrafish thinks the stimulus is “new” (Appendix B). This habituation

assay will be a valuable addition to the current behavioral assays as it would allow comparison between the observed neurodevelopmental aberrations and learning, which may be relevant to human development.

Finally, we have carried out preliminary experiments using sound as a stimulus to assay the behavior of the fish. The current preliminary experiments show that with pulses of sound, zebrafish will show a “freezing” response (i.e. slower swim speed). After the sound pulses stop, they slowly recover to their basal swim speed (Appendix B). This additional type of stimulus will provide additional behavioral data, creating a more complete view of behavioral perturbations. This new stimulus will allow us to differentiate between visual defects and behavioral differences, as response to sound is independent of vision.

Cyclosporine and beyond

Prior to our work, research surrounding calcineurin inhibiting immunosuppressant drugs cyclosporine and tacrolimus was focused on the side effects in adult patients, especially those affecting the kidney and liver [3]. Both cyclosporine and tacrolimus are considered class C drugs by the FDA, meaning that potential benefits may warrant use of the drug in pregnant women despite potential risks. Our goal of research was to expand on the known risks of these drugs. We found that there were neurodevelopmental defects in overall brain size after treatments early in development as well as behavioral defects after treatments later in development (Chapter 2). Unfortunately, pregnant women do not have any safer alternatives than these drugs, as stopping the immunosuppressant drugs would mean risking organ rejection and potential death. Our research on cyclosporine is a

promising first step in allowing these women to make more informed decision when planning their families. Additionally, our research acts to bring more attention to this issue and warrants further investigation in the human population.

In testing the developmental disruption of cyclosporine, we further illustrated how the analysis of zebrafish behavior can be used to test developmental toxicity *in vivo*. This type of analysis has been also utilized in our lab for pesticides and neurological modulators [4–6]. Many of these compounds are unavoidable in everyday life or are without viable alternatives during pregnancy. Due to these factors, it is important to be able to test the effects these compounds may have during development, especially neural development. While aberrations in physical development are usually easily observable after birth, subtle differences in brain development are harder to observe and may not fully manifest until several years later. Since the brain continues developing until a person is in their mid-20s [7], it is oftentimes difficult to pinpoint the exact moment when developmental disturbances occur and what may cause them. This phenomenon has been observed in the United States with the anti-vaccine movement. While there is no link between vaccines and autism [8], concerned parents may associate the earliest autism diagnosis (typically occurring between ages 6 to 24 months) with the time when their children are obtaining many vaccines, creating a false connection between the two. My research using zebrafish to model brain and behavioral consequences of developmental toxicity could be useful to more accurately determine effects of toxicant exposures during early development in humans and to avoid potential spurious correlations.

Alternative medications

While cyclosporine is used as an inhibitor of calcineurin/NFAT signaling to suppress the immune system, cyclosporine inhibits calcineurin indiscriminately [9]. This indiscriminate inhibition may lead to a myriad of off-target effects that do not contribute to immunosuppression. Additionally, the cyclosporine-cyclophilin complex has been reported to interact with mitochondria in a calcineurin independent manner. As a result of these off-target functions, there is interest in creating more specific inhibitors of calcineurin/NFAT signaling. One class of these compounds is called inhibitor of NFAT-calcineurin signaling or INCA [10]. Since calcineurin is a multi-substrate enzyme [11], INCAs hold promise in inhibiting the immune system in a more specific way, which may decrease side effects of immunosuppression. This specificity could also create a safer class of immunosuppressant for use during pregnancy for women who have had a solid organ transplant. If such a compound is considered for use, our model would be an ideal way to test it. We have already observed the effects of cyclosporine in brain development, and we could test various INCA compounds to determine if there are INCAs that do not negatively affect brain and/or behavioral development.

The ability of compounds to more specifically inhibit the calcineurin/NFAT pathway also creates additional possibilities for treating calcineurin-related diseases. An analysis of transplant patient data showed that taking cyclosporine or tacrolimus lowered the prevalence of Alzheimer's disease compared to the prevalence in the general population [12]. If this effect is calcineurin dependent, researchers can attempt to determine the specific calcineurin signaling pathway that is involved (i.e. if it is a specific NFAT or a different substrate) and can direct research to a discovering a specific

inhibitor of this pathway. In this case, a specific inhibitor could decrease the incidence of Alzheimer's disease without immunosuppression or other side effects of these immunosuppressants.

Zebrafish model of calcineurin inhibition

The main target of cyclosporine is the phosphatase calcineurin and our results from Chapter 2 furthered our interest in testing the role of calcineurin during early brain development. In Chapter 3, I showed how calcineurin inhibition during early development affected brain development. Calcineurin inhibition has been implicated in Down syndrome, and our model could illuminate some effects of this inhibition. In Down syndrome, calcineurin is directly inhibited by RCAN and calcineurin signaling is suppressed by DYRK1A [13,14]. In addition, research on the catalytic activity of calcineurin suggests that the catalytic pocket is nonspecific and that the regulatory subunits may lend substrate specificity to its activity. There are two regulatory subunits of calcineurin in zebrafish (*ppp3r1a* and *ppp3r1b*) which may confer some specificity to calcineurin holoenzyme substrate activity [15,16]. The most interesting results were found by knocking down the regulatory subunits individually, as they did not show the same phenotypes. While both knockdowns displayed decreases in the midbrain size, the *ppp3r1a* knockdown showed additional phenotypes of decreases in forebrain and hindbrain size. Behaviorally, both knockdowns showed response to the moving bar. In *ppp3r1a* knockdowns, there was an increase in social interactions and in the *ppp3r1b* knockdown, there was less overall activity. It is clear that there are at least two different pathways involved in calcineurin's role in brain development when the holoenzyme

includes either Ppp3r1a or Ppp3r1b, and the downstream targets of these holoenzymes warrant further investigation.

An alternative hypothesis is that these two subunits are expressed differently within the brain. In our immunolabeling experiments, we have shown the expression of the regulatory subunits throughout the brain, but the antibody used recognizes both subunits. Previously published literature about calcineurin did not show distinct mRNA localization of the subunits at 1dpf [16]. To determine the localization of the subunits, we could immunolabel embryos after knockdown of one of the subunits. The localization of the Ppp3r1a subunit can then be observed when the embryo is injected with the *ppp3r1b* morpholino and vice versa. One problem with this approach is that there is not full knockout of the calcineurin regulatory subunits in the morphants as seen in the western blots in Chapter 3. A better approach could be to create lines of fish with each subunit knocked-out using CRISPR/Cas9. Individual subunit knock-outs would provide important information on localization and a more complete picture of the individual subunit roles.

Overall, our results suggest that there is a critical role for calcineurin in the brain during development. We have shown that there is a decrease in brain size when calcineurin is inhibited perhaps due to the increase in apoptosis in the head of the embryos at 1dpf. Although we only measured apoptosis in the head, and not specifically in the brain, there is a marked increase in apoptosis by inhibiting calcineurin. In the future, we will use immunolabeling for active caspase 3 and neuronal markers (e.g. Elavl3 [17]) to test if apoptosis specifically occurs in neurons. These apoptosis experiments will also be performed in the regulatory subunit morphants. Based on the

difference in brain size between the two subunit morpholinos at 3dpf, we should be able to detect differences in apoptosis between the two morphants.

Calcineurin inhibition in Down syndrome

In Chapter 3, I discussed how we used morpholinos to knockdown calcineurin as a model for Down syndrome. While I showed that calcineurin inhibition leads to brain and behavioral aberrations, it is not known how calcineurin inhibition is related to Down syndrome phenotypes as a whole. Due to the known increases in DYRK1A and RCAN in Down syndrome, calcineurin signaling has been a target for designing drugs to alleviate some Down syndrome phenotypes [18–20]. These inhibitors include CX-4945 [18], inhibitor of DYRK (INDY) [19], and harmine [20]. While many developmental effects may be irreversible, these drugs could alleviate ongoing symptoms caused by decreased calcineurin signaling. Our calcineurin inhibited zebrafish would be an ideal model to test these compounds. Future experiments could knockdown *ppp3r1a* and/or *ppp3r1b* in zebrafish larvae and treat them with these compounds. After treatment, we could assess the treated larvae, compare them to the untreated larvae, and determine if they have any potential to rescue the observed larval phenotypes.

The calcineurin conundrum

In addition to the evidence that decreased calcineurin plays a role in Down syndrome, calcineurin has been implicated in a range of neurodevelopmental diseases, neurodegenerative diseases, and psychiatric disorders. Alzheimer's disease is another common example of a calcineurin-related disease. In contrast to the potential role of

decreased calcineurin signaling in Down syndrome, it has been reported that *increased* calcineurin is associated with Alzheimer's disease [21]. This association between increased calcineurin and Alzheimer's disease is further supported by the previously discussed association between cyclosporine and tacrolimus use and decreased incidences of Alzheimer's disease [12]. The calcineurin association in these two diseases is not as simple as presented. It well known that humans with Down syndrome are at a high risk of developing Alzheimer's disease at a young age [22,23]. While this seems contradictory to the increased calcineurin in Alzheimer's model, it actually reveals the complexity of these multifactor diseases. In addition to DYRK1A and DSCR1, the gene for amyloid precursor protein (APP) is located on the 21st chromosome [24] and an increase in APP may cause Alzheimer's disease in Down syndrome patients. Additionally, there is research suggesting DYRK1A directly phosphorylates APP which may also contribute to the instances of Alzheimer's disease in Down syndrome [25]. It is important that when discussing these associations, we are careful to assess the whole disease and not just one symptom.

These associations lead me to the hypothesis that calcineurin plays many roles throughout brain development and aging over an organism's lifetime. The function of calcineurin may be context dependent and related to other signaling factors that are simultaneously present. One prime example is the research linking decreases in calcineurin signaling to decreased apoptosis and neural protection after injury. Studies in rats have shown that cyclosporine or tacrolimus treatment can increase neuronal survival after brain hemorrhage [26], spinal cord injury [27], and after traumatic brain injury [28]. In zebrafish, a decrease in calcineurin signaling after tail fin injuries leads to a quicker

recovery from injury [29]. These results seem to be contradictory to my results showing that decreases in calcineurin during development lead to increased apoptosis in the head of zebrafish larvae (Chapter 3).

My hypothesis is that calcineurin has specific roles that help pattern the brain during development, but when calcineurin is inhibited proper connections cannot be made. When these neurons make improper connections, or no connection at all, they may undergo apoptosis to rectify the error. After development, calcineurin may only function in a maintenance capacity in controlling apoptosis and regeneration. While these experiments are outside the realm of this current dissertation, this is an interesting topic of research to identify what may be involved in this switch. Additionally, cyclosporine treatments have calcineurin independent effects that may be involved in these pathways as discussed previously. With so many paths leading back to calcineurin, it seems that this may be an integral part of proper brain function, not only during early brain development, but also throughout one's life.

Tissue specific calcineurin inhibition

In future experiments we would like to take advantage of zebrafish as a genetic system to focus on specific perturbations of calcineurin signaling. In the current experiments in Chapter 3 we inhibited calcineurin throughout the entire embryo. To more directly test the role of calcineurin inhibition in brain development we can take more specific approaches to target the nervous system for inhibition. For one, we could take advantage of CRISPR/Cas9 technology to knock-out the calcineurin regulatory subunits specifically in the nervous system. Previous research in zebrafish has developed a vector

system for tissue-specific gene editing [30]. We could use this system to express Cas9 protein specifically under the control of the *elavl3* promoter to target neurons [17], and to express guide RNAs against calcineurin. We could target both regulatory subunits, for total inhibition of calcineurin, and the individual subunits to test the role for the different subunits in the nervous system.

In addition to directly targeting calcineurin, we could overexpress negative regulators of calcineurin, such as Rcan and Dyrk1a, under control of the *elavl3* promoter. Overexpression of these genes would lead to an overall decrease in calcineurin signaling, as previously described and as may be the case in Down syndrome [13,14]. Analysis of these fish would illuminate the nervous system specific effects of calcineurin signaling inhibition. This would allow for testing of general inhibition of calcineurin signaling in the brain, and by screening for copy number and assuring there is only one copy of these genes we could more accurately model Down syndrome. While this model would not be directly comparable to human Down syndrome, it could shed light on some of the nervous system targets of calcineurin that would warrant further research in Down syndrome.

In these new lines we could measure eye size, brain size and perform behavioral tests as in Chapters 2 and 3 to assess the brain development of these larvae. If the phenotypes we have observed in this dissertation are dependent on the knock-down of calcineurin in neurons we would expect to see similar phenotypes in these tissue specific knockouts.

Assay for the loss and recovery of vision

Chapter 4 focused on the development of new tools to help screen for a loss and recovery of vision in zebrafish. As previously discussed, zebrafish are excellent models for high-throughput screening and we found behavioral analysis to be an efficient system for screening the loss and recovery of vision. The effectiveness of our system was demonstrated by performing both photoablations and genetic ablations as complementary approaches to affect larval vision. We began with our assay of avoidance behavior, and while it was effective at detecting loss of vision it had some inherent flaws. One glaring issue was that the control larvae would not avoid bars that were cyan colored. This was strange as cyan is a secondary color comprised of green and blue, and the fish showed robust responses to green and blue separately. We updated our assay to measure the direction the fish were facing (clockwise or counterclockwise) in response to a rotating stimulus. When we tested this new system using a cyan-colored rotating cross, we found that the zebrafish larvae positively responded. This was one indication that our update was a better test of vision. This could be due to the extra movement necessary to avoid the bar in our avoidance assay, versus just turning in one direction or another in the vision assay. It could also be a result of the avoidance assay relying on zebrafish avoidance, and not all colors may induce this avoidance. A cyan bar may not be threatening to larval zebrafish, and therefore they don't avoid it, but they still do see it (Appendix C).

It is important to test various secondary colors on our system for future experiments where we may be able to detect deficiencies in specific cones that detect such colors. The importance of testing secondary colors is determined by how we show

stimuli to zebrafish. Our source of stimulus is a laptop screen which emits red, green, and blue (RGB) light to create images. The visual stimuli are shown on a white background, which is bright in red, green and blue. This background would appear cyan-colored (bright in blue and green) to a fish with defective red photoreceptor cells. Consequently, such a fish would have trouble seeing a cyan-colored stimulus on a background that appears to have a similar color. Thus, secondary colors on a white background are well suited for detecting defects in specific photoreceptor cells. Subsequently, we wanted to be sure that we could effectively test all secondary colors in our system.

“Eye” can see clearly now

Now that we have developed an efficient system for high-throughput analysis of loss and recovery of vision, future research can be focused on using this system to test compounds that may aid in the recovery of vision. The most promising therapies that are being developed to treat human blindness are stem cell-based therapies. A phase 1 clinical trial using stem cells to regrow the retinal pigment epithelium in human patients has recently been published after achieving success in two patients [31]. Future experiments in the Creton laboratory will focus on testing pharmaceuticals in our assay of visual behavior to try to identify compounds that may assist in regeneration. Using our system, we could test large libraries of compounds with relative ease as fish can be mass irradiated to ablate their vision, and then the larvae can be treated with compounds that may have uses in regeneration. This would be a good first step in identifying compounds for testing that could be useful in complementing stem-cell therapies in the treatment of human eye diseases.

Additional future experiments could examine the different layers of the eye. Disruptions in different eye layers can lead to different diseases in humans. Our current method of visual ablation involves exposing the entire fish to UV light before behavioral testing. Future experiments will aim to target the eye with more precision and even to target individual cell types. One promising system we have available in the lab, but not yet implemented, is a transgenic line that has bacterial nitroreductase expressed under a blue cone specific promoter (*sws2*) [32]. These fish behave normally and do not show any deficiencies, but when they are treated with the prodrug metronidazole, the nitroreductase enzyme will alter the prodrug into a cytotoxic form. This converted metronidazole will only kill the cells expressing nitroreductase, allowing for cell-type specific control of the ablation. This system is very promising since it would allow us to ablate the eyes specifically and with great temporal control. Additionally, other laboratories have used a transgenic nitroreductase line under the control of a UAS promoter (UAS:*nfsB*) that would allow even more flexibility with this system [33]. By pairing the UAS:*nfsB* with various Gal4 lines, we could target other parts of the optic system, such as the optic nerve, optic tectum, and choroid. By ablating different parts of the visual system, we could better model human visual degeneration and learn more about how regeneration may occur in these areas.

Regeneration or recovery?

In this dissertation I have discussed our current research on the loss and recovery of vision in zebrafish larvae. In this research, we have observed the loss and recovery of vision, but have not determined the state of the retinal cells. In future experiments, we

will ablate the vision of zebrafish as in Chapter 4, via light or morpholinos, and then process the embryos for histology of the retina. To get an effective look at the morphology of the retina, we will paraffin section the larvae and stain with standard histology dyes to observe the general structure of the retina. If we are ablating the cells within the eye, we will be able to observe the loss and regeneration of photoreceptors. Previous research on retinal damage has shown that the photoreceptors are regenerated through Müller cell reentry into the cell cycle to repair the damage [34–36]. Proliferation is evident through BrdU incorporation in zebrafish between 24 and 48 hours after damage is induced [35]. Light induced retinal damage and regeneration through Müller glial cells has been previously characterized [37], which leads us to believe that in our light based system the loss and recovery of vision is likely a proxy for this regeneration. In the previously characterized system retinal ablation is not immediately evident after light treatment, but becomes clear within the first 48 hours post ablation [37], so histology on our larvae would be performed at various time points after ablation to confirm that our system is working in a similar fashion.

The good, the bad, and the ugly

While zebrafish are an excellent model system for testing neurological perturbations as discussed in this dissertation, they are not perfect. As discussed, zebrafish are great models for large scale screening of compounds, but obviously a fish is far from a human. The similarity between pathways in fish and humans allows potential compounds to have observable effects in zebrafish, but this requires knowing what effects to look out for.

Throughout this dissertation I have discussed the uses for zebrafish as a model of behavior. It has been reported that activation or inhibition of specific pathways will result in similar behavioral profiles within zebrafish, it is oftentimes difficult to translate these behaviors to human behavior. For example, can we really say if the social interaction we observe in zebrafish is comparable to aberrant social behavior in autism? As zebrafish become a more popular and widely used model, it is important to consider these questions when trying to model human disease, especially diseases with substantial behavioral components.

Final Thoughts

As medicine advances, it becomes increasingly important to have efficient models to test human development and disease in relation to current and emerging pharmaceutical drugs. Having high-throughput models of human development and disease will be integral in decreasing the time between creation or discovery of a drug and implementation in the human population. In this dissertation I have discussed how zebrafish can be a model of developmental toxicity (Chapter 2), human disease (Chapter 3), and regeneration (Chapter 4). Zebrafish have been gaining in popularity as a multifunctional model and I contend that they will become a vital first step in discovering and testing new pharmaceutical drugs. While zebrafish will not fully replace current models and operating procedures, they can be used to greatly supplement current methods of drug discovery and testing, as discussed in this dissertation.

References:

1. Akerboom J, Chen T-W, Wardill TJ, *et al.* Optimization of a GCaMP calcium indicator for neural activity imaging. *J Neurosci* 2012; **32**:13819–40.
2. Rankin CH, Abrams T, Barry RJ, *et al.* Habituation revisited: An updated and revised description of the behavioral characteristics of habituation. *Neurobiol Learn Mem* 2009; **92**:135–138.
3. Rezzani R. Cyclosporine A and adverse effects on organs: histochemical studies. *Prog Histochem Cytochem* 2004; **39**:85–128.
4. Richendrer H, Creton R. Cluster analysis profiling of behaviors in zebrafish larvae treated with antidepressants and pesticides. *Neurotoxicol Teratol* 2017.
5. Richendrer H, Pelkowski SD, Colwill RM, Créton R. Developmental sub-chronic exposure to chlorpyrifos reduces anxiety-related behavior in zebrafish larvae. *Neurotoxicol Teratol* 2012; **34**:458–65.
6. Richendrer H, Creton R. Chlorpyrifos and malathion have opposite effects on behaviors and brain size that are not correlated to changes in AChE activity. *Neurotoxicology* 2015; **49**:50–58.
7. Stiles J, Jernigan TL. The basics of brain development. *Neuropsychol Rev* 2010; **20**:327–348.
8. Taylor LE, Swerdfeger AL, Eslick GD. Vaccines are not associated with autism: An evidence-based meta-analysis of case-control and cohort studies. *Vaccine* 2014; **32**:3623–3629.
9. Hogan PG, Chen L, Nardone J, Rao A. Transcriptional regulation by calcium, calcineurin, and NFAT. *Genes Dev* 2003; **17**:2205–32.
10. Roehrl MHA, Wang JY, Wagner G. Discovery of small-molecule inhibitors of the NFAT-calcineurin interaction by competitive high-throughput fluorescence polarization screening. *Biochemistry* 2004; **43**:16067–16075.
11. Shibasaki F, Hallin U, Uchino H. Calcineurin as a multifunctional regulator. *J Biochem* 2002; **131**:1–15.
12. Tagliatalata G, Rastellini C, Cicalese L. Reduced Incidence of Dementia in Solid Organ Transplant Patients Treated with Calcineurin Inhibitors. *J Alzheimer's Dis* 2015; **47**:329–333.
13. Kurabayashi N, Sanada K. Increased dosage of DYRK1A and DSCR1 delays neuronal differentiation in neocortical progenitor cells. *Genes Dev* 2013; **27**:2708–21.
14. Arron JR, Winslow MM, Polleri A, *et al.* NFAT dysregulation by increased dosage of DSCR1 and DYRK1A on chromosome 21. *Nature* 2006; **441**:595–600.
15. Rodríguez A, Roy J, Martínez-Martínez S, *et al.* A conserved docking surface on calcineurin mediates interaction with substrates and immunosuppressants. *Mol Cell* 2009; **33**:616–26.
16. Hammond DR, Udvardia AJ. Cabin1 expression suggests roles in neuronal development. *Dev Dyn* 2010; **239**:2443–51.
17. Kim CH, Ueshima E, Muraoka O, *et al.* Zebrafish elav/HuC homologue as a very early neuronal marker. *Neurosci Lett* 1996; **216**:109–12.
18. Kim H, Lee K-S, Kim A-K, *et al.* A chemical with proven clinical safety rescues Down-syndrome-related phenotypes in through DYRK1A inhibition. *Dis Model Mech* 2016; **9**:839–848.

19. Ogawa Y, Nonaka Y, Goto T, *et al.* Development of a novel selective inhibitor of the Down syndrome-related kinase Dyrk1A. *Nat Commun* 2010; **1**:1–9.
20. Adayev T, Wegiel J, Hwang Y-W. Harmine is an ATP-competitive inhibitor for dual-specificity tyrosine phosphorylation-regulated kinase 1A (Dyrk1A). *Arch Biochem Biophys* 2011; **507**:212–8.
21. C. Reese L, Tagliatela G. A Role for Calcineurin in Alzheimers Disease. *Curr Neuropharmacol* 2011; **9**:685–692.
22. Wisniewski KE, Wisniewski HM, Wen GY. Occurrence of neuropathological changes and dementia of Alzheimer's disease in Down's syndrome. *Ann Neurol* 1985; **17**:278–282.
23. Mann DMA. The pathological association between down syndrome and Alzheimer disease. *Mech Ageing Dev* 1988; **43**:99–136.
24. Castro P, Zaman S, Holland A. Alzheimer's disease in people with Down's syndrome: the prospects for and the challenges of developing preventative treatments. *J Neurol* 2017; **264**:804–813.
25. Ryoo S-R, Cho H-J, Lee H-W, *et al.* Dual-specificity tyrosine(Y)-phosphorylation regulated kinase 1A-mediated phosphorylation of amyloid precursor protein: evidence for a functional link between Down syndrome and Alzheimer's disease. *J Neurochem* 2008; **104**:1333–44.
26. Dai Y, Sun Q, Zhang X, Hu Y, Zhou M, Shi J. Cyclosporin A ameliorates early brain injury after subarachnoid hemorrhage through inhibition of a Nur77 dependent apoptosis pathway. *Brain Res* 2014; **1556**:67–76.
27. Hui KKW, Liadis N, Robertson J, Kanungo A, Henderson JT. Calcineurin inhibition enhances motor neuron survival following injury. *J Cell Mol Med* 2010; **14**:671–86.
28. Sullivan PG, Sebastian AH, Hall ED. Therapeutic Window Analysis of the Neuroprotective Effects of Cyclosporine A after Traumatic Brain Injury. *J Neurotrauma* 2011; **28**:311–318.
29. Kujawski S, Lin W, Kitte F, *et al.* Calcineurin regulates coordinated outgrowth of zebrafish regenerating fins. *Dev Cell* 2014; **28**:573–87.
30. Ablain J, Durand EM, Yang S, Zhou Y, Zon LI. A CRISPR/Cas9 vector system for tissue-specific gene disruption in zebrafish. *Dev Cell* 2015; **32**:756–64.
31. da Cruz L, Fynes K, Georgiadis O, *et al.* Phase I clinical study of an embryonic stem cell-derived retinal pigment epithelium patch in age-related macular degeneration. *Nat Biotechnol* 2018.
32. Yoshimatsu T, D'Orazi FD, Gamlin CR, *et al.* Presynaptic partner selection during retinal circuit reassembly varies with timing of neuronal regeneration in vivo. *Nat Commun* 2016; **7**:10590.
33. Agetsuma M, Aizawa H, Aoki T, *et al.* The habenula is crucial for experience-dependent modification of fear responses in zebrafish. *Nat Neurosci* 2010; **13**:1354–1356.
34. Vihtelic TS, Soverly JE, Kassen SC, Hyde DR. Retinal regional differences in photoreceptor cell death and regeneration in light-lesioned albino zebrafish. *Exp Eye Res* 2006; **82**:558–575.
35. Yurco P, Cameron DA. Responses of Müller glia to retinal injury in adult zebrafish. *Vision Res* 2005; **45**:991–1002.
36. Fausett B V., Goldman D. A Role for γ Tubulin-Expressing Muller Glia in

Regeneration of the Injured Zebrafish Retina. *J Neurosci* 2006; **26**:6303–6313.
37. Meyers JR, Hu L, Moses A, Kaboli K, Papandrea A, Raymond PA. β -catenin/Wnt signaling controls progenitor fate in the developing and regenerating zebrafish retina. *Neural Dev* 2012; **7**:1.

Appendix A: High-throughput analysis of behavior in zebrafish larvae: effects of feeding.

Clift, D., Richendrfer, H., Thorn, R. J., Colwill, R. M. & Creton, R. High-Throughput Analysis of Behavior in Zebrafish Larvae: Effects of Feeding. *Zebrafish* 11, 455–461 (2014).

I assisted in the experiments and design of the experiments and writing of the manuscript.

Abstract

Early brain development can be influenced by numerous genetic and environmental factors, with long-lasting effects on brain function and behavior. Identification of these factors is facilitated by high-throughput analyses of behavior in zebrafish larvae, which can be imaged in multiwell or multilane plates. However, the nutritional needs of zebrafish larvae during the behavioral experiments are not fully understood. Zebrafish larvae begin feeding at 5 days post fertilization, but can live during the first 7 days solely on nutrients derived from the yolk. To examine if feeding affects behavior, we measured a broad range of behaviors with and without feeding at 5, 6, and 7 days post fertilization. We found that feeding did not have a significant effect on behavior in 5 day-old larvae. In contrast, fed 6 and 7 day-old larvae displayed increased avoidance responses to visual stimuli, increased swim speeds and decreased resting in comparison to unfed larvae. In addition, the fed 7 day-old larvae displayed an increase in thigmotaxis and a decrease in the distance between larvae in the presence of visual stimuli. Thus, feeding affects a range of behaviors in 6 and 7 day-old larvae. We conclude that 5 day-old larvae are well-suited for high-throughput analyses of behavior, since effects of feeding can be avoided at this time. For high-throughput analyses of behavior in older larvae, standard feeding protocols need to be developed.

Key Words

Zebrafish larvae; Behavior; Avoidance; Thigmotaxis; High-throughput imaging; Feeding

Introduction

Developmental disorders such as attention deficit hyperactivity disorder, intellectual disability, cerebral palsy, autism, seizures, hearing loss, blindness and learning disorders affect approximately 15% of children between the ages of 3 and 17 years [1,2]. The etiology of these developmental disorders is often poorly understood and may include multiple genetic and environmental factors. A better understanding of the underlying factors can be facilitated by analyses of behavior in animal model systems. Behavioral analyses are non-invasive and can reveal subtle defects in neural signaling that are easily missed by morphological analyses. In addition, behavioral analyses can be used to examine neural function in a wide variety of organisms, ranging from nematodes in a culture dish to large mammals in their natural environment.

The zebrafish is an emerging model system in the behavioral sciences [3–6]. The signaling pathways that regulate brain development and function are highly conserved in vertebrate species. Adult zebrafish colonies are relatively easy to maintain and are cost efficient. A mixed adult female and male population in a tank on a 10 hour dark/14 hour light cycle will spawn year round and hundreds of synchronously developing embryos can be collected from the bottom of a tank on a daily basis. The embryos develop predictable neural patterns, which are amenable to genetic manipulation and can be imaged in living embryos using state-of-the-art molecular tools. Moreover, the behavior of zebrafish larvae can be examined in multiwell plates, which provides unique opportunities for high-throughput applications [7–10]. Zebrafish embryos develop rapidly

and the larvae emerge from their chorions between 2 and 3 days post fertilization (dpf). At 5 dpf, the larvae have inflated swim bladders and actively hunt for food [11–15]. A broad range of behaviors have been analyzed in zebrafish larvae, including scoot swimming, burst swimming, routine turns, J-, C-, and O-bend turns, optokinetic and optomotor responses, prey tracking, phototaxis, thigmotaxis, escape and avoidance behaviors, non-associative learning, and visual recognition memory [6,16,17]. Due to the rapid development of larvae, these behaviors can be studied within the first week after fertilization.

Various feeding protocols are used when studying larval behavior. Larvae start feeding at 5 dpf but can live during the first 7 days solely on nutrients derived from the yolk. Only a few studies indicate that the larvae are fed before behavioral testing [18–20].

Withholding external food from larvae helps to prevent contamination of the culture medium and variability caused by differences in food intake. However, it is not known if larval behavior is affected by feeding.

In the present study, we examined zebrafish larvae at 5, 6, and 7 dpf with and without feeding, using a custom-developed imaging system for automated analysis of behavior [8,9]. The larvae were first imaged on a white background and were then imaged in the presence of visual stimuli. This experimental paradigm allows for an analysis of a broad range of behaviors, including spontaneous behaviors in a neutral environment and various behaviors that are only displayed in the presence of aversive visual stimuli.

We found that feeding did not have a significant effect on behavior at 5 dpf, but did affect behavior at 6 and 7 dpf. Based on these results, we conclude that 5-day-old larvae are well-suited for high-throughput analyses of behavior, since effects of feeding can be avoided at this time.

Materials and Methods

Zebrafish larvae and feeding. Adult wild type zebrafish were originally obtained from Carolina Biological and are maintained at Brown University as a genetically diverse outbred strain. The fish are kept in a mixed male and female population on a 14 hour light / 10 hour dark cycle. Embryos were collected from the tanks between 10:30 and 11:30 am and were raised at 28.5°C in egg water, containing 60 mg/L sea salt (Instant Ocean) in deionized water and 0.25 mg/L methylene blue as a fungal inhibitor. Embryos were grown at an approximate density of 200 embryos per liter in Aquatic Habitats 2-liter breeder tanks. Unfertilized eggs were removed from the breeder tanks and 50% of the egg water was changed daily, at approximately 10 am. Starting at 5 dpf, larvae in the ‘fed’ group were fed daily, immediately after the water change, with 0.04 grams of Zeigler AP100 LD50 larval diet (Pentair Aquatic Eco-systems) per 2-liter tank. Thus, fed 7 day-old larvae had continuous access to food from 5-7 dpf.

The zebrafish imaging system. A high-throughput imaging system for automated analysis of behavior in zebrafish larvae was developed in our laboratory [8]. Briefly, the system was built in a tall cabinet; the top shelf of the cabinet holds a 15 megapixel Canon

EOS rebel T1i digital camera and the bottom shelf holds an Acer Aspire 5517 laptop with a 15.6 inch screen to provide visual stimuli to the larvae. The camera is controlled with Canon's Remote Capture software and is connected to a second laptop computer to run the software and store the acquired images.

Imaging zebrafish larvae. Zebrafish larvae were imaged at 5, 6 and 7 dpf, three hours after feeding. The larvae were imaged in 5-lane plates, with lanes that are 70 mm long x 18 mm wide and have 60° sloping edges to reach a 66 x 14 mm bottom at a 3.5 mm depth [9]. The multilane plates were made using a 1-well plate (Thermo Fisher Scientific Cat no. 267060), 50 ml of agarose (0.8% agarose in deionized water with 60 mg/L Instant Ocean), and a custom-designed 5-lane mold, as described previously [9]. Twenty minutes prior to the start of the experiment, the lanes were filled with egg water and five larvae were transferred to each lane. Four plates (2 plates with fed larvae and 2 plates with unfed larvae) were placed on the screen of the laptop computer in the imaging cabinet. A plastic diffuser (Pendaflex 52345) was placed between the 5 lane plates and the laptop screen in order to avoid moiré patterns on the images. Canon's software has a 'Remote Shooting' feature for computer-controlled image acquisition in interval mode. The camera was programmed to collect high-resolution images every 6 seconds for a half hour for a total of 300 images per experiment.

Visual stimuli. Visual stimuli are shown to the larvae as PowerPoint presentations on the laptop's LCD screen. The presentation used in this study starts with a blank white

background for 15 minutes, followed by 15 minutes of a moving red bar (Fig 1). The red bar is 1.3 cm wide and moves up and down at a speed of 2 cm/sec in the upper half of the lanes. Our laboratory has previously shown that zebrafish larvae display robust avoidance responses when exposed to these visual stimuli [9]. The PowerPoint file is included in the supplementary information (Supplement 1).

Automated image analysis in ImageJ. The acquired images were analyzed in ImageJ, which can be downloaded free of charge from the National Institutes of Health (<http://rsb.info.nih.gov/ij/>). Our laboratory developed an ImageJ macro that automatically measures the location and orientation of the zebrafish larvae in a large number of images, which can go beyond the available RAM of the image analysis computer [8,9]. This macro, called zebrafish_macro25k, can be downloaded from the supplementary information (Supplement 2). The macro automatically removes the visual stimuli by splitting the color channels, subtracts the background, applies a threshold, detects the larvae by particle analysis, and repeats this process for subsequent images in a folder. We recently added a display of the larval centroid and center of the ‘bounding box’, the tightest box that can be drawn around a larva. In addition, we added a display for all possible distances between larvae (10 distances in a group of 5 larvae). The macro creates a ‘results’ file containing the image name, larval area in pixels, mean intensity, X, Y coordinates of the centroid, X, Y coordinates of the center of mass, X, Y, width, and height of the bounding box (the tightest box containing a larva), lane number, and X, Y coordinates of the midpoint of the lane. The Results file is opened in MS Excel for further analysis.

Data analysis in MS Excel. The coordinates of the ‘Results’ file are copied in a MS Excel template, which calculates the location, orientation and swim speed of the larvae, as described previously [21,22]. The location of the larvae along the main axis of the lane is calculated by comparing the Y coordinates of the larval centroids to the Y coordinates of the lane’s midpoint. If the Y coordinate of a larva is smaller than the Y coordinate of the midpoint of a lane, the larva is located in the upper half of the lane (‘up’). If not, the larva is located in the lower half of the lane (‘down’) or away from the visual stimuli when such stimuli are presented. It should be noted that ‘up’ or ‘down’ is a measure in the horizontal plane. A larva is considered to be on the ‘edge’ if the larval centroid is in the outer 3 mm of the 70 x 18 mm swimming area. If not, the larva is considered to be located in the ‘center’ of the swimming area. The swim speed is calculated by comparing the XY coordinates of larval centroids to the XY coordinates of the larval centroids in the next image. Larvae that move less than 1 mm in a 6 second interval are considered at rest. The ‘social distance’ or average of all possible distances between larvae was measured by comparing the centroids of larvae that are together in a well. Diagonal distances were calculated using the equation $a^2 + b^2 = c^2$. The ‘COUNTIFS’ function in Excel was used to determine how often the larvae were located down in the well, were located on the edge of the well, or were at rest. Behavioral parameters of a single lane were averaged for the first 15 minutes without visual stimuli and the second 15 minutes with visual stimuli. The bar graphs display the average and standard error of 20 lanes per experimental group.

Statistical Analyses. Statistical analyses were carried out using SPSS software. To assure that the measurements are independent, the data were analyzed on a per-lane basis

(n = number of lanes). The effects of feeding (fed and unfed) and age (5, 6 and 7 dpf) on various behaviors were analyzed using a two-way ANOVA. If the ANOVA showed a significant effect ($p < 0.05$), specific groups were compared by post hoc analyses using a two-tailed t-test (fed vs. unfed) or Tukey HSD test with a correction for multiple comparisons (5, 6 and 7 dpf).

Results

Zebrafish larval behavior in multilane plates

The behavior of zebrafish larvae was measured in multilane plates. The multilane plates were designed to give the larvae ample space to avoid aversive stimuli and interact with other larvae, which allows for the automated analysis of a broad spectrum of complex behaviors [9]. We found that the larvae display a clear avoidance response to a red moving bar (Fig 1). During the first 15 minutes of the recording, the larvae swim on a white background and move freely throughout the lane (Fig 1A). The larvae are then exposed for 15 minutes to a moving red bar, which moves continuously up and down in the upper half of the lanes. The larvae move into the lower half of the lanes to avoid the stimulus (Fig 1B). All experimental groups, including 5, 6 and 7 dpf larvae fed and unfed, displayed clear avoidance behaviors in response to visual stimuli. For example, the fed 5 dpf larvae shown in Fig 1 were located down in the lane 53% of the time without visual stimuli vs. 75% of the time with visual stimuli (Fig 2A). This avoidance response is significant ($p < 0.0001$, $n = 20$ lanes, two-tailed t-test). The substantial avoidance response and level of significance indicate that the multilane assay is a robust assay for

measuring avoidance behaviors. Other behaviors were similar to the behaviors measured previously in multiwell plates [8]. For example, the fed 5 dpf larvae shown in Fig 1 spent 60% of their time on the edge of the swimming area, displayed an average swim speed of 29 mm / min and rested 50% of the time (n=20 lanes). The developed algorithms for calculating ‘social distance’, the average of all possible distances between the larvae, revealed that the larvae display a social distance ranging from 23 mm (7 dpf fed with visual stimuli) to 32 mm (6 dpf unfed without visual stimuli) in the 70 x 18 mm lane. The effects of age and feeding were analyzed using a two-way ANOVA. This analysis revealed that none of the measured behaviors is significantly affected by age, between 5 and 7 dpf ($p>0.05$). We then further examined the effects of age within their respective feeding groups by using a one-way ANOVA. This revealed that there were no behaviors significantly affected by age, between 5 and 7dpf, except the resting behavior without bar when comparing 5dpf to 7dpf larvae in the not fed group ($P=0.032$). There is a significant interaction between age and feeding for the swim speed without visual stimuli and resting with or without visual stimuli ($p<0.05$). In addition, all behaviors, except social distance without visual stimuli, are significantly affected by feeding ($p<0.05$).

Effects of feeding on avoidance behavior

At 5 dpf, fed and unfed larvae display similar avoidance responses. In contrast, feeding induced a significant increase in the avoidance response of 6 and 7 dpf larvae (Fig 2A). The 6 dpf larvae, exposed to visual stimuli, were 68% down in the lane without feeding vs. 82% down in the lane with feeding. This difference between the fed and unfed groups

is significant ($p < 0.05$, t-test $n = 20$ lanes). The 7 dpf larvae, exposed to visual stimuli, were 68% down in the lane without feeding vs. 85% down in the lane with feeding. This difference between the fed and unfed groups is significant ($p < 0.01$, t-test, $n = 20$ lanes). Based on these findings, we conclude that feeding affects avoidance behaviors in 6 and 7 dpf zebrafish larvae.

Effects of feeding on thigmotaxis

Zebrafish larvae are known to display a preference for the edge of a circular well when imaged in a multiwell plate [23,24]. This edge preference or thigmotaxis was also observed in the current experiments with rectangular lanes. For example, Figure 2B shows the 5 dpf fed larvae spent 60% ($n = 20$ lanes) of their time in the outer 3 mm of the swimming area. This outer area corresponds to 39% of the total swimming area or only 29% of the total volume of water, since the lanes have sloping edges. Thus, the larvae display a clear preference for the outer edge compared to the center of the swimming area. Similar percentages were observed with and without visual stimuli. The 7 dpf larvae without visual stimuli were 69% on the edge without feeding vs. 58% on the edge with feeding. This difference between the fed and unfed groups is significant ($p < 0.01$, t-test, $n = 20$ lanes). The 7 dpf larvae with visual stimuli were 73% on the edge without feeding vs. 65% on the edge with feeding. Again, this difference between the fed and unfed groups is significant ($p < 0.05$, t-test, $n = 20$ lanes). Based on these results we conclude that feeding affects thigmotaxis at 7 dpf.

Effects of feeding on swim speed

The swim speeds of fed and unfed larvae were analyzed at 5, 6, and 7 dpf with and without visual stimuli (Fig 2C). At 5 dpf, the fed and unfed larvae did not display significant differences in swim speed. In contrast, fed larvae swam significantly faster than the unfed larvae at 6 dpf, both without visual stimuli ($p < 0.01$, t-test) and with visual stimuli ($p < 0.05$). Similarly, fed larvae swam significantly faster than the unfed larvae at 7 dpf, both without visual stimuli ($p < 1 \times 10^{-8}$, t-test) and with visual stimuli ($p < 1 \times 10^{-5}$, t-test). Based on these results, we conclude that feeding leads to an increase in larval swim speeds at 6 and 7 dpf.

Effects of feeding on resting behavior

Resting behavior of fed and unfed larvae was analyzed at 5, 6, and 7 dpf with and without visual stimuli (Fig 2D). A larva was considered to be 'resting' if the larva moved less than 1 mm in a 6 sec interval. At 5 dpf, the fed and unfed larvae did not display significant differences in resting. In contrast, fed larvae rested less than unfed larvae at 6 dpf. This effect of feeding was observed without visual stimuli ($p < 0.01$, t-test) and with visual stimuli ($p < 0.05$). Similarly, fed larvae rested less than unfed larvae at 7 dpf. Again, this effect of feeding was observed without visual stimuli ($p < 1 \times 10^{-6}$, t-test) and with visual stimuli ($p < 0.0001$, t-test). Based on these results, we conclude that fed larvae rest less than unfed larvae at 6 and 7 dpf.

Effects of feeding on social distance

The social distance of fed and unfed larvae was analyzed at 5, 6, and 7 dpf with and without visual stimuli (Fig 3). At 5 and 6 dpf, feeding did not induce significant differences in social distance. In contrast, feeding did induce a significant decrease in social distance in 7 dpf larvae exposed to visual stimuli. Thus, the fed larvae swim closer together than the unfed larvae ($p < 0.05$, t-test). Based on these results, we conclude that feeding can affect the average distance between larvae at 7 dpf.

Discussion

The present study examined zebrafish larvae at 5, 6, and 7 dpf with and without feeding, using a custom-developed imaging system for automated analyses of behavior. We found that feeding did not have a significant effect on behavior in 5 day-old larvae. In contrast, fed 6 and 7 day-old larvae displayed increased avoidance responses to visual stimuli, increased swim speeds and decreased resting in comparison to unfed larvae. In addition, the fed 7 day-old larvae displayed a decrease in thigmotaxis and a decrease in the distance between larvae in the presence of visual stimuli.

The observed changes in behavior may be explained, in part, by an increase in available energy when additional nutrients are provided by feeding. This increased energy level corresponds well with the increased swim speeds and reduced resting times observed in fed larvae, as compared to unfed larvae. In addition, avoidance responses may depend on

available energy, since larvae need to swim down the lane to avoid the aversive visual stimuli. While the feeding-induced changes in swim speed, resting, and avoidance behavior may all be explained by a general increase in available energy, these behaviors are not automatically linked. For example, unfed larvae display a substantial decrease in swim speed between 6 and 7 dpf, without a corresponding change in the avoidance response. Possibly, the unfed 7 dpf larvae swim as little as needed to save their energy for avoidance responses, which may be an effective adaptation for predator avoidance in nature. Feeding may also change behaviors that are unrelated to activity. For example, thigmotaxis, a preference for the edge of the swimming area, was affected at 7 dpf with or without visual stimuli. Thigmotaxis is used as a measure of anxiety in various organisms, including zebrafish larvae [23,24]. Thus, the feeding-induced decrease in thigmotaxis could reflect a reduced level of anxiety in well-fed larvae. Finally, the feeding-induced decrease in social distance at 7 dpf may be a direct result of the increased avoidance response to visual stimuli. When larvae display a strong avoidance response to visual stimuli in the upper half of the lane, they would be expected to end up close together in the lower half of the lane. In future experiments, it may be interesting to look in more detail at social behaviors during the first 15 minutes, before visual stimuli are presented to the larvae.

Zebrafish larvae are used in various high-throughput assays that screen for behavioral defects [7,10,25]. These assays can provide a wealth of information on the genes, pharmaceuticals and environmental toxicants that affect brain development and function. There is no consensus on feeding in such behavioral assays. In studies that do not pursue

behavior, larvae are typically fed at 5 dpf and beyond to ensure that energy needs are met during development [26–28]. Food intake and energy expenditure can be measured quantitatively [29,30] and effective feeding protocols have been developed to improve larval survival [31,32]. However, feeding protocols have not been standardized in behavioral studies. There have been several different feeding protocols used in previous studies that examined behavior of 5-7 dpf zebrafish larvae. These protocols include feeding with paramecia [18], feeding with a diet of TetraMin baby fish food and Artemia [19,20] or without feeding [8,10,23,33] demonstrating the wide variety of feeding protocols used during behavioral experiments. Our study is the first to directly examine the effect of feeding on larval behavior. Feeding can be problematic in behavioral assays, especially when raising larvae in multiwell plates. First, left-over food can quickly lead to bacterial or fungal contamination of the water. Second, feeding protocols need to be fast and consistent to avoid variability in food intake. Third, feeding will add another layer of complexity in the interpretation of the results, i.e. behavioral defects may be a direct result of changes in neural function or may be caused indirectly by changes in food intake. A possible solution is to examine behavior in 5 day-old zebrafish larvae without feeding. The 5 day-old larvae have a large yolk sac filled with nutrients and the results of the present study show that 5 day-old larvae do not display significantly different behaviors with or without feeding. Thus, the practical issues of feeding in a high-throughput setting can be avoided at this time. However, some behaviors can only be studied later in development. For example, shoaling behaviors develop as zebrafish age [34]. When studying such behaviors in a high-throughput setting, it will be important to develop protocols for consistent feeding while avoiding a detrimental decrease in water

quality. Ultimately, the development of methodologies for automated analyses of behavior will provide the high-throughput tools that are needed to better understand the genetic and environmental factors that cause developmental brain disorders.

Acknowledgements We thank Mrinal Kapoor and Sean Pelkowski for the initial testing of the multilane plates. This work was supported by the Eunice Kennedy Shriver National Institute of Child Health and Human Development (R01 HD060647). Holly Richendrfer, Ruth Colwill and Robbert Creton received funding from the National Institute of Environmental Health Sciences (F32 ES021342, R03ES017755, P42 ES013660) and Robert Thorn received funding from a NIH training grant in molecular biology, cell biology and biochemistry (T32 GM007601).

References:

1. Boyle CA, Boulet S, Schieve LA, *et al.* Trends in the prevalence of developmental disabilities in US children, 1997-2008. *Pediatrics* 2011; **127**:1034–42.
2. CDC: Center for Disease Control and Prevention DD. No Title.
3. Levin ED, Cerutti DT. Behavioral Neuroscience of Zebrafish. In: Buccafusco J, ed. *Methods of Behavior Analysis in Neuroscience*. 2nd Editio. Boca Raton: CRC Press; 2009.
4. Gerlai R. Using zebrafish to unravel the genetics of complex brain disorders. *Curr Top Behav Neurosci* 2012; **12**:3–24.
5. Kalueff A V, Gebhardt M, Stewart AM, *et al.* Towards a comprehensive catalog of zebrafish behavior 1.0 and beyond. *Zebrafish* 2013; **10**:70–86.
6. Wolman M, Granato M. Behavioral genetics in larval zebrafish: learning from the young. *Dev Neurobiol* 2012; **72**:366–72.
7. Kokel D, Bryan J, Laggner C, *et al.* Rapid behavior-based identification of neuroactive small molecules in the zebrafish. *Nat Chem Biol* 2010; **6**:231–237.
8. Richendrfer H, Créton R. Automated High-throughput Behavioral Analyses in Zebrafish Larvae. *J Vis Exp* 2013:1–6.
9. Pelkowski SD, Kapoor M, Richendrfer H a, Wang X, Colwill RM, Creton R. A novel high-throughput imaging system for automated analyses of avoidance behavior in zebrafish larvae. *Behav Brain Res* 2011; **223**:135–44.
10. Rihel J, Prober DA, Arvanites A, *et al.* Zebrafish behavioral profiling links drugs to biological targets and rest/wake regulation. *Science* 2010; **327**:348–51.
11. Westerfield M. *The zebrafish book. A guide for the laboratory use of zebrafish (Danio rerio)*. 4th Editio. Eugene: Univ. of Oregon Press; 2007.
12. Kimmel CB, Ballard WW, Kimmel SR, Ullmann B, Schilling TF. Stages of embryonic development of the zebrafish. *Dev Dyn* 1995; **203**:253–310.
13. Bianco IH, Kampff AR, Engert F. Prey capture behavior evoked by simple visual stimuli in larval zebrafish. *Front Syst Neurosci* 2011; **5**:101.
14. Muto A, Kawakami K. Prey capture in zebrafish larvae serves as a model to study cognitive functions. *Front Neural Circuits* 2013; **7**:110.
15. Westphal RE, O'Malley DM. Fusion of locomotor maneuvers, and improving sensory capabilities, give rise to the flexible homing strikes of juvenile zebrafish. *Front Neural Circuits* 2013; **7**:108.
16. Colwill RM, Creton R. Imaging escape and avoidance behavior in zebrafish larvae. *Rev Neurosci* 2011; **22**:63–73.
17. Colwill R, Creton R. Automated imaging of visual recognition memory in larval zebrafish. In: Kallueff A, Stewart A, eds. *Zebrafish protocols for neurobehavioral research*. Springer Protocols; 2012.
18. de Esch C, van der Linde H, Slieker R, *et al.* Locomotor activity assay in zebrafish larvae: influence of age, strain and ethanol. *Neurotoxicol Teratol* 2012; **34**:425–33.
19. Airhart MJ, Lee DH, Wilson TD, Miller BE, Miller MN, Skalko RG. Movement disorders and neurochemical changes in zebrafish larvae after bath exposure to fluoxetine (PROZAC). *Neurotoxicol Teratol* **29**:652–64.
20. Airhart MJ, Lee DH, Wilson TD, *et al.* Adverse effects of serotonin depletion in developing zebrafish. *Neurotoxicol Teratol* **34**:152–60.

21. Colwill RM, Creton R. Zebrafish Neurobehavioral Protocols. In: Kalueff A V., Cachat JM, eds. *Zebrafish Neurobehavioral Protocols*. Vol 51. Neuromethods. Totowa, NJ: Humana Press; 2011.
22. Creton R. Automated analysis of behavior in zebrafish larvae. *Behav Brain Res* 2009; **203**:127–36.
23. Richendrfer H, Pelkowski SD, Colwill RM, Creton R. On the edge: pharmacological evidence for anxiety-related behavior in zebrafish larvae. *Behav Brain Res* 2012; **228**:99–106.
24. Schnörr SJ, Steenbergen PJ, Richardson MK, Champagne DL. Measuring thigmotaxis in larval zebrafish. *Behav Brain Res* 2012; **228**:367–374.
25. Kokel D, Peterson RT. Using the zebrafish photomotor response for psychotropic drug screening. *Methods Cell Biol* 2011; **105**:517–24.
26. Avdesh A, Chen M, Martin-Iverson MT, *et al.* Regular care and maintenance of a zebrafish (*Danio rerio*) laboratory: an introduction. *J Vis Exp* 2012:e4196.
27. Lawrence C. Advances in zebrafish husbandry and management. *Methods Cell Biol* 2011; **104**:429–51.
28. Varga ZM. Aquaculture and husbandry at the zebrafish international resource center. *Methods Cell Biol* 2011; **104**:453–78.
29. Renquist BJ, Zhang C, Williams SY, Cone RD. Development of an assay for high-throughput energy expenditure monitoring in the zebrafish. *Zebrafish* 2013; **10**:343–52.
30. Shimada Y, Hirano M, Nishimura Y, Tanaka T. A high-throughput fluorescence-based assay system for appetite-regulating gene and drug screening. *PLoS One* 2012; **7**:e52549.
31. Best J, Adatto I, Cockington J, James A, Lawrence C. A novel method for rearing first-feeding larval zebrafish: polyculture with Type L saltwater rotifers (*Brachionus plicatilis*). *Zebrafish* 2010; **7**:289–95.
32. Hensley MR, Leung YF. A convenient dry feed for raising zebrafish larvae. *Zebrafish* 2010; **7**:219–31.
33. Richendrfer H, Pelkowski SD, Colwill RM, Créton R. Developmental sub-chronic exposure to chlorpyrifos reduces anxiety-related behavior in zebrafish larvae. *Neurotoxicol Teratol* 2012; **34**:458–65.
34. Buske C, Gerlai R. Shoaling develops with age in Zebrafish (*Danio rerio*). *Prog Neuropsychopharmacol Biol Psychiatry* 2011; **35**:1409–15.

Figures:

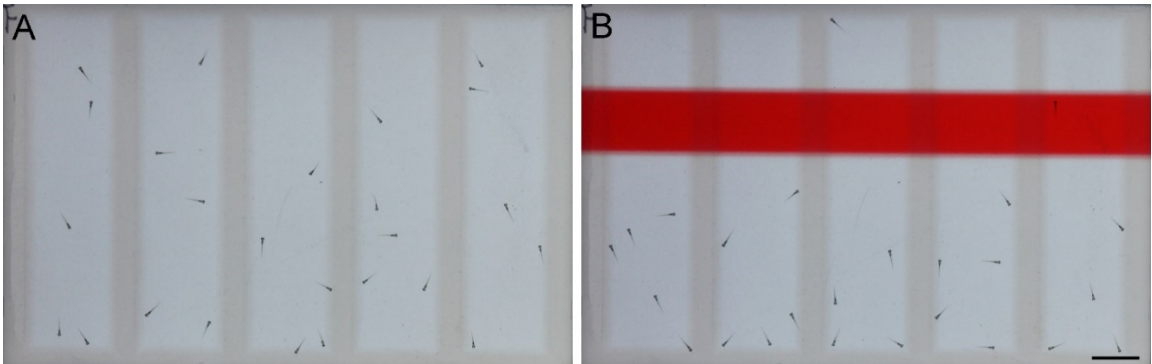


Figure 1. Imaging of zebrafish larvae in five-lane plates. A) Larvae are first imaged for 15 minutes without visual stimuli. B) Larvae are then exposed to a red bar that moves up and down in the upper half of the lanes. The images show 5-day-old larvae that were fed 3 hours prior to imaging. Note that the larvae avoid the visual stimulus. Scale bar = 1 cm.

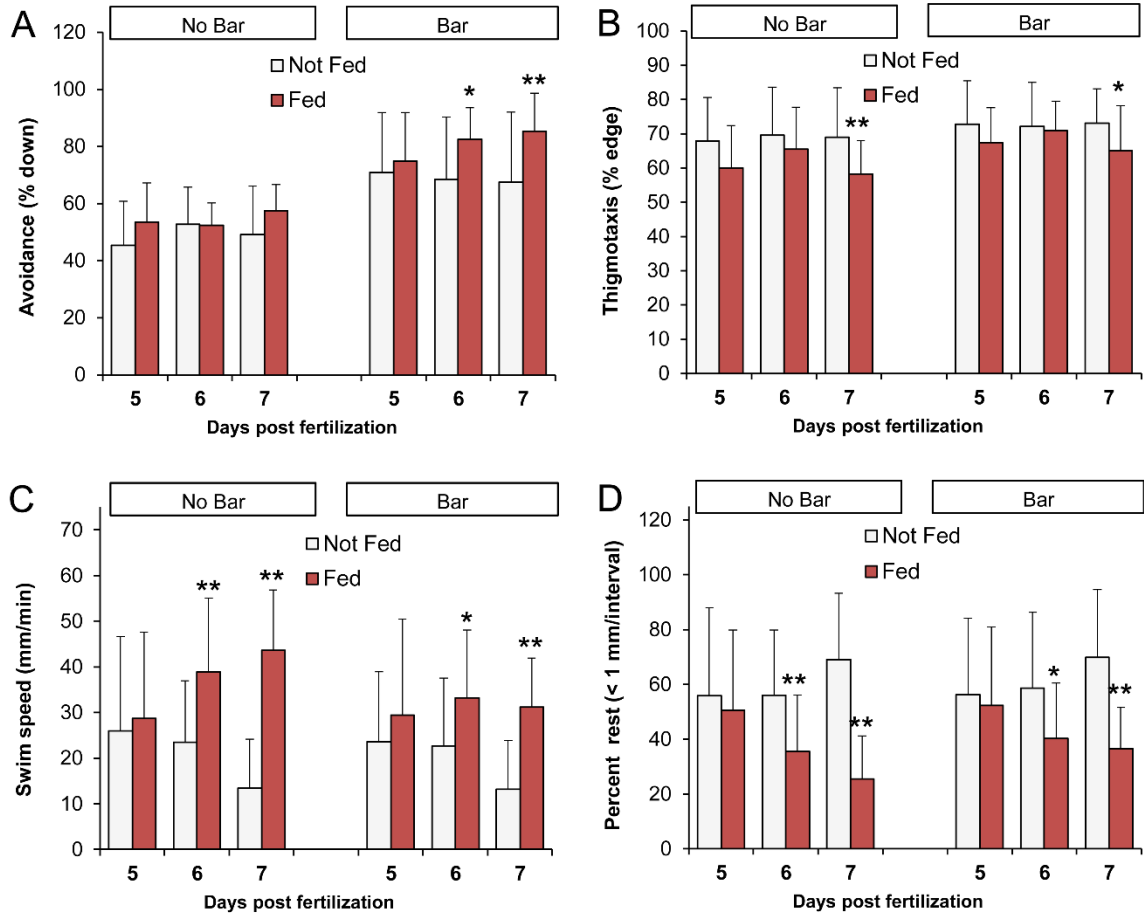


Figure 2. The behavior of 6- and 7-day-old zebrafish larvae is affected by feeding.

A) Avoidance behavior: the percentage of time that larvae are down in the lane, away from the visual stimulus. B) Thigmotaxis: the percentage of time that the larvae are located in the outer 3 mm of the swimming area. C) Swim speed: the average swim speed in mm / min. D) Percent rest: the percentage of time that larvae move less than 1 mm in a 6 second interval. White = measurements from the ‘not fed’ group, Red = measurements from the ‘fed’ group. * $p < 0.05$, ** $p < 0.01$ (t-test, fed vs. not fed, $n = 20$ lanes). Error bars indicate the standard deviation (SD).

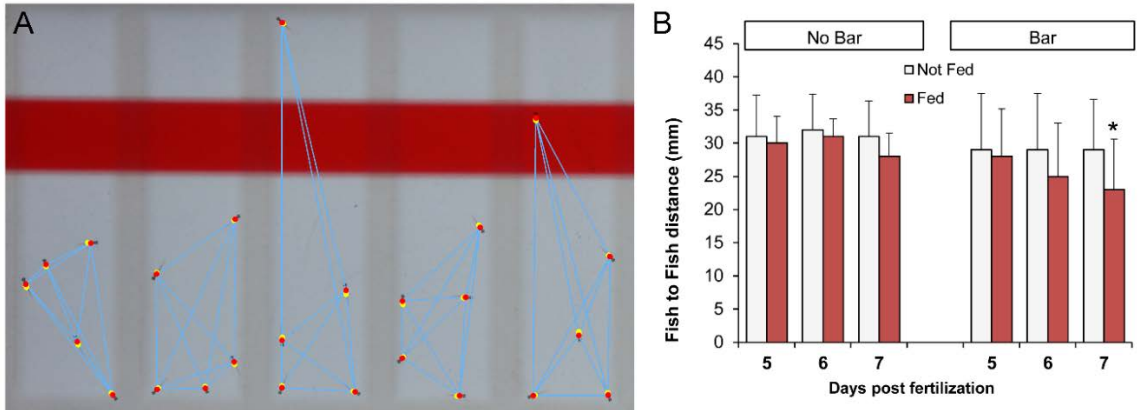


Figure 3. Fish-to-Fish Distance. A) Updated algorithms in our ImageJ macro automatically measure the larval centroid (red dot) and the center of the bounding box (yellow dot) and plot the distance between larvae in all possible combinations (blue lines). B) Feeding decreases the larval distance at 7 dpf in the presence of visual stimuli (* $p < 0.05$, t-test, fed vs. not fed). White = measurements from the ‘not fed’ group, Red = measurements from the ‘fed’ group. * $p < 0.05$, ** $p < 0.01$ (t-test, fed vs. not fed, $n = 20$ lanes). Error bars indicate the standard deviation (SD).

Appendix B: Updates and additions to Creton Lab behavioral assay

I performed all experiments presented in this appendix.

Introduction:

In the Creton Lab we have taken advantage of an affordable and customizable zebrafish behavioral setup that was previously designed and optimized in the lab [1,2]. While small things have changed to the assay such as the shape of the movement area (lanes [2] or wells [1,3]) and what stimuli was used (bouncing ball [1], moving bar [2], rotating cross [3]), most of the assayed behaviors and relative throughput has stayed fairly consistent. In this appendix, I will describe preliminary experiments I have performed to increase throughput, assay new stimuli and assay more complex behaviors.

Materials and Methods:

Behavioral Cabinets All experiments were performed in cabinets as previously described [2,4].

96-Well Plates. For preliminary experiments, one 5dpf larva was placed in each well of a costar 96-well plate. Water was added to fill the wells as much as possible to try to reduce shadowing. For initial experiments larvae were exposed to 15 minutes of a blank screen and 15 minutes of a bouncing ball in each well.

Sound Experiments. To test the sound larvae were placed in wells as in Thorn et al. 2017 [3]. Five larvae were placed in each well. A subwoofer was placed on the outside of the behavioral cabinet and plugged into the laptop to control the time and duration of the

sound. There was 9 minutes of silence followed by 1 minute of sound, and then a final 9 minutes of silence. The minute of sound consisted of a 200Hz pure tone at approximately 80 decibels that played for 0.5 second and then stopped for 0.5 second over the entire minute.

Habituation. For the habituation experiments, the 6-well plate setup from Thorn et al. 2017 [3] was used. Five larvae were added per well and the rotating red cross was used as a stimulus. The larvae were given 20 minutes without visual stimuli to adjust to the behavioral cabinet. Subsequently, either an additional 90 minutes without visual stimuli, or a 90-minute training period. The training period consisted of pulses of the red cross rotating on and off every 30 seconds. After the training period, both groups were exposed to 10 minutes of the clockwise rotating red cross. As a test of fatigue, a final 10 minute period consisting of counter clockwise rotating red cross was shown.

Analysis. All behavioral were analyzed with an updated version of the imageJ macro [3] that allowed for more wells and more periods than the previously used macros.

Results and Discussion:

The 96-well plate experiments (results not shown) were analyzed using imageJ. Due to inconsistent filling of wells the data was not consistent and could not be properly analyzed. In some wells that were overfilled a magnifying effect occurred when larvae

where in some locations, and they would disappear from view when they moved out of focus (Fig 1). In underfilled wells, the shadowing led to extra data points that confounded the analysis (Fig 1). Since the preliminary experiment R. Creton and D. Clift have been further optimizing the experiments, including more larvae per well and updating the macro to add iterative image subtraction to contend with shadowing.

The experiments were performed by exposing the larvae to a 200Hz pure tone for .5s followed by .5s of silence, repeated over a minute. We analyzed the swim speed of the larvae over time for the total duration of the experiment. The sound experiment showed that larvae do respond to sound. While we thought they would respond by moving faster, their swim speed decreases during the sound pulses and slowly recover in the silent time afterwards (Fig 2). This slowdown may be as a result of a “freezing” behavior that deserves further research.

To test habituation, we split the larvae into two groups, one that would be trained, and one that one would remain untrained. The untrained group was allowed to swim freely with no visual stimulus during the 90 minute “training” period, and the trained group was exposed to a rotating clockwise red cross for 30s and a period of no stimulus for 30s repeated over “training” period. In the habituation experiments, we analyzed the images for swim speed in response to the stimulus over the duration of the experiment. The trained larvae showed an increase in swim speed when they were first shown the moving cross during the testing period, but after the testing period they showed no addition

response. On the other hand, the untrained larvae showed a spike in swim speed at the onset of the testing period when first seeing the moving cross stimulus. After the testing phase, both groups were showed the counter clockwise rotating red cross. This stimulus did not stimulate the larvae to swim faster, suggesting it is not novel enough to act as a control. Preliminary tests (not shown) show rotating red dots could be useful as a novel stimulus control for the end of the habituation experiment. We found that the trained zebrafish larvae had significantly lower swim speed during the training period than the untrained group (Fig 3a, 33 mm/min vs. 26 mm/min; $p=.0003$). This assay will be a strong addition to our current battery of measured parameters, as we can now measure learning in zebrafish larvae. Additionally, when observing the change in swim speed from image to image, there seems to be a return to normal in swim speed, suggesting that the larvae may display habituation on a shorter time frame than the 90 minutes currently used and this assay could be further shortened (Fig 3b).

Overall, these behavioral experiments represent a step forward in testing a new set of behaviors and stimuli. Future experiments will focus on continuing the optimization of these behavioral experiments. We could also start combining these behavioral data in ways that could allow for even more robust behavioral analyses, as we could test a combination of different behavioral responses (i.e. – response to sound, and learning) and could perform the experiments in a more high-throughput manner by using 96-well plates.

References:

1. Pelkowski SD, Kapoor M, Richendrfer H a, Wang X, Colwill RM, Creton R. A novel high-throughput imaging system for automated analyses of avoidance behavior in zebrafish larvae. *Behav Brain Res* 2011; **223**:135–44.
2. Richendrfer H, Créton R. Automated high-throughput behavioral analyses in zebrafish larvae. *J Vis Exp* 2013:e50622.
3. Thorn RJ, Clift DE, Ojo O, Colwill RM, Creton R. The loss and recovery of vertebrate vision examined in microplates. *PLoS One* 2017; **12**:e0183414.
4. Clift D, Richendrfer H, Thorn RJ, Colwill RM, Creton R. High-Throughput Analysis of Behavior in Zebrafish Larvae: Effects of Feeding. *Zebrafish* 2014; **11**:455–461.

Figures:

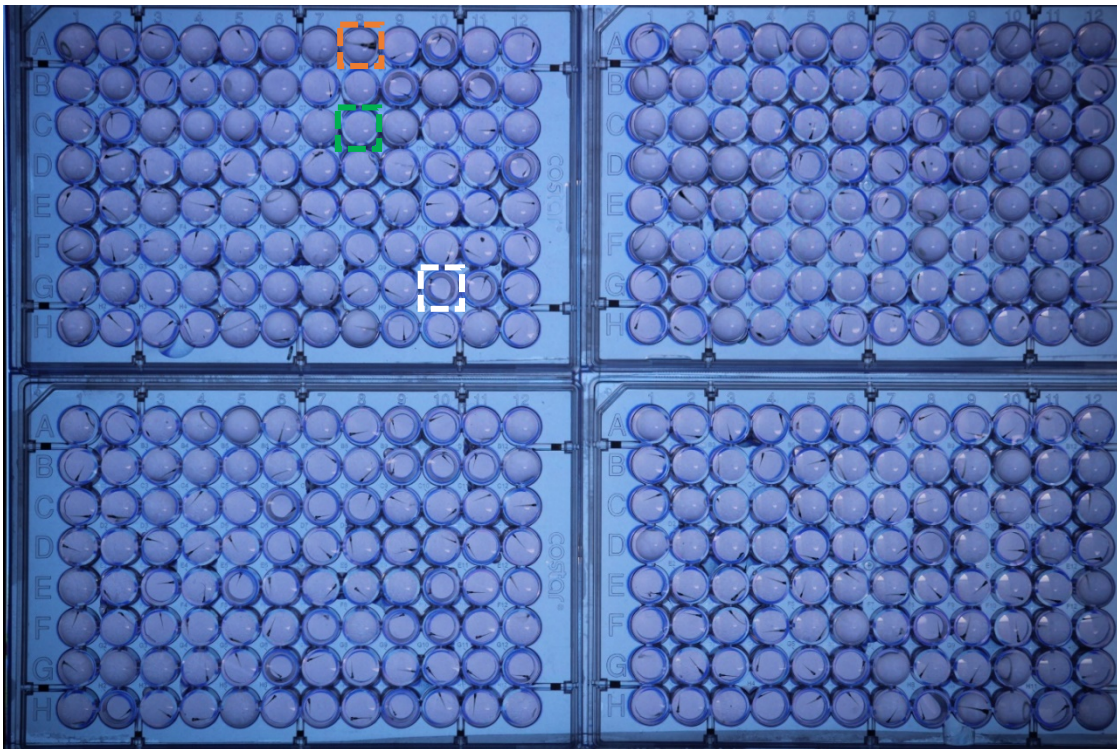


Figure 1: 96-well plate setup. One larva was placed in each of the 384 wells. The highlighted areas are examples of well filling differences that made the analysis difficult. Orange box shows an overfilled well that has ‘magnified’ the larva. Green box shows an overfilled well that has ‘magnified’ the background and is missing the larva. White box shows an underfilled well with a shadow.

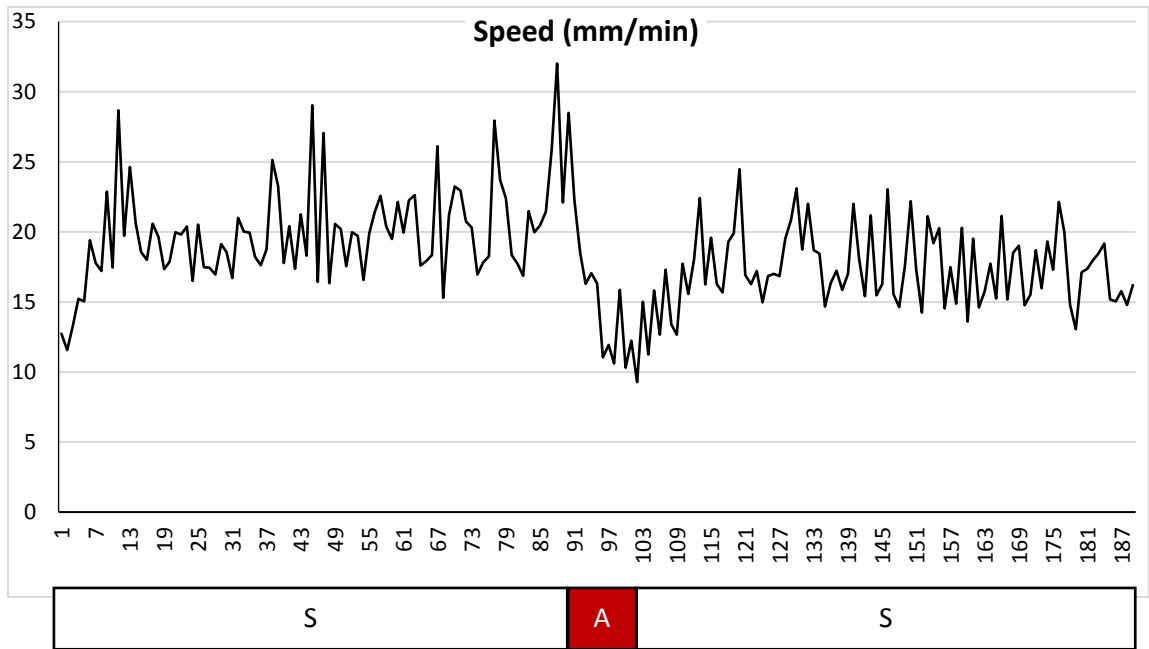


Figure 2. Response of zebrafish to audio stimulus. 5 larvae were placed in each well of a 6 well plate. Periods of silence (S) and audio stimulus (A) are denoted below graph. n = 24 wells

1 min

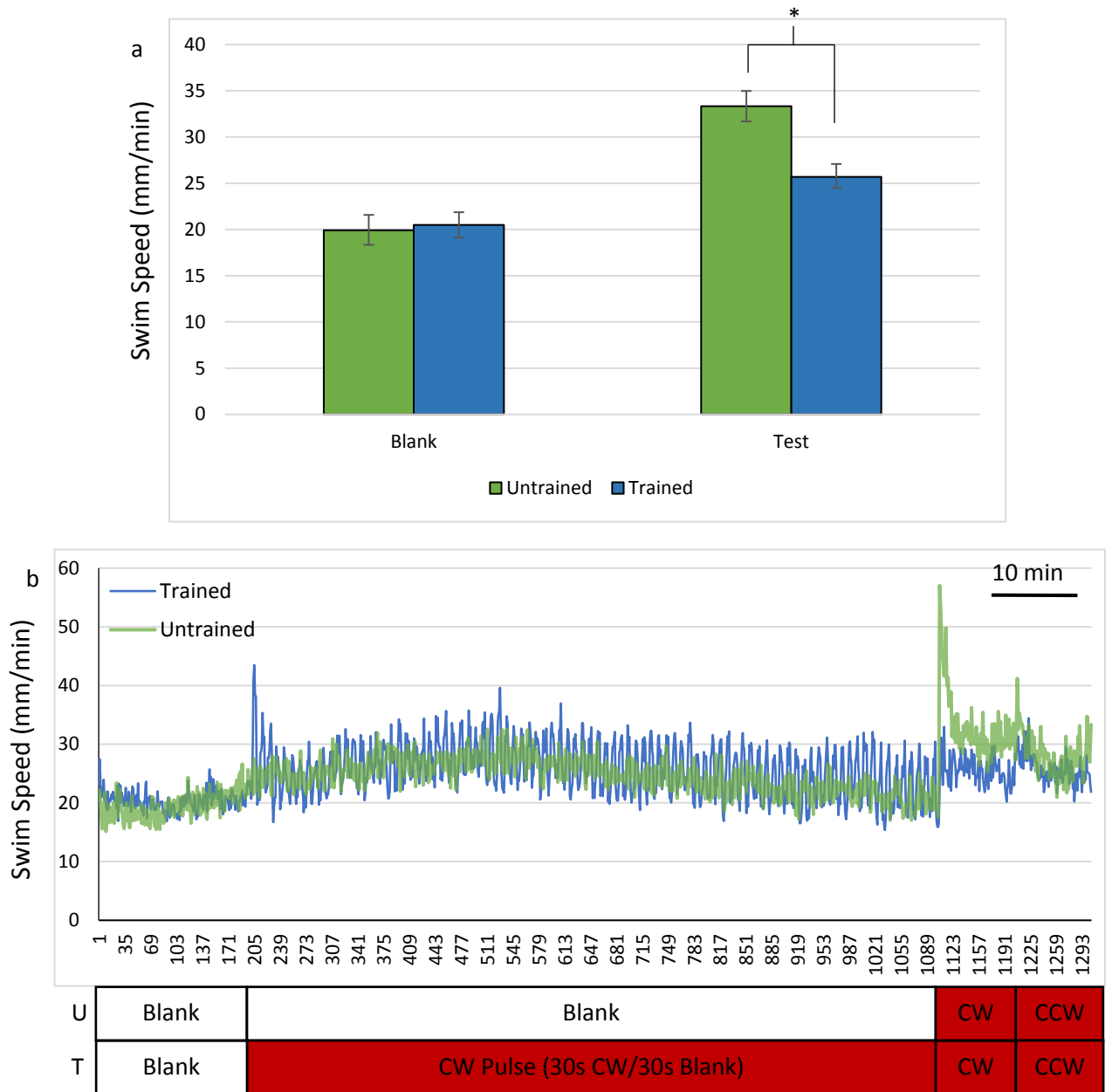



Figure 3: Habituation of zebrafish to a visual stimulus. The response of zebrafish after habituation to a red clockwise spinning cross for 30 minutes. a) Average of swim speed of two groups of fish during the initial blank period and during the test phase. The trained group that had previously been exposed to the rotating red cross shows significant ($p=0.0003$) lower in response to the test stimulus compared to the untrained group. b) Analysis of swim speed over the entirety of the behavioral assay. Below a representation of what stimulus each group is receiving at the time represented above. U = Untrained group, T = Trained group, CW = red clockwise rotating cross, CCW = red counter-clockwise rotating cross. N = 36 for each group

Appendix C: Test of zebrafish response to visual stimuli of primary and secondary colors

I performed all experiments presented in this appendix.

Introduction:

In the process of optimizing the assay of loss and recovery of vision (chapter 4), we tested the vision of zebrafish on all primary and secondary colors in our assay of avoidance behavior. The ability to assay both primary and secondary colors could become useful when testing for the loss and recovery of specific cones in vision loss and regeneration.

Materials and Methods:

Behavioral Experiments: Behavioral experiments were performed as outlined in Thorn et al. 2017 [1]. Briefly, we assayed avoidance by using the various colored stimuli in the top half only (bar) or by showing dots moving up throughout the entire well (dots). In the red and cyan test, we used a bar in both the top half of the lanes, to move larvae down, followed by a bar in the bottom half of the lane, to move larvae up. In the 6-well plate experiments of vision we showed larvae a rotating cross moving clockwise (CW) and then counter clockwise (CW) and used crosses that were colored red or cyan for testing purposes.

Results and Discussion:

We started by testing 5dpf larvae in our assay of avoidance behavior using bars and dots of all primary (red, green, blue) and secondary (magenta, yellow, cyan) colors and measuring what percent were in the top half of the lanes (%up). To determine if the

larvae responded we compared the response to the bar, which should move the larvae down in the lanes, to the response to dots, which should move the larvae up in the lanes. We found that in larvae showed significant response to stimuli that were colored red (18% vs 67%; $p=2.9 \times 10^{-7}$), green (17% vs 58%; $p=9.0 \times 10^{-7}$), blue (28% vs 67%; $p=6.0 \times 10^{-6}$), magenta (20% vs 52%; $p=5.0 \times 10^{-5}$) and yellow (16% vs 50%; $p=2.1 \times 10^{-6}$) but there was no significant difference in the response to the cyan stimuli (41% vs 51%; $p = .2$) (Fig 1).

This result showed us that the assay of avoidance behavior was not suitable as a measure of vision. While the larvae did show robust response to all other colors, for our future experiments we wanted to be sure we could test all colors. To test vision, we moved to an assay in 6-well plates that did not involve avoidance of the stimulus. We showed larvae a colored cross that would rotate clockwise or counter clockwise based on past research on the optokinetic response (OKR) [2]–[4]. In the OKR, zebrafish are shown a rotating stimulus, and their eyes will orient in the same direction as the rotation stimulus. We hypothesized that this eye movement would also translate to larval movement in our system. To test this hypothesis, we compared the response of larvae to red and cyan colored stimuli in the 5-lane assay of avoidance behavior and the 6-well assay of vision. In the 5-lane assay we replicated the results from earlier, where larvae responded strongly to the red bars (19% vs 61%; $p=1.1 \times 10^{-7}$) and not at all to the cyan bar (46% vs 46%; $p=.3$) (Fig 2a). In the 6-well assay of vision we found that the larvae responded to both the red cross (62% vs 29%; 5.3×10^{-4}) and the cyan cross (64% vs 35%; $p=3.4 \times 10^{-5}$)

(Fig 2b). These results suggest that the 6-well plates are a better assay of vision than the 5-lane avoidance assay, and we will be able to use this for color vision in the future.

References:

1. Thorn RJ, Clift DE, Ojo O, Colwill RM, Creton R. The loss and recovery of vertebrate vision examined in microplates. *PLoS One* 2017; **12**:e0183414.
2. Beck JC, Gilland E, Tank DW, Baker R. Quantifying the ontogeny of optokinetic and vestibuloocular behaviors in zebrafish, medaka, and goldfish. *J Neurophysiol* 2004; **92**:3546–61.
3. Rinner O, Rick JM, Neuhauss SCF. Contrast sensitivity, spatial and temporal tuning of the larval zebrafish optokinetic response. *Investig Ophthalmol Vis Sci* 2005; **46**:137–142.
4. Haug MF, Biehlmaier O, Mueller KP, Neuhauss SC. Visual acuity in larval zebrafish: behavior and histology. *Front Zool* 2010; **7**:8.

Figures:

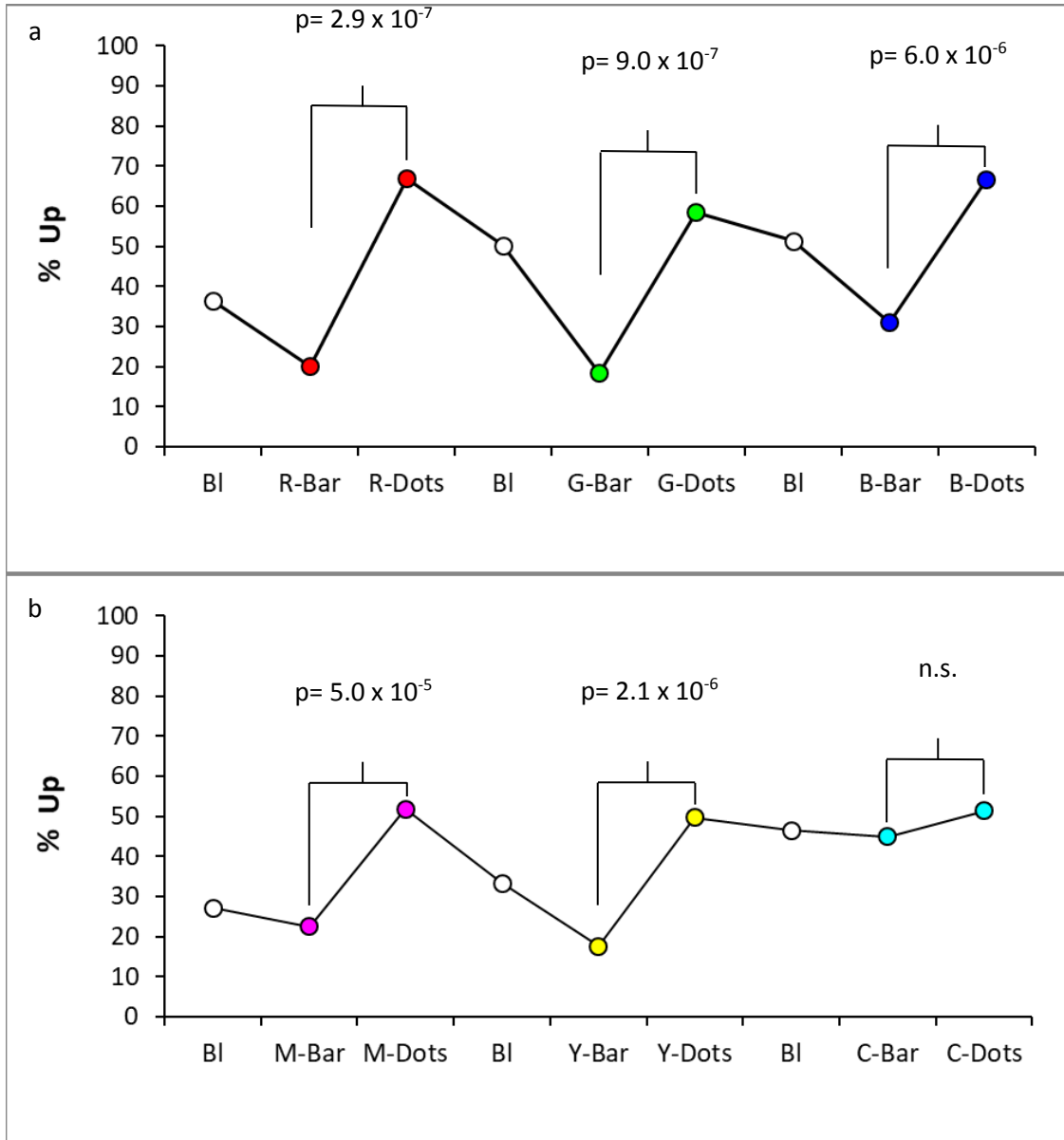


Figure 1. Test of zebrafish visual response in lanes with primary and secondary colors. The response of zebrafish to visual stimuli that are primary (a) or secondary (b) colored. Every color was able to elicit a response from the zebrafish (Bar vs. Dots) except for Cyan. Two-tailed t-tests were performed to compare the response to the bars and dots, and the p-values are shown for significant values. N=10 lanes (50 larvae) per group. Bl = Blank, R = Red, G = Green, B = Blue, M = Magenta, Y = Yellow, C = Cyan

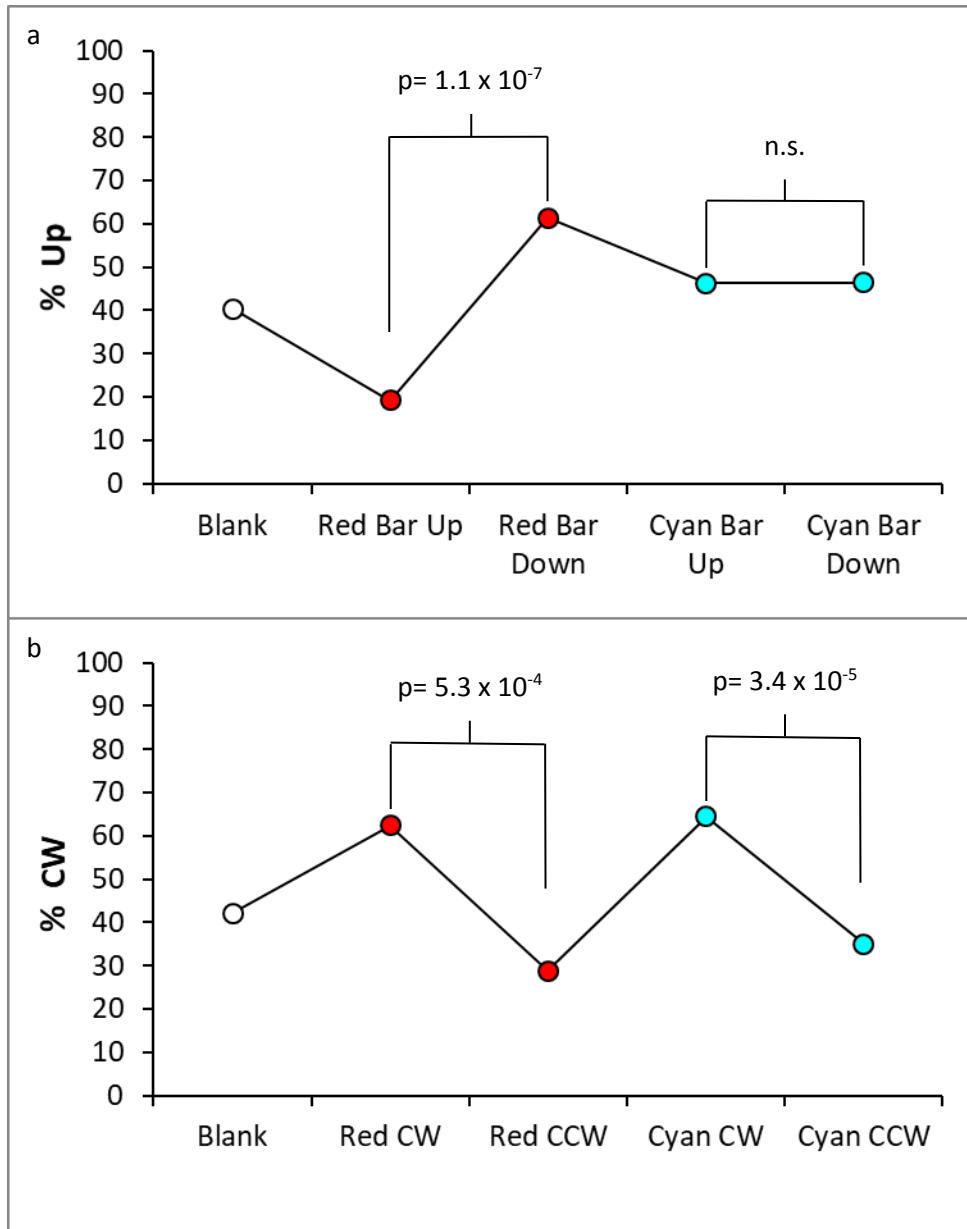


Figure 2. Test of zebrafish visual response to cyan colored stimuli. The response of zebrafish to cyan colored visual stimuli in the assay of avoidance behavior (a) and the test of vision (b). In the assay of avoidance in the 5 lanes 5dpf zebrafish larvae showed no significant response to the cyan bar. In the assay of vision in 6-well plates, 5dpf 11 larvae showed significant response to both the red rotating cross and the cyan rotating cross. Two tailed t-tests were performed and the p-values reported for significant differences. N= 10 lanes (50 larvae) or 12 wells (60 larvae). CW = clockwise, CCW = counter-clockwise.